2 DoF surgical training eye phantom for cataract surgery in a low-cost setting

Kadabettu Rajath Shenoy

TU Delft

2 DoF surgical training eye phantom for cataract surgery in a low-cost setting

by

Kadabettu Rajath Shenoy
BioMechanical Design Engineering
(5462916)

Thesis committee:	Prof. dr. J Dankelman, TU Delft, supervisor
	Dr. ir. R M Oosting, TU Delft, supervisor
	Dr. ir. A Sakes
Project Duration:	June, 2023 - March, 2024
Faculty:	Faculty of Mechanical Engineering, Delft

Cover:	Eye Pictures by Umesh Soni under Unsplash License (free)
Style:	TU Delft Report Style, with modifications by Daan Zwaneveld

TU Delft

Preface

The human body has been one of the most fascinating things I find. As a biomechanical design student by education and passion, I always wanted to create something that could closely imitate a part of the body- just like an intricate origami piece resembling a swan. The dream was slightly vague to begin with and it took me quite a while to finally be able to settle in on the topic of a human eye. A year and a half ago, I had almost no knowledge about the intricacies and complexities of the human eye, its detailed anatomy, and eye surgeries. The first step that swayed me further into this topic was when I began my internship at DORC (Dutch Ophthalmic Research Center) International BV in Zuidland on the topic of phacoemulsification needle design and manufacturing. The first surgical videos and knowledge about eye and cataract surgery can be traced back to the internship training over the 3 months I had at the company. As I tried out the surgical tools I was working with on an eye phantom, I realized how complex the surgery steps were as I made many 'lethal' mistakes on the dummy eyepiece with the tool piercing many synthetic structures inside. Bad as I may be, this piqued my interest in the question that ignited and fueled this thesis project - "How do the surgeons get their training for cataract surgeries?". This question evolved into a more refined problem statement for this thesis.

I would first like to acknowledge Roos M Oosting and Jenny Dankelman, my two supervisors on my master's thesis topic, for guiding me through the journey of this thesis. Your insights, discussions, recommendations, and even feedback on my presentations have come a long way. I would like to acknowledge Dr. Thomas Kuriakose from India who has been one of the most important people in this thesis. He always made time to answer my fundamental questions about eye anatomy, tools, and surgery techniques while also being the 'academic trainer' in this thesis validating the final prototype. I would like to thank Mart Gahler, my internship supervisor in the company, and DORC for not only giving me the internship opportunity but also igniting that spark in me and helping me throughout the project, especially in the 'Surgical trials' part of my thesis. I would like to thank Dr. Efe who took part as the 'surgeon' in those trials. I would like to thank Paul Breedweld, not only for the amazing course on 'bio-inspired design' but also for letting me get the opportunity of interning at DORC. I would like to thank Jan van Frankenhuyzen from Phantom Lab and the IWM department for your insights about specific queries I had and for helping me create the parts. Finally, I would like all my friends, and family for directly and indirectly helping me out during this one year of the project.

I hope you, the reader, find this report interesting and appreciate the hard work, passion, and knowledge I have poured into this project.

Kadabettu Rajath Shenoy
TU Delft, February 2024

Abstract

The human eye is a very delicate yet highly intricate organ, and treatments such as cataract surgery call for meticulous precision. Ophthalmologists hone their skills over years of practice, which they initially acquired during their studies in medical schools. Basic skills such as globe fixation and capsulorhexis training have a very steep learning curve as they are fundamental, albeit very challenging from the get-go. There is a lack of training simulators that can combine both surgical techniques as effectively and economically as animal eye setups. In this respect, the present research work aims at designing a cataract surgery eye phantom for capsulorhexis and globe fixation, which can replicate the movement of the eyeball in the orbit coupled with the inherent passive stiffness. The project culminates in the design of a 2-degree-of-freedom anterior human eye phantom with anatomically similar features of the human eye needed for training the aforementioned surgical steps. A significant part of the prototype structure is 3D printed using Draft resin V2 on the Formlabs Form 3+ printer to create minute yet almost anatomically impeccable components. Mechanical analyses were performed to tune the passive stiffness of the compliant mechanisms, and materials such as PlatSil Gel-00, hydrogel, and eggshell membrane were chosen and utilized to replicate the interactions between the tools and various tissues in the human eye. Clinical evaluations were conducted by a surgeon performing capsulorhexis on the prototype in a wet lab environment and several validation tests by an academic trainer for the suitability and practicality of the prototype. In that context, the present research serves as the first step toward creating innovative designs for training phantoms in the field of eye surgery.

Keywords: eye phantom, ophthalmology, capsulorhexis, training, 3D printing, compliant mechanism.

Contents

Preface i

Abstract ii

1 Introduction 1
- 1.1 Cataract . . . 1
- 1.2 Cataract Surgery . . . 2
- 1.3 Ophthalmology and cataract surgery training . . . 4
- 1.4 Problem description and research goal . . . 7
- 1.5 Requirements . . . 7
  - 1.5.1 Primary Requirements . . . 7
  - 1.5.2 Secondary Requirements . . . 8
- 1.6 Thesis outline . . . 8
- 1.7 Thesis model overview . . . 9

2 Human Eye Anatomy 10
- 2.1 Eye and optic muscles . . . 10
- 2.2 Cornea and sclera . . . 10
- 2.3 Iris and pupil . . . 11
- 2.4 Lens and capsular membrane . . . 11

3 Design methodology 14
- 3.1 Strategy . . . 14
- 3.2 Design of the rotating eyeball . . . 15
- 3.3 Tension Element . . . 16
  - 3.3.1 Choice of tension elements . . . 16
  - 3.3.2 Design of the tension elements . . . 18
- 3.4 Lower eyeball plate . . . 22
- 3.5 Eyeball piece . . . 22
- 3.6 Corneal piece and anterior chamber . . . 23
- 3.7 Tolerances and fixtures . . . 24
- 3.8 Full model overview . . . 25

4 Materials and preparation 28
- 4.1 Structural components . . . 28
- 4.2 Ball joint . . . 29
- 4.3 Corneal tissue . . . 29
- 4.4 Corneal cover . . . 29
- 4.5 Capsular membrane . . . 30
- 4.6 Cataractous lens . . . 32

5 Experimental setups, protocols, and verification 34
- 5.1 Preliminary experiments . . . 35
  - 5.1.1 Stiffness of a single compliant strip . . . 35
  - 5.1.2 Tear, fit, and water retention test of the silicone ring . . . 37
- 5.2 Secondary Experiment: Torsional stiffness test of the setup . . . 37
- 5.3 Clinical Evaluation . . . 38
- 5.4 Validation by training surgeon . . . 39

6 Results and discussions 41
- 6.1 Preliminary experiments . . . 41
  - 6.1.1 Change in thickness of the compliant strip . . . 41

6.1.2 Changing the speed of the platform motion . . . 42
6.1.3 Variation in the stiffness profile after 20 cycles of loading . . . 43
6.1.4 Other preliminary experiments: . . . 45
6.2 Secondary experiment . . . 45
6.3 Cost estimation . . . 48
6.4 Clinical Evaluation . . . 49
6.4.1 Assessment overview . . . 49
6.4.2 Concerns . . . 50
6.4.3 Implications . . . 53
6.5 Validation by the training surgeon . . . 53
6.5.1 Structural flaws and improvement in the design of the training model . . . 54
6.5.2 Positive remarks . . . 56
6.5.3 Proposed training methodology . . . 57
6.5.4 Recommended design changes for future improvements . . . 58
6.6 Limitations of the project and experiments . . . 58
6.7 Accomplishment of the set requirements . . . 58

7 Conclusion **59**

References **60**

A Appendix: Parts creation and assembly steps **65**
A.1 Molding the silicone membrane membrane on corneal piece . . . 65
A.2 Prototype setup guide . . . 68

B Appendix: Major dimensions of prototype and graphs **75**
B.1 Dimensions . . . 75
B.2 Additional graph . . . 82

1

Introduction

1.1. Cataract

Cataracts are one of the most prevalent eye problems in the world accounting for 47.8% of global blindness according to the surveys of 2020 [1]. A cataract is a medical condition in which the natural eye lens gets cloudy as the proteins begin to break down and clump together [2], which leads to a cloud vision eventually leading to blindness. While the eventual cause for cataract formation is the degradation of lens proteins, many preliminary factors lead to this chain reaction. One of the most common causes is the natural aging of the person – a decline of α-crystallin chaperone in the 40s which leads to aggregation of proteins and loss of lens transparency [3]. Any previous eye surgery may put the person at a higher risk of contracting a cataract in that eye. It is estimated that about 80% of the patients who undergo vitrectomy have a chance of developing cataracts within 2 years [4]. Other causes include exposure to UV radiation, malnutrition, trauma, and genetic abnormality [5].

Cataracts are more prevalent in low and middle-income countries (LMICs) than in other re-

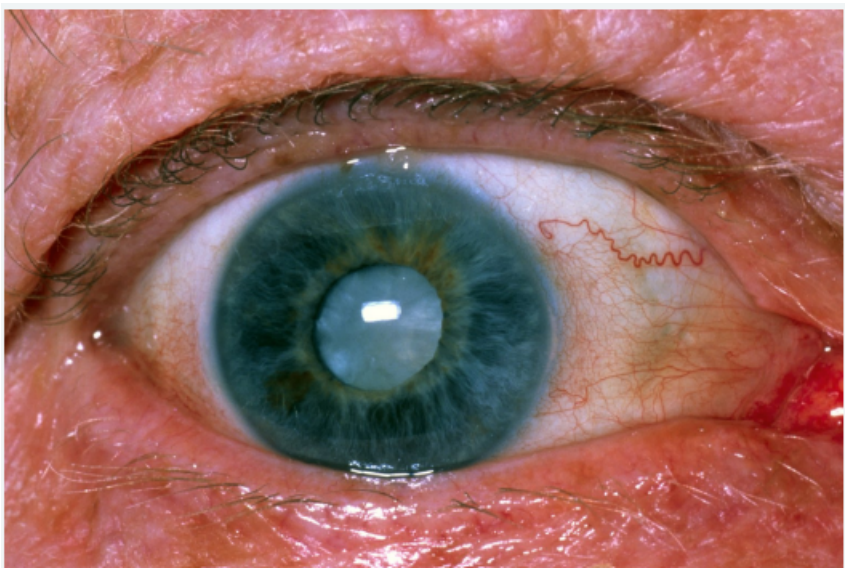

Figure 1.1: Cataract eye [6]

gions and often lead to material poverty in such countries. Figure 1.2 shows the demography of the cases found in the population. South Asian countries account for the largest burden of the cataract cases. Cataract is often linked with a decrement in quality of life in the people affected by it in society in many ways. People are not able to earn an adequate amount of living or be handle their household. This not only exacerbates the spread of poverty but also has psychological implications. Reduced social interaction often leads to isolation, lack of social support, and depression [7]. Nevertheless, there has been a significant decrease in cataract-related blindness rates in high-burden countries between 2000 and 2020 [8]. This can be attributed to improvements in the healthcare system, access to healthcare camps, and

educating the public about the treatments.

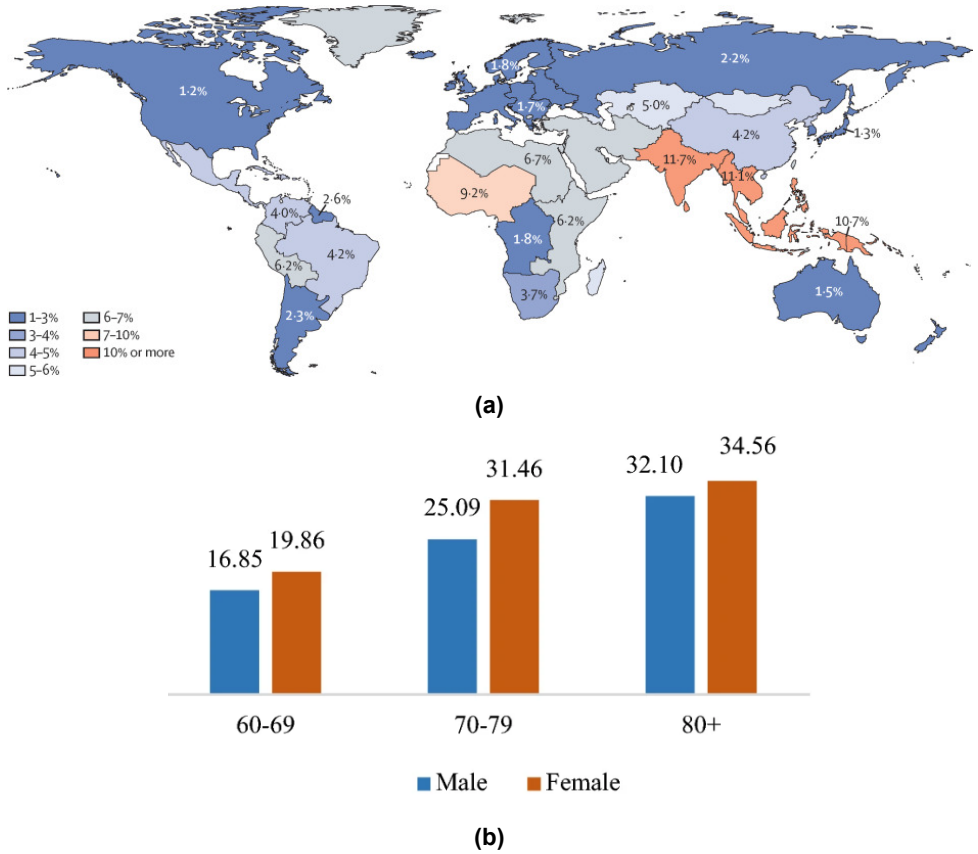

Figure 1.2: (a) Distribution of cataract cases throughout the world [8] and (b) Prevalence of cataract among older adults in India in 2017-2018 [9]

1.2. Cataract Surgery

Although there is ongoing research on drugs that can delay the progress or onset of age-related cataracts such as N - acetylcarnosine (NAC) [10], these trials are mostly in their initial phases. Currently, there are no alternatives to surgery as a treatment for cataracts. Cataract surgeries are not new. Ancient and medieval cultures around the world as old as 800 BCE often show records of couching as a method of cataract treatment which involved dislocating the clouded lens from the visual axis and into the vitreous cavity using sharp tools [11]. The first true and recorded instance of extracapsular cataract extraction (ECCE) was done in France by Jacques Daviel [12]. Intracapsular Cataract Surgery (ICCE) and Extracapsular Cataract Extraction (ECCE) surgery are two practices that are rarely performed these days as compared to Manual Small Incision Cataract Surgery (MSICS) and phacoemulsification due to the complication rates [13]. ECCE involves the removal of the entire hard cataractous lens as a single entity while leaving behind the capsular bag wherein the IOL is implanted whereas ICCE involves the removal of the lens along with the capsular bag with IOL implanted in front of the iris. Phacoemulsification involves using a handpiece whose tip vibrates at around 40 KHz frequency. This probe is inserted after capsulorhexis to emulsify the lens using the phaco tip and aspirating the fragments via the hollow tip. Laser-assisted cataract surgery is also one of the newer means of performing cataract surgery, although scarcely used due to its

novelty and completely different machines and tools requirements. Phacoemulsification and laser-assisted cataract surgery are the most commonly performed surgery for cataracts in developed countries due to their low complication rates while MSICS has been proven to be the most cost-effective intervention in LMICs [14]. Figure 1.3 shows the progression of the surgery techniques over the decades.

A regular small incision cataract surgery (SICS) involves 6-7 major steps with some of them

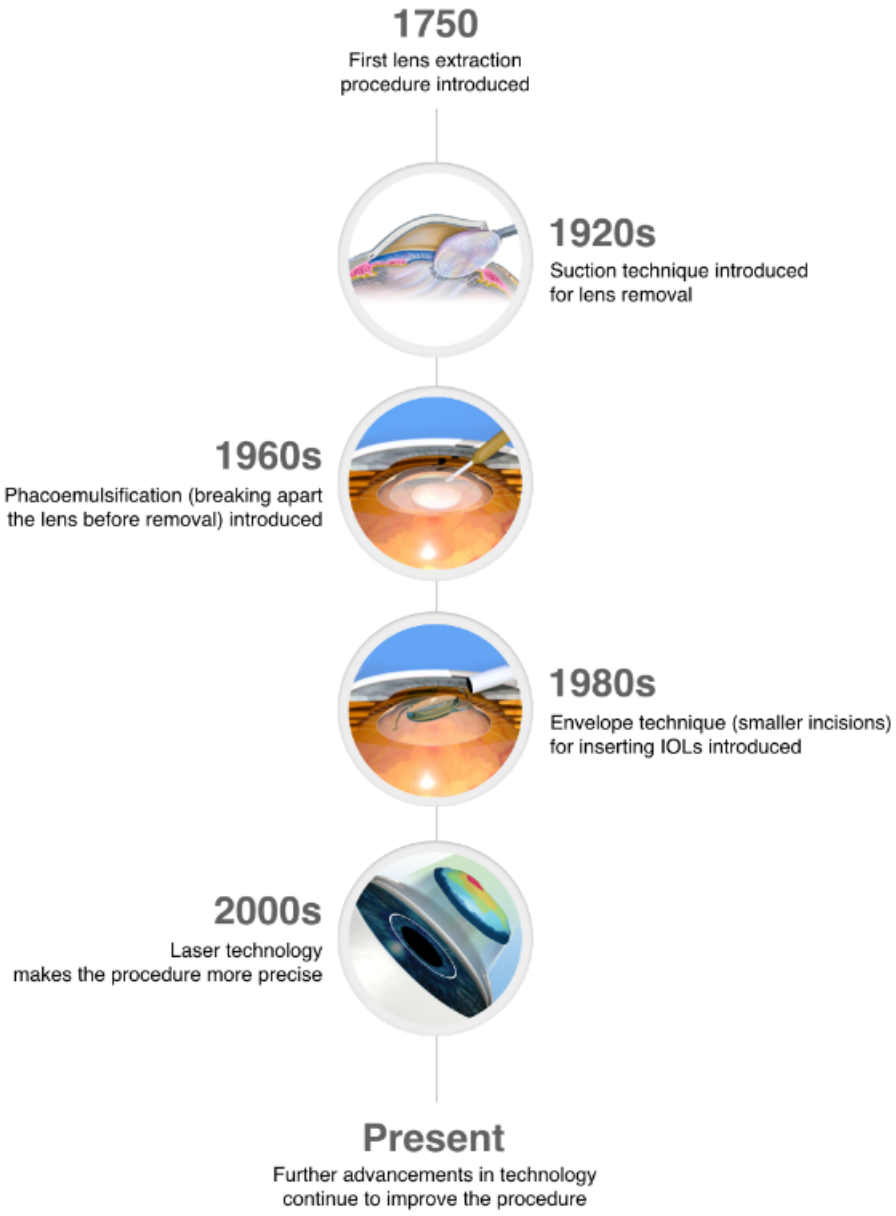

Figure 1.3: Progression of cataract surgery over the years [15]

being specialized based on the type of cataract surgery chosen for the case [16]. After the patient's eye has been anesthetized, a corneal incision is made with a keratome near the limbus of the cornea to insert other surgical tools into the eye. Using a cystotome, a small cut is made on the anterior face of the capsular membrane, and capsulorhexis is carried out wherein the membrane is torn in a circular manner using microforceps. The softer lens cortex is separated from adhering to the capsule and a fluid wave is utilized to reach the cataractous region of

the lens nucleus (hydro dissection). A sharp tip along with some forceps, the hard lens nucleus is broken into pieces in a process called lens sculpting. This process is often specialized and named based on the tool used- a vibrating phaco tool for phacoemulsification and a laser in laser cataract surgery. The fragments are carefully removed from the eye. Irrigation and aspiration is done to extract the softer lens cortex without damaging the remaining capsular bag using vacuum suction and liquid injection into the chamber to maintain the pressure. An intraocular lens is implanted using a thin probe into the empty capsular bag. The steps, in order from least to most difficult, were lens insertion, wound construction, hydro dissection, aspiration/removal of cortex, sculpting/cracking of the lens, quadrant removal of the lens, and capsulorhexis [17].

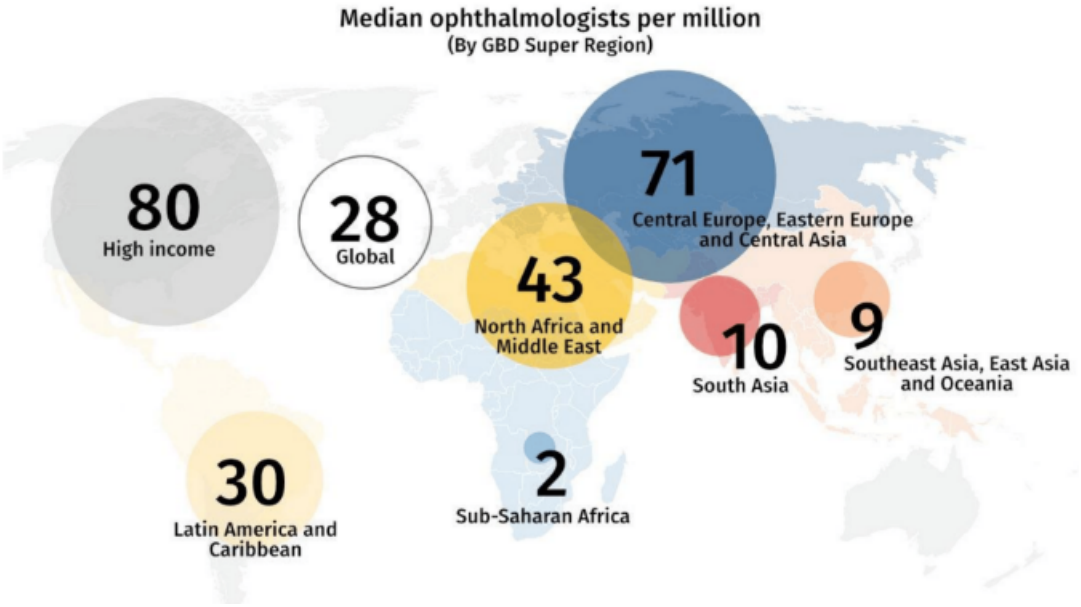

Figure 1.4: Ophthalmologist distribution around the world [18]

1.3. Ophthalmology and cataract surgery training

Figure 1.4 shows the considerable difference in the number of ophthalmologists per million population between the developed and developing countries, with South Asia having 10 and Sub-Saharan African (SSA) regions having 2 which is very low compared to the global average of 28. Quality of training and facilities available for both training and real surgery are among several other reasons. Until the recent decades, cataract surgery training in LMICs was imparted on an apprenticeship style of training under the classic Halstedian model of 'see one, do one, teach one' [19]. This apprenticeship style of training has come under the lens of ethical views and the safety of real patients. The alternative to this is expensive and resourceful, with a lot of widespread unawareness which often leads to lack of quality imbued. Cataract surgery training is often not restricted to students in medical universities. Most of the cataract surgery training curricula in developing countries, especially in Asia, are for extracapsular cataract extraction (ECCE) surgery, which is outdated, and manual small incision cataract surgery (MSICS) rather than the more novel and advanced phacoemulsification surgery and laser-based cataract surgery [20], [21].

Nonetheless, the research institutes and companies hold several collaborative bridging and training programs for the resident and practicing surgeons. One such example is the two-week 'Phaco Development Program' (PDP) introduced by Alcon Inc, Switzerland in India which was noted to be effective at not only garnering the collective pickup of the phaco method but also addressing and reducing the complication rates during surgery training [20]. Although somewhat controversial, non-physician cataract surgeons (NPCS) have been trained and allocated for cataract surgeries due to the rise in the number of cataracts and the lack of trained surgeons. Studies show that there was considerable variation in acceptance of these non-physician cataract surgeons in SSA with real impact in the treatment of cataracts in these regions [22]. This is in complete contrast to the less common cataract surgery training programs beyond the institutions in developed countries such as the USA and much of Europe which are often regarded as supplementary. This is due to their well-balanced curriculum, state-of-the-art training techniques, and facilities. In such a high-income setting, the cost of training and/or the practiced surgical procedure is of less concern as compared to the results obtained, therefore more sophisticated procedures such as phacoemulsification are the go-to norm for all the surgeons.

Each country has its timeline, career path, and course of action for students pursuing a qualification in ophthalmology. In India, a student who cleared their 12th grade attempts the National Eligibility-cum-Entrance Test [NEET (UG)] to get admission into any of the medical schools for their bachelor's program called MBBS (Bachelor of Medicine and Bachelor of Surgery) [23]. MBBS is a 5.5-year program wherein the students are taught the know-how about human physiology, medicine, ailments, and theories about surgery in general [24]. It should be known these students do not perform any live surgeries during or immediately after their program as they are not deemed specialists. They then enter the bond years after the 12-month internship during which they are expected to work in rural/ urban settings depending upon their allocation by the respective state government or pay a penalty and forgo the bond [25]. This period let them gain real-life experience with the existing healthcare and hone their basic skills. If the individual is interested in pursuing a career in specialization programs such as ophthalmology, they need to once again clear a nationwide entrance exam of NEET meant for postgraduates (PG) and choose their options by getting a seat at medical universities [26]. During this program, the students, who have now taken up the residency in that institute/ medical facility, learn more about eye problems, and treatments, and get the training necessary to be able to perform live surgeries over their residency years.

Cataract surgery training is the most basic surgical procedure taught in the ophthalmology program. Apart from the theories and lectures, the residents gain their skills by practicing through various means. Virtual Reality (VR) simulator training setups such as EyeSi, Phacovision, and MicrovisTouch have been developing rapidly over the decades in terms of training modules offered and technology. It has been proven to improve the abstract as well as certain procedural skills whilst reducing the complication rates of the trainees [27], [28], [29]. Research has been progressive on the usage of animal and cadaveric eyes in wet labs as newer, affordable, and anatomically similar eyes are being used in almost every training center in a wet lab environment. It helps in letting students experience and work on the biological eye. Both these methods of training have their own sets of merits and demerits especially in terms of finances [30], [31], versatility [32], [33], and realism [34],[35],[36],[37]. A surgical training phantom can be described as an object made to imitate a real human or a part of the body using non-living or synthetic materials to obtain specific physical or chemical properties and primarily used for training purposes. Figure 1.5a shows the earliest known cataract surgery

training eye phantom in the market made by Maloney [38] while Figure 1.5c and 1.5d are the modern-day phantom made by Philips [39] and Eyecre.at GMbH [40]. Although being a less prominent choice of training compared to other training techniques in general, surgical training eye phantoms have the potential to able to take the best qualities of both the VR and animal eyes in wetlabs as they can be customized to fit the need of the case study/ training style [41].

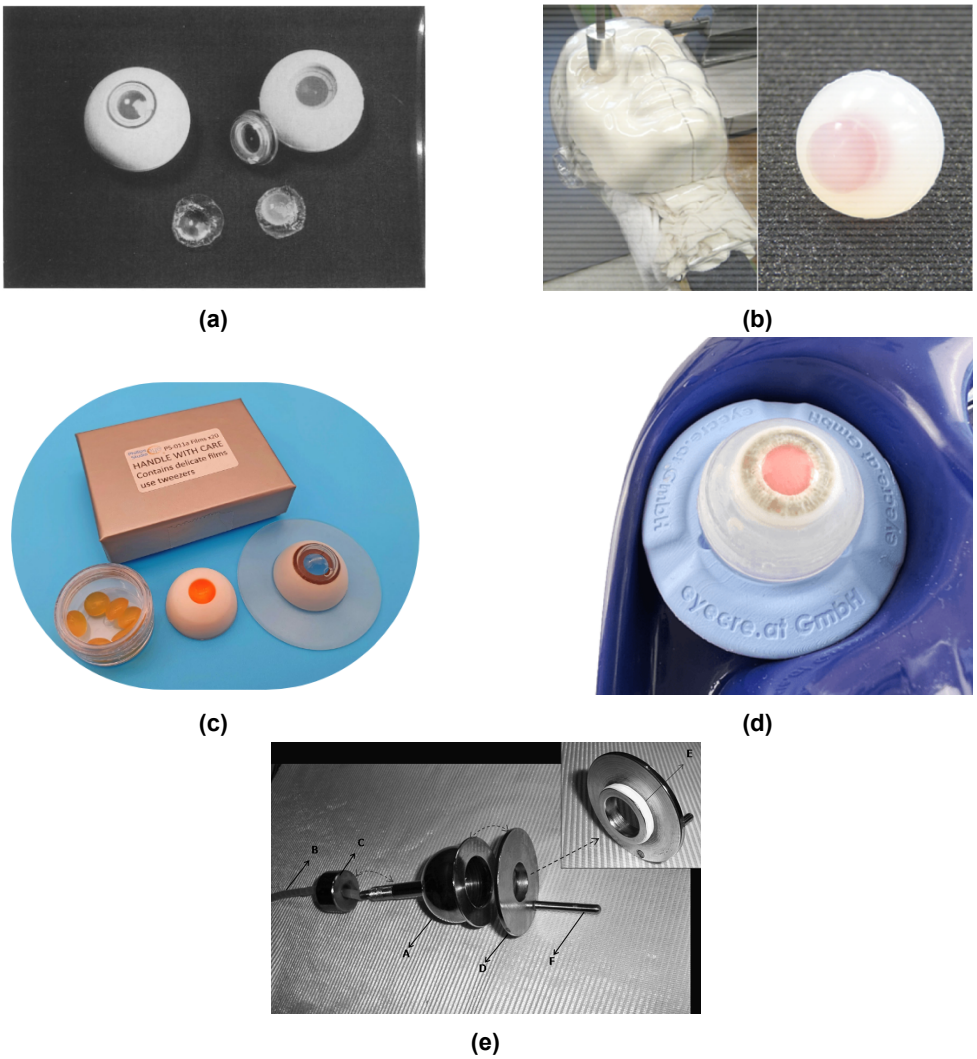

(a) **(b)** **(c)** **(d)** **(e)**

Figure 1.5: Cataract surgery phantoms used in the field- (a) One of the earliest eye phantom for cataract surgery training by Maloney [38], (b) Lab made synthetic gelatinous eye with custom head [42], (c) Cataract training eye made by Phillips studio [39], (d) Single unit cataract surgery training phantom by Eyecre.at GMbH [40] and (e) A globe holder for animal eyes during cataract surgery training [34]

The curriculum for surgery training in the ophthalmology program varies among countries, regions, and even among individual universities. Reforms in the existing curriculum and special lab-based training programs have been held in the past few years to fix these issues [43]. However, the backbone of any such curriculum often follows the guidelines set by the Accreditation Council for Graduate Medical Education (ACGME). This international council lists 6 core competencies that the training program must inculcate – patient care and procedural skills, medical knowledge, system-based practice, practice-based learning and improvement, professionalism, and interpersonal and communication skills [44]. Furthermore, in India, professional organizations such as the All India Ophthalmological Society (AIOS) and the In-

dian Medical Association present various assessment strategies, scoring, goals, and timelines within the whole curriculum [43]. An accredited medical training facility/university is open to forming its curriculum based on these fundamentals.

1.4. Problem description and research goal

The current project is based on the academic study from Kerala in India given by Dr. Thomas Kuriakose. Dr. Thomas is a Senior consultant and the Director of Academics at Giridhar Eye Institute in Kochi, Kerala. He presented the project idea around the training phantoms to help the students get accustomed to the real human eye during their surgical training period. There was a need for a training model that could simulate the free movement of the eyeball in the human head when interacting with surgical tools.

Due to the delicate and highly intricate nature of the surgeries in the eye, any small unregulated movements of the eye may result in moderate to severe complications. To avoid this, the students are trained to gently stabilize the globe using tools such as cotton tips while performing the surgical steps using the other hand. Such a free-moving eye, be it real or phantom, is generally not available as the wetlabs use enucleated eyes fixed firmly on dummy heads either through pins or hollow bulb setups. Such arrangements do not simulate the passive stiffness of the eye in the head when pushed around during surgery. The author consulted with Dr. Thomas if there is any specific step from the cataract surgery training program that could be incorporated to narrow the project down towards cataract surgery training models. The doctor saw the great potential in consolidating the capsulorhexis training course since it not only involves the mentioned stability training but also continuous curvilinear capsulorhexis (CCC) being one of the more difficult and often practiced cataract surgery steps among others. The proposed solution should be low-cost, require minimal maintenance, and be able to be manufactured or prepared very easily so that multiple models can be used in a training environment for all the trainees involved.

Thus, the research goal of the project is as follows: To prepare a cataract surgery training eye phantom for capsulorhexis and globe stability training in a low-cost setting.

1.5. Requirements

The requirements of this project is as follows

1.5.1. Primary Requirements

- The eyeball model should be able to maneuver in all four directions- adduction, abduction, supraduction, and infraduction with restoring tensile forces like that of the human eye as shown in Figure 1.6.
- The eyeball should have a phantom material representing the anterior lens capsular membrane that could be worked on during the capsulorhexis training. The setup needs to be akin to the anatomical arrangement as seen in the human eye.

Explanation:

- During a live surgery, the patient is sedated and is unable to voluntarily move their eyeballs. These motions are induced when any surgical tool meets the eye, especially while interacting with the cornea. This is often observed in the initial training lessons wherein the trainees get used to the precise movement of the tool. Although extorsion and intorsion are possible, this movement is often too little and can be ignored for the proposed model.

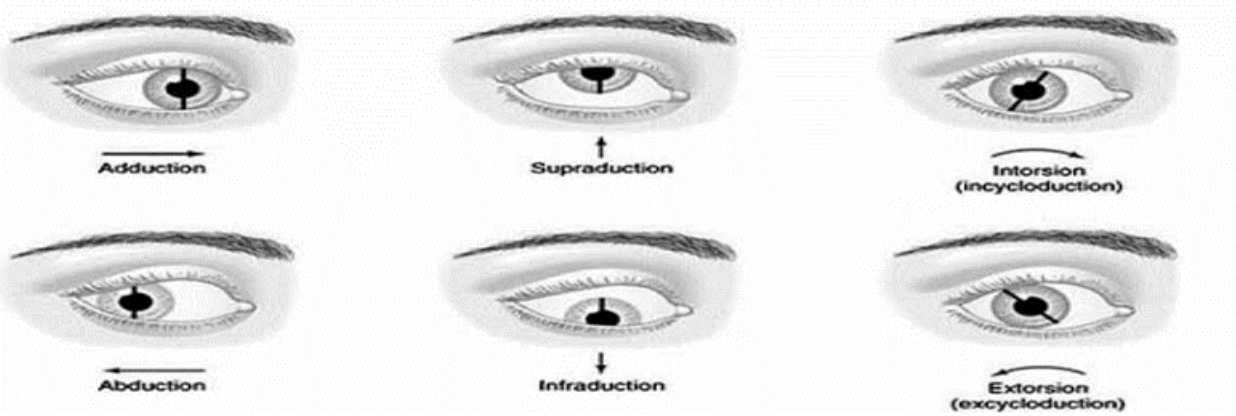

Figure 1.6: Movements of the eye.

- The membrane needs thickness and shear strength like that of the capsular membrane. The distance between the anterior capsular membrane and the corneal element along with the anterior chamber volume should be close to the anatomical distance.

1.5.2. Secondary Requirements

- The model is designed to be able to use multiple times. Since the phantom membrane is meant for single use, the design must incorporate an easy replacement feature.
- It should also be noted that the build and the phantom membrane need to be created/obtained very easily due to technological constraints and low-cost settings.
- The user has the option to either use the model with flexible rotation elements, alter the flexibility or remove this element and fix the eye like a standard setup. This modification needs to be pre-set and not be subjected to manual iterative design or reliant on the user's knowledge of design.

1.6. Thesis outline

The contents of the following chapters are as follows:

- **Human Eye Anatomy**: This chapter provides the anatomical dimensions and properties of the human eye that are necessary in designing the phantom model.
- **Design methodology**: This chapter gives insight into the strategies used to select and design various components of the prototype with 3D modeled images.
- **Materials and preparation**: This chapter lists various materials used to create specific components of the prototype along with material specifications, properties, and preparation guidelines.
- **Experimental setups, protocols, and verification**: This chapter explains in detail the objectives, experimental setups/software, protocols, and expected outcomes. The chapter is divided into 4 major parts- preliminary experiments on certain isolated components, secondary experiment of the whole prototype, clinical evaluation, and validation by training surgeon. The first two experiments are mechanical analyses while the other two are done by medical professionals.
- **Results and discussions**: This chapter contains the findings of the experiments conducted during the research. The results from mechanical analyses are predominantly about the force-displacement and stiffness behavior of the prototype. The chapter also includes a cost analysis for creating a whole prototype. The assessment form and insights

from the surgeons from the clinical trials are described in detail along with the findings of the validating tests conducted by Dr. Thomas. Critical remarks, areas of improvement, and possible ways to assimilate the prototype into the curriculum are summed up in this chapter. A description of meeting the set requirements of the study, the limitations of the current study, and future work marks the end of this chapter.

- **Conclusion**: This short chapter gives an overview of how the project progressed and met the expectations and requirements of the research.

1.7. Thesis model overview

The thesis design is based on the 'V-model' approach, augmented slightly to adhere to this project. Figure 1.7 shows the layout of the approach.

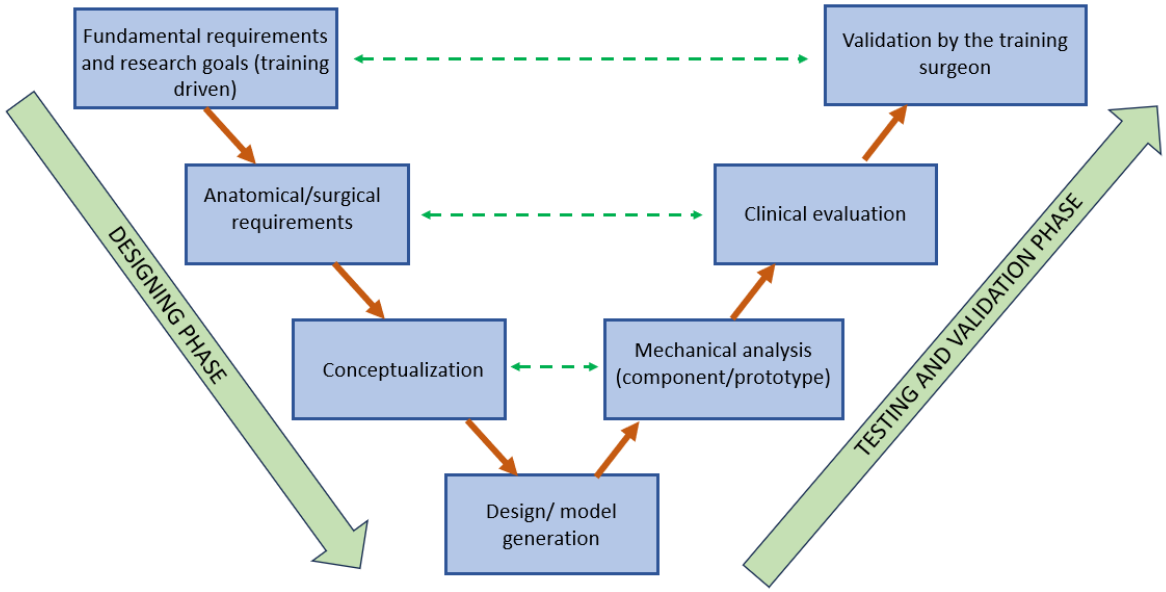

Figure 1.7: V-model approach towards thesis structuring.

2

Human Eye Anatomy

2.1. Eye and optic muscles

The human eyeball is about 24.2 mm (transverse) x 23.7 mm (sagittal) x 22.0-24.8 mm (axial) in size [45]. It sits in the orbit of the skull on a cushion of orbital fat. The eyeball has two sections- the posterior segment behind the posterior lens capsule which makes up the vitreous chamber, retina, macula and optic nerves [46], and the anterior segment made of the lens capsule with lens, zonules, iris and cornea enclosing the anterior chamber containing aqueous humor [47]. Figure 2.1 shows the anatomy of the entire human eye.

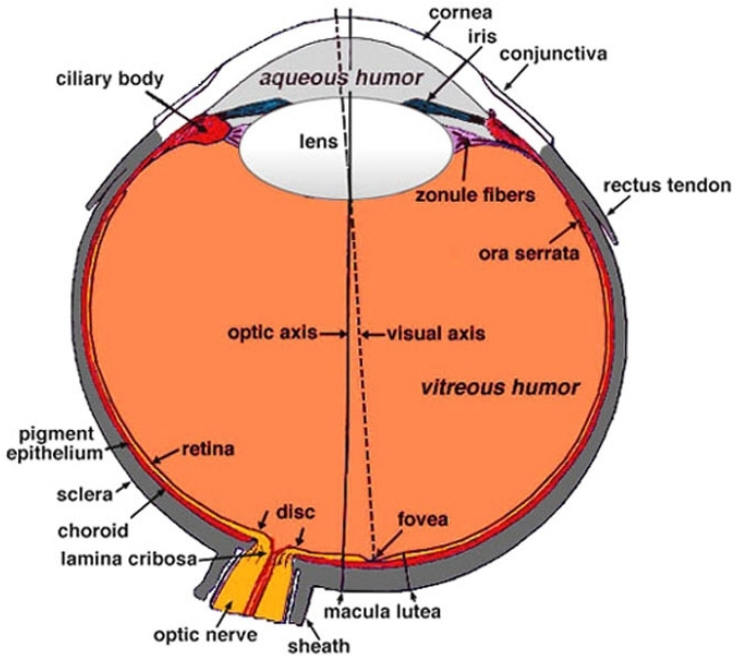

Figure 2.1: Anatomy of the human eye in the sagittal section [48]

The six muscles around the eye globe move the eyeball in various directions as shown in Figure 2.2. The passive spring stiffness in each of the 4 directions of movement (abduction, adduction, infraduction, and supraduction) is about 0.7-1.5 g/deg [49],[50] but can be higher depending upon the individual.

The following sections shall only mention the parts in the anterior segment, especially those that are relevant to the project.

2.2. Cornea and sclera

The sclera is the hard white tissue that forms the outer coat of the eye. Around the visual axis, the cornea forms a dome-shaped structure holding the aqueous chamber over the iris. The circular border between the cornea and the sclera is called the limbus and is often the

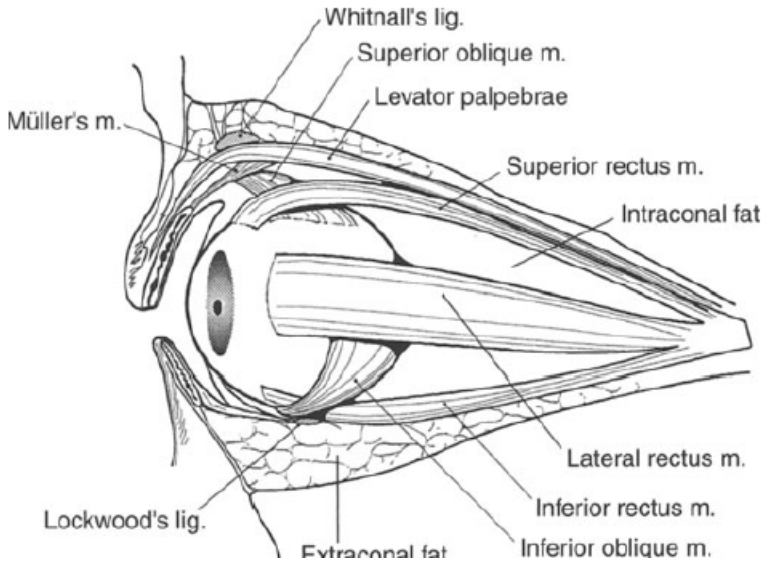

Figure 2.2: Ocular muscles and fat around the eye in the orbit [51]

incision site for cataract and glaucoma surgeries. Unlike the sclera, the cornea is completely transparent as it allows the light to pass through it into the eye. It has a diameter of 11.7 mm with a central and peripheral thickness of about 560 micrometers and 640 micrometers respectively [52]. The cornea exhibits a layered structure made up of about 200 lamellae along with other thinner membranes made of epithelial cells on the periphery. The cornea has a stiffness between 0.068 N/mm to 0.08 N/mm depending on the point of testing [53]. The cornea also has a complex anisotropic viscoelastic property that allows it to act as a mechanotransducer for stress depending on the strain rate [54],[55]. It can self-heal by being able to close the sharp wounds made by sharp and very fine gauge surgical tools over some time [56]. The distance between the posterior surface of the cornea and the anterior capsular membrane is called the anterior chamber depth (ACD) and it is about 3-4 mm [57].

2.3. Iris and pupil

Iris is the colored part of the human eye and is composed of multiple folds of sphincter and dilator muscles that modulate the central opening, called pupil, by contraction and dilation. The outer diameter of the iris is between 12-13 mm with a thickness of 0.2 mm [59]. The maximum and minimum pupil diameters vary between 2 mm in bright light and 8 mm in the dark [60]. During surgery, medications allow the pupils to fully dilate for maximum visual acuity for the surgeon to see into the eye.

2.4. Lens and capsular membrane

The lens is positioned directly beneath the iris along the visual axis. It has an asymmetric biconvex structure with the posterior surface more curved than the anterior surface [61]. The equatorial diameter of the lens is about 6.5 mm at birth and continues to grow at a different rate throughout the teenage years and stays at 9 mm with less than 1 mm change for decades in adult life [62]. The thickness of the lens at its maximum is 4 mm at birth, growing at about 25 micrometers per year until it is about 5.5mm [61]. The volume of the lens is about 160 mm3 in adults [63]. The lens can be divided broadly into two parts- the nucleus and the cortex. Each of these zones is made of concentric layers of lens fibers made of transparent proteins.
The stiffness of the lens cortex and nucleus at the age of 60 years is about $4x10^{-3}$ N/mm2 and

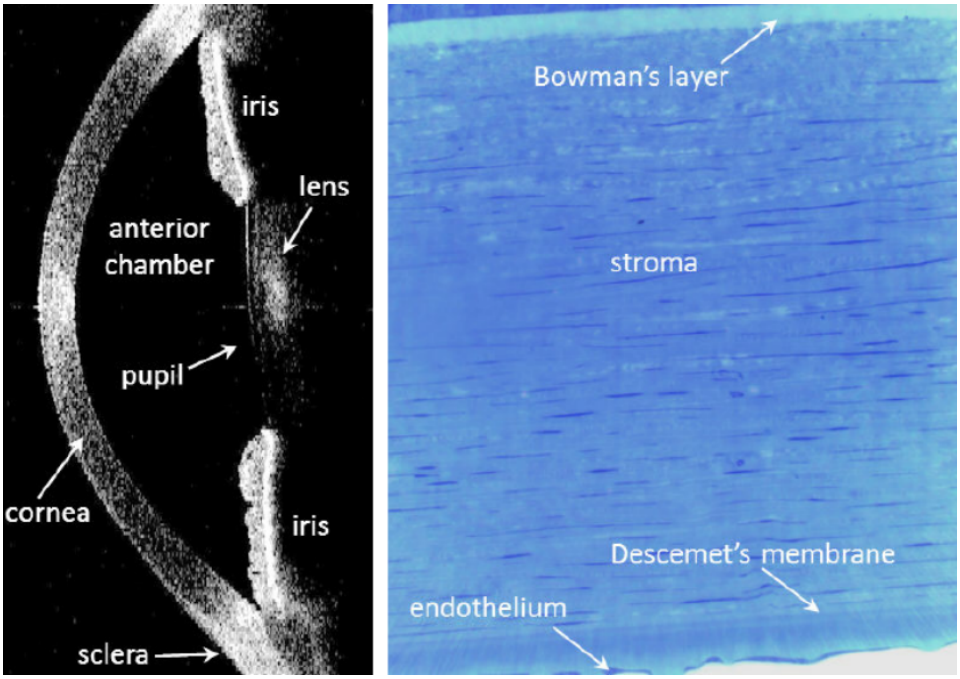

Figure 2.3: Cross section of the corneal structure [58]

$2x10^{-3}$ N/mm2 respectively [64]. The mean hardness, expressed in terms of force required by a medical guillotine to bisect a cataractous lens, is about 0.47 N for grade 1 which increased to 1.89 N for grade 4 [65].

The lens is encapsulated by a bag of capsular membrane. This is the thickest basement membrane in the human body and has a lamellar structure [66]. This capsular membrane tends to grow through the life of the individual, getting thicker on the anterior surface. The thickest region of the membrane is around the anterior pole as it reaches up to 30 micrometers [66],[67] and it is the thinnest at the posterior pole at about 3.5 micrometers [66], [68]. The elastic modulus of the lens capsule is a hundred times greater than the lens material, at about 1.5 N/mm2, and plays the role of a force transmitter to change the shape of the lens. The lens with the capsule is held in its place by a mesh of thin zonules connected to the ciliary bodies as shown in Figure 2.4.

The ciliary muscles contract or relax based on the neural signals and pull the capsule enclosing the lens through the zonules. The membrane experiences an outward force perpendicular to the membrane surface due to the pressure of the lens material and a radially outward force directed towards the equatorial boundaries along the membrane due to the tension of the zonules and ciliary muscles as shown in Figure 2.5. This is relevant during the capsulorhexis as an improper tear in the anterior surface can result in radial tear, a complication that leads to collapse or loss of integrity of the capsular bag.

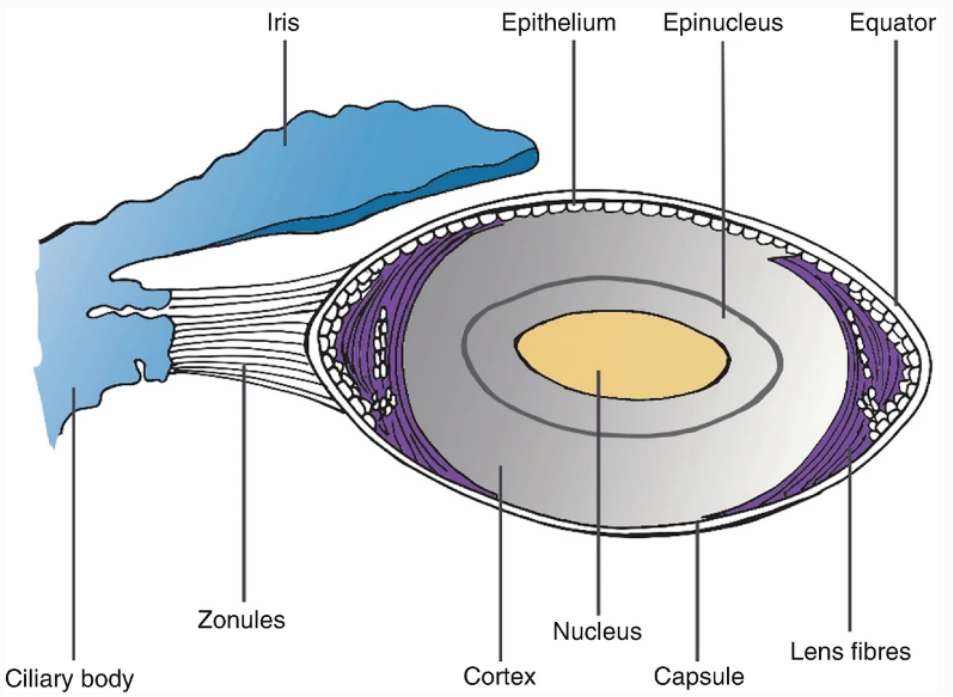

Figure 2.4: Anatomy of lens and associated structures [69]

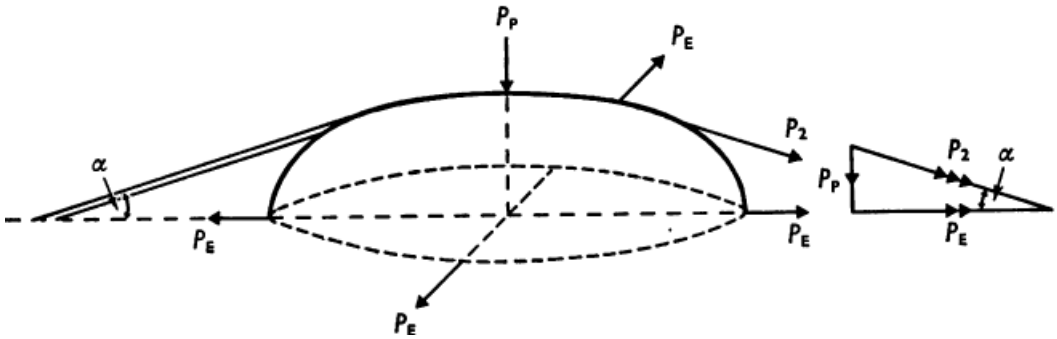

Figure 2.5: Diagram showing the forces on the anterior portion of the lens. P_s = force acting through the zonular fibres, P_p = polar force, P_E = equatorial force, and α = angle of inclination of anterior zonule fibres to lens equator [64]

3

Design methodology

3.1. Strategy

Figure 3.1 shows the overview of the design strategy implemented in the project (part of the V-model approach mentioned in the Introduction chapter). Note that the materials were chosen, tested, and utilized on a part-by-part basis similar to and in tandem with the design process. The methodology extends from this chapter to the 'Major experiment' section of the 'Experimental setups, protocols, and verification' (Chapter 5).

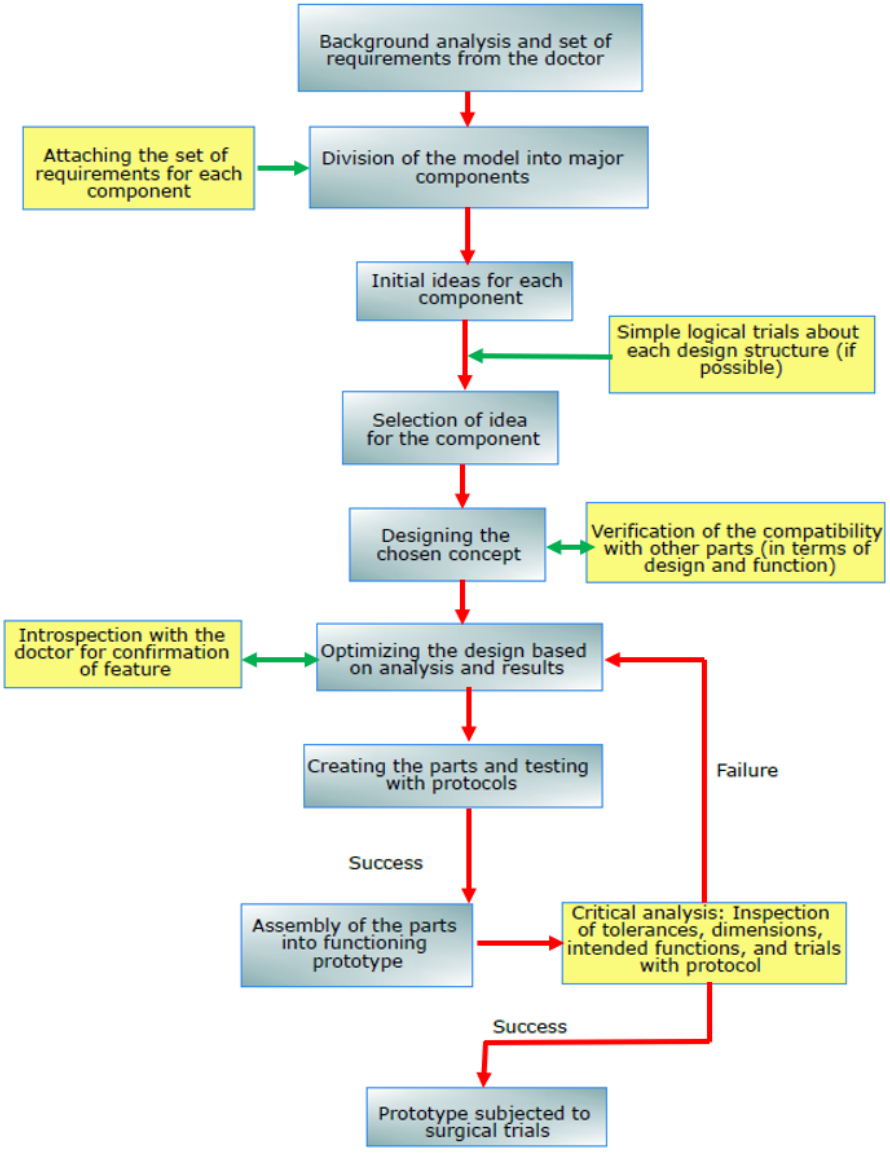

Figure 3.1: Overview of the design strategy

3.2. Design of the rotating eyeball

According to the opinions of the doctor, the trainees need to familiarize themselves with working in the limited volume of the anterior chamber of the eye while also knowing that this eye of the patient is under passive muscular tension of the eye.

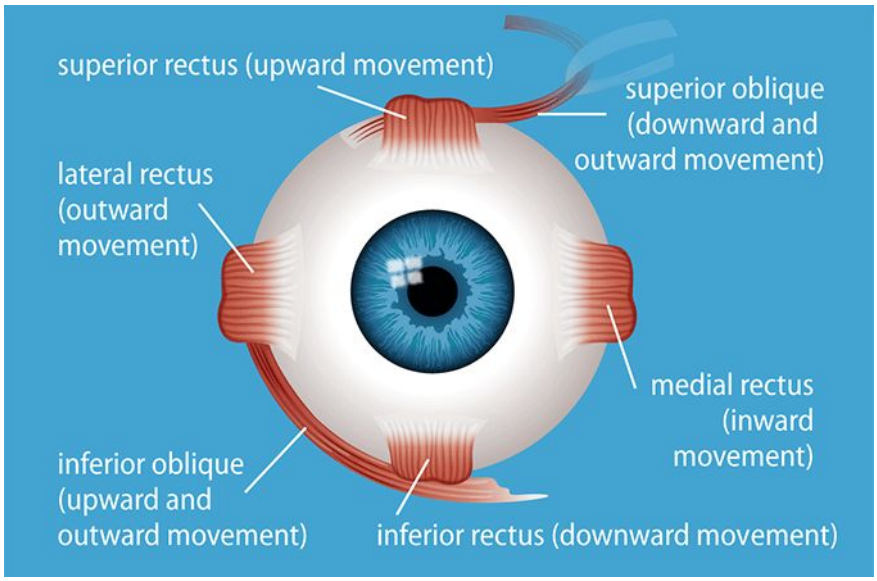

Figure 3.2: Eye muscles and movement directions [70]

In the human eye as seen in Figure 3.2, 4 rectus muscles allow the motion of the eye, each in a particular major direction, and 2 oblique muscles move the eyeball in diagonal directions. There are also intornsion and extorsion which are rotations along the axis passing perpendicular to the plane (z-axis henceforth) of this image. When the patient is sedated, these muscles do not constrict voluntarily and therefore the eyeball is stationary. However, there exists a passive stiffness in each of these muscles which creates tension force when any surgical tool interacts with the eyeball. A skilled surgeon, especially during corneal incision and capsulorhexis, makes minimal induced eye movement with his tools whereas the early-stage trainees often push the eyeball with their tools and need to stabilize it with other tools such as a cotton bud. The eyeball moves back to the initial default position due to the restoring forces due to the passive stiffness of the muscles.

An intact biological eyeball is a typical ball or a spherical joint model inside the eye socket. Therefore, a spherical joint seems to be a better option over a gimbal design since the latter not only adds complexity to the design and movement efficiency (DOFs) but also leads to more instances of unchecked friction at each hinge. Since the project focuses primarily on the anterior section of the eye, designing a hemispherical model makes more sense. Due to this, a ball joint can be incorporated from the inside out (Figure 3.3a) rather than outside in (Figure 3.3b) since the former has lesser frictional resistance due to a relatively larger moment arm while applying external force.

The issue with a hemispherical design is that the inner dome needs to cover less than or equal to half the ball inside to be able to fit in which conversely, also makes the eyeball fall off (Figure X to be added). Therefore, a lower eyeball plate is designed in such a way that while the eyeball is exactly (almost) enclosing the top half of the ball, the lower eyeball plate covers a ring-sized area beneath the eye model and can be attached to the upper half with pins. Such a design makes sure that the eyeball is secure onto the ball and can be detached when nec-

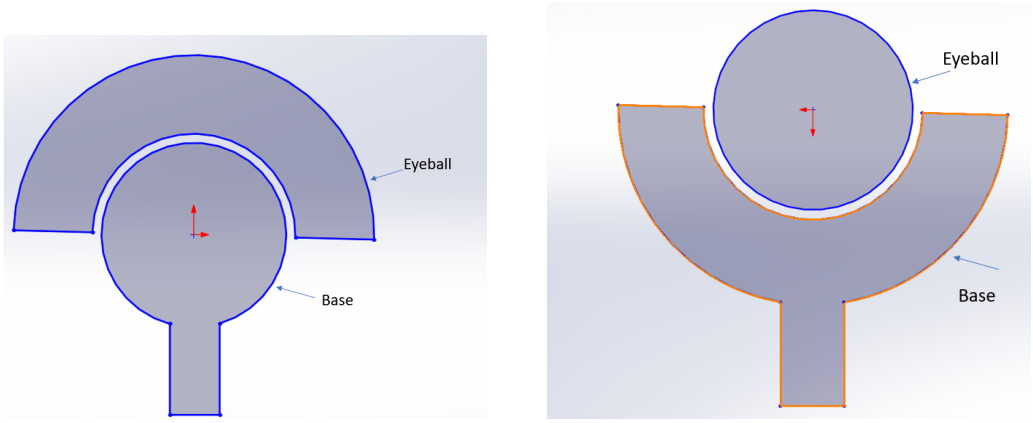

(a) (b)

Figure 3.3: Orientation of half eyeball over the base

essary. Having such an eyeball model has two major benefits:

1. Ease of changing the consumable materials inside the model without damaging the delicate structures.
2. It helps in training the students who find the additional DOFs provided by the model difficult I the initial stages. The eyeball can be removed from the setup and fixed on a more stable/rigid structure.

3.3. Tension Element

3.3.1. Choice of tension elements

The choices of tension elements to be used in the prototype are based on the following key requirements.

Desired stiffness and radial deflection: Anatomically, the effective passive stiffness of the eyeball in any of the four major directions is 0.7 - 1.5 g/deg (Chapter 2), which makes the design inherently delicate. Based on the footage and notes from the surgeons/ medical professors, the desired deflection for which this stiffness is desired is about 10-15 degrees. This is because although the eyeball can freely rotate for 27 degrees in elevation and about 44 degrees in the other three directions [71], the induced movement is often very less. Furthermore, it becomes difficult to maintain a constant spring stiffness over a larger range of motion, especially for delicate structures. Therefore, effective stiffness needs to be designed over this range of motion.

Energy loss: Friction plays a major detrimental role in the model design. The tension element should not only have inherently low friction in its design but also be able to compensate for the friction at other junctions, especially on the spherical surface of the ball joint.

Performance over time and calibration: The tension elements need to be chosen and designed in such a way that their performance remains the same over the model's functional period. Manual calibration is not desirable since the operator/user may not be skilled enough to properly maintain the desired properties. The robustness of the design choice is highly desired as it minimizes the need for calibration.

Design complexity: A tension element of choice can be set up in two different ways which, in action, can perform the same intended motion – pull design and push design. These are shown in Figure 3.4. The choice of the arrangement of the tension element in the prototype

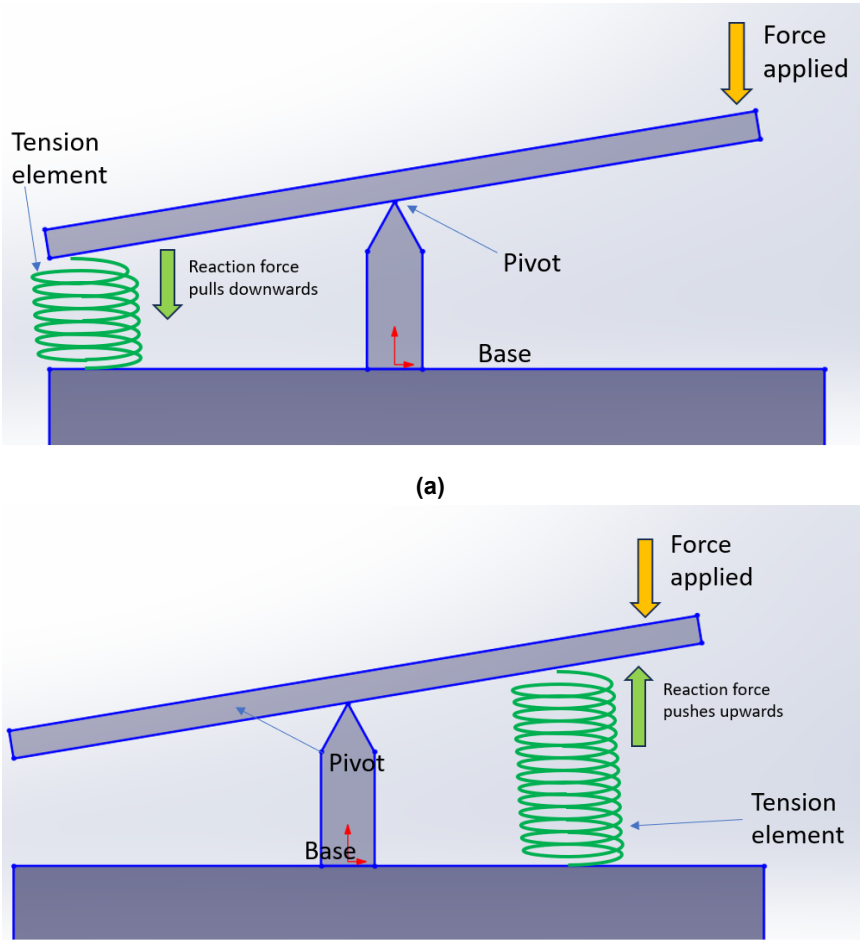

Figure 3.4: (a) Pull-design arrangement of tension element and (b) push-design arrangement of tension element

can be attributed to the other conditions set.

Pretension: The pretension of the elements requires careful design to maintain equilibrium. Due to the delicate design requirements (thickness of components, desired low stiffness, and material choices), pretension should be avoided. Not only does adding pretension create additional complications in calibration, but it also tends to move the eyeball in the restricted direction (z-axis rotations), may induce creep, and generate normal forces leading to more frictional forces.

Design complexity and constraints: All the mechanisms and structures should be below the eyeball structure. Any protrusion of the structures above the eye hemisphere would cause interference with the tools and possible future eyelids and other dummy facial structures of the mount.

Based on these prerequisites, there were 7 different choices of design:

1. Hydraulic
2. Pneumatic
3. Magnetic
4. Linear spring
5. Torsional spring
6. Compliant wire
7. Compliant strip

The selection of the design element is based on the Harris profile as seen in Table 3.1 which compares each choice based on the attribute and scores from 1 (Less suitable) to 3 (more suitable). The design with the highest aggregate score is chosen.

Table 3.1: Harris profile for scoring and choosing the best-suited choice

Requirements / **Design**	Desired flexibility	Energy loss	Stability	Ease of maintenance/ compatibility	Design complexity	Cost per unit	Total (out of 18)
Hydraulic	1	2	2	2	1	1	9
Pneumatic	2	1	2	2	1	1	9
Magnetic	2	3	1	1	2	1	10
Torsional spring	2	2	2	3	2	3	14
Linear spring	2	2	2	3	2	3	14
Compliant wire	3	2	2	3	3	2	15
Compliant strip	3	2	3	3	3	2	16

The desired flexibility of the tension element is very low at around 0.7 - 1.5 g/deg. Hydraulic elements are almost insensitive or may not work at that desired stiffness. Energy losses are predominantly friction along the element and at contact. Pneumatic element also tends to lose energy due to compression of air along with friction in pistons. Lack of stability is measured by the tendency of the element to move the bodies or redirect most of the reaction forces in the restricted direction. The element needs to be compatible with stainless steel or other metallic surgical tools (magnetic element would interfere due to proximity) while also being easy to clean and set up. The design should be simple enough while also being foolproof. The cost to produce or purchase one unit must be cheap. Based on the total score obtained, the compliant strip design is chosen.

3.3.2. Design of the tension elements

The design of the compliant strip (referred as tension element from now on) is based on the following parameters:

Positioning of the elements: Among the two configurations of the element concerning the structure as shown in Figure 3.5a and 3.5b, the former is less space-consuming but for the project, it is difficult to run trials and make replacements. Although it has not been tested, the single-point contact of the element on the lower eyeball plate may turn to a multi-point contact after a certain deflection point. Therefore, Figure 3.5b is adopted for the prototype.

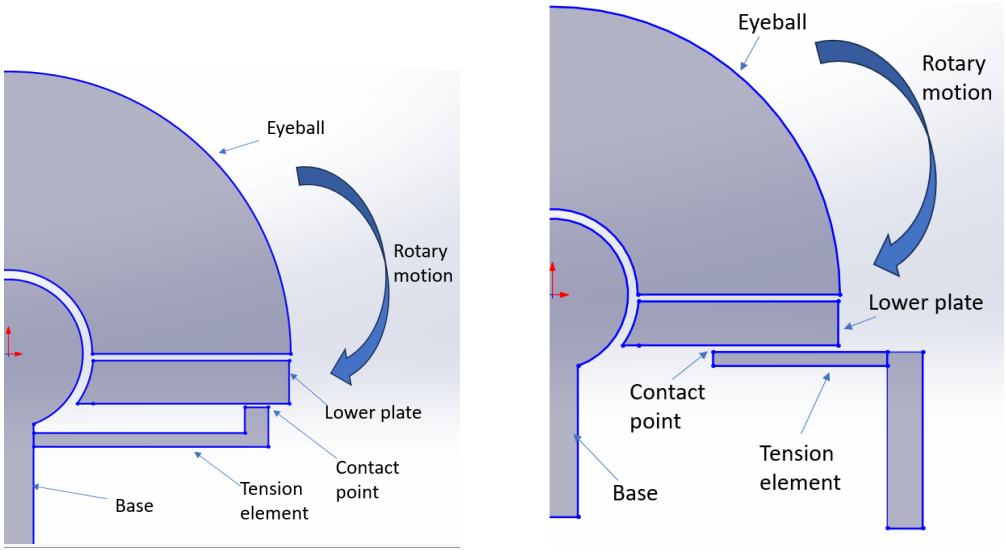

Figure 3.5: Possible orientations of the tension elements

Number of elements: Since there are 4 major directions of movement in the eye, the number is elements in the design is restricted to 4. Each additional direction, which is a vector sum of two major directions, is managed by a parallel spring system.

Restriction of the rotation of the eyeball along the Z-axis: The width of a cantilever beam is the critical parameter that restricts the sideways movement. Therefore, the width of the element needs to be such that it offers the most resistance while not increasing the stiffness in the downward direction. The point of contact/attachment also needs to be designed to restrict sideways motion.

Categorization of the motion: The motion of the eyeball and the attached lower eyeball plate follows an arc pattern as shown in Figure 3.6a. The allowable range of the motion is about 20-25 degrees from the horizontal. The circular motion of the lower eyeball plate can be categorized into three parts – a moment or twist, linear downward, and linear inward, as shown in Figure 3.6b.

The tension element can either take consider the deflection due in all these three modes, resulting in a larger restoring force, or choose one of the motions while ignoring the other two modes. In the preliminary phase, both choices were chosen and tested.

Selection of the element design: Tension element 1 (‘T1’ for short) was designed to consider all three modes of deflection. Its design was improved from the failed basic design ‘T0’ (Figure 3.7a) and was based on the curved profile of an archery bow, shown in Figure 3.7b. Since it needs to be secured on the lower eyeball plate to deform in all modes, a pin profile was made at this contact point. This would reduce the effective spring stiffness of the system (when tilted in a major direction) to two times a single element rather than a combination of all four elements, two of which need to twist. A single proposed design was made and tested. Even without considering the entire system, the stiffness of bending an isolated element far exceeded the stiffness desired. Therefore, this category of design consideration was not selected.

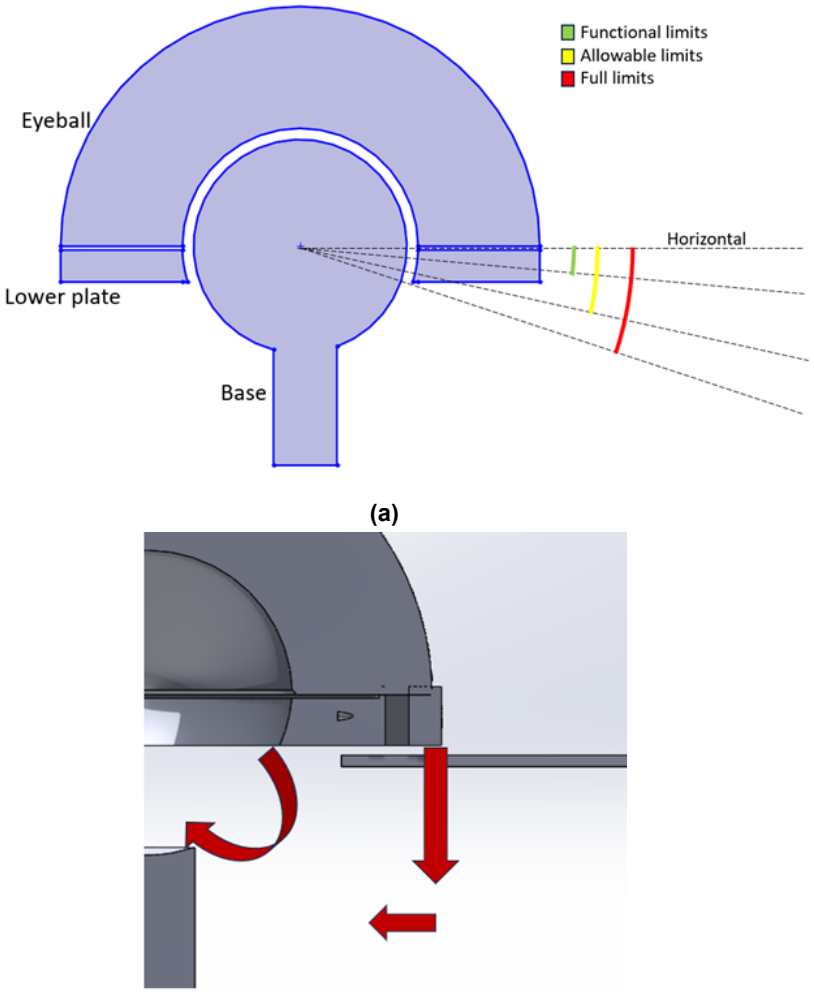

Figure 3.6: (a) Possible limits of motion and (b) Simplification of motions at the joint and contact surfaces

Tension element 2 (‘T2’ for short) was designed considering only the downward movement of the eyeball and lower eyeball plate being monitored while freely allowing the twist component of the eyeball motion. The linear inward movement is very small compared to the linear downward movement in the functional range, therefore this motion is also allowed to be free. The resulting design was a simple cantilever beam with a width wide enough to restrict sideways motion as shown in Figure 3.7c. Each of the four elements is just in contact with the lower eyeball plate without any pretension. The lower eyeball plate has ridges along which the tension element can move. The contact surfaces of this lower eyeball plate and the tension element must be very smooth to reduce friction during the free inward movement. While bending the setup in a major direction, only the spring directly under it comes into play, therefore the resulting effective stiffness is far less than the system with four T1 elements. The effective stiffness in additional direction, in theory, has an effective stiffness twice that of a single element due to the two-parallel spring system. Thus, design T2 is selected for the prototype.

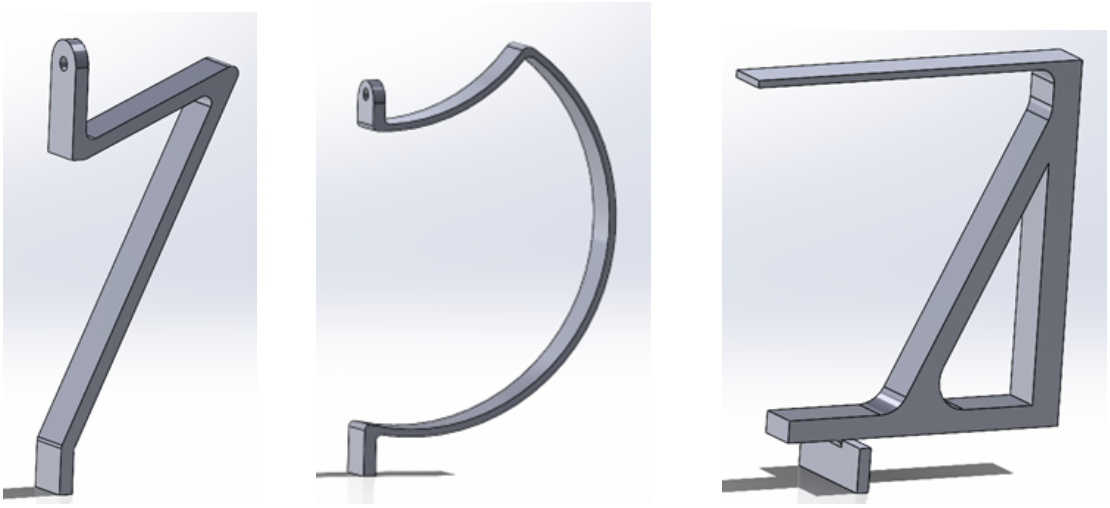

(a) (b) (c)

Figure 3.7: (a) T0 basic design, (b) T1 design, and (c) T2 design (selected)

Primary dimension of the element: The compliant strip design chosen has a simple rectangular strip of a certain thickness. This thickness is the most important dimension of the design due to many reasons-

1. It is the critical dimension in the direction in which the force is applied, and the element is most likely to fail.
2. Compared to the width, the thickness has the smallest value but has the most relevant role in the stiffness of the element, alongside the length of the element.
3. The lower the thickness, the lesser the stiffness, and this thickness of the element depends on the choice of the manufacturing method.

The stiffness of a cantilever beam design for a point load is given by k = 3.E.I/L^3 wherein 'E' is Young's modulus of the material, 'I' is the moment of inertia which for a rectangular cross-section is I=(b.h^3)/12 with 'b' being the width, 'h' as thickness and 'L' as the length of the beam. The width is set to 2.5 mm to avoid Z-axis clatter and the length to 25 mm to be within the workable volume range.

However, this formula is only for small deflections and assumes linear mechanics, which may not be suitable for our tension elements. The non-linearity arises from both the large functional range of motion of about 15-20 degrees as well as the material being used. The manufacturer of the 3D printing material had specified that the hardened 3D printed resin used in this project has the drawback of not having a consistent mechanical behavior profile which could be due to inherent material properties as well as the printing specifications.

Rather than theoretically determining the material behavior, a simpler technique was used. First, the thinnest possible strip was printed with the mentioned values of width and length. This thickness was advised to be 0.5 mm by the lab technicians since anything thinner would fail to be printed. Primary tests were carried out as mentioned in Chapter 5 to find its stiffness in g/deg and compare it with the necessary range. Assuming the stiffness 'k' is highly influenced by the thickness 'h' (i.e. stiffness, k α h^n where n is some rational number), the thickness was doubled, and the stiffness was checked again. Upon checking, the overshoot of stiffness of 1 mm thick strip was slightly small, therefore based on trial and error or deduction of 0.05 mm each time and checking, the thickness of 0.85 mm tension element gave us the stiffness value

within the range we needed it to be in. Note: In this report, this part is being called ’compliant strip’, ’compliant arm’, ’flexible element’, and ’tension element’- all being the same names that can be used interchangeably.

3.4. Lower eyeball plate

The primary function of the lower eyeball plate is to hold the eyeball over the steel ball so that the former can move over the latter. This is done using a 2-pin design on the top of this piece which fits into two of the four circular slots in the eyeball. It also comes in contact with the tension element and works as an extension of the eyeball piece. Based on the initial basic evaluation followed by the choice of tension element design, the slits to hold the arched tension element is replaced by 4-way ridges on which the tension element would slide. The ridges would prevent the Z-axis rotation. The height of the ridges is such that it prevents the tension element from being dislocated under extreme motion. The contact surfaces are smooth to reduce friction. Figure 3.8 show the new and old designs of the component.

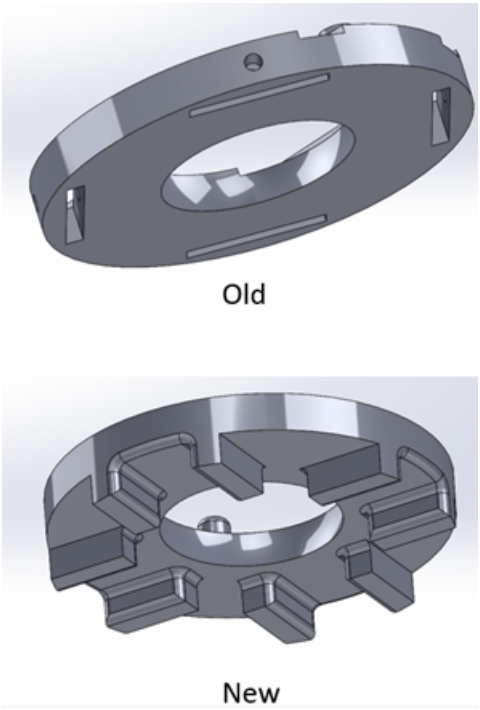

Figure 3.8: lower eyeball plates

3.5. Eyeball piece

The eyeball piece is designed based on the anatomical dimensions- a diameter of 24 mm. It is a solid hemisphere with a flat surface underneath having 4 small pinholes and a larger central hemispherical groove to fit on the lower eyeball plate and the 12 mm steel ball respectively. The upper surface of the hemisphere has a stepped circular groove feature, with the other diameter being about 13 mm. When the cornea piece, lens, and membrane are fitted on the grooves and locked in the notches, the anterior chamber is recreated within the cornea piece with similar anatomical values. The notch feature is a newer feature added after the surgical trials to the pre-existing ‘slot’ in the eyeball. Figure 3.9 a, b, c, and d show the design of the eyeball pieces.

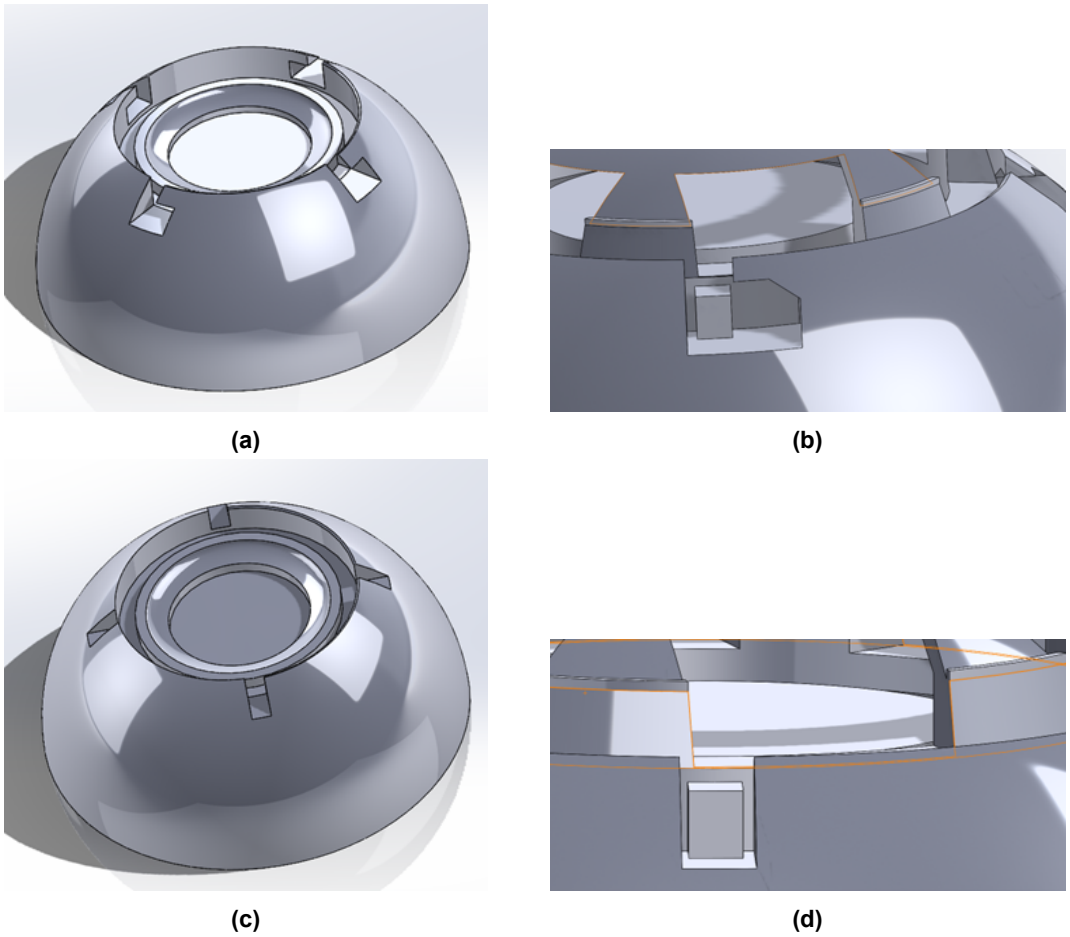

Figure 3.9: (a) Eyeball with notch feature, (b) close-up of notch connection, (c) eyeball with slot feature, and (d) close-up of slot connection

3.6. Corneal piece and anterior chamber

The anterior chamber is the space of focus of the prototype where the tools are being used by the trainees. The sharp scalpel-like tool called the keratome is used to make a small cut on the cornea near the limbus, a ring-like visual structure on the outer edge of the cornea. This interaction and the further movement of the micro forceps through this cut leads to the movement of the eyeball, commonly seen by the unsteady hands of the inexperienced trainees. Therefore, the design of the prototype needs to incorporate this interactive design.

One of the most important design aspects of the cornea design is the size- the volume enclosed by the cornea and the resulting anterior chamber needs to be as identical to that of a human eye as possible. The artificial cornea structure also needs to be transparent so that everything is visible from the top to the surgeon. The pupils are always dilated during a real surgery, so they are not necessary to be made in the proposed model. Based on these requirements, the options were either to use something off the shelf that has the necessary features or to create something using chemical mixtures such as transparent plastic or silicone. Based on the detailed analysis mentioned in Chapter 4, a soft lens is cut to the desired shape. The cornea piece is an attachment that goes on the top of the eyeball piece, in the specially designed ridge. It has a dome ring with a wide circular opening at the top held by a few thin columns with windows in between them. The dome ring is primarily to support the lens which is placed on top of it and the windows are opening through which the keratome and other instruments can enter

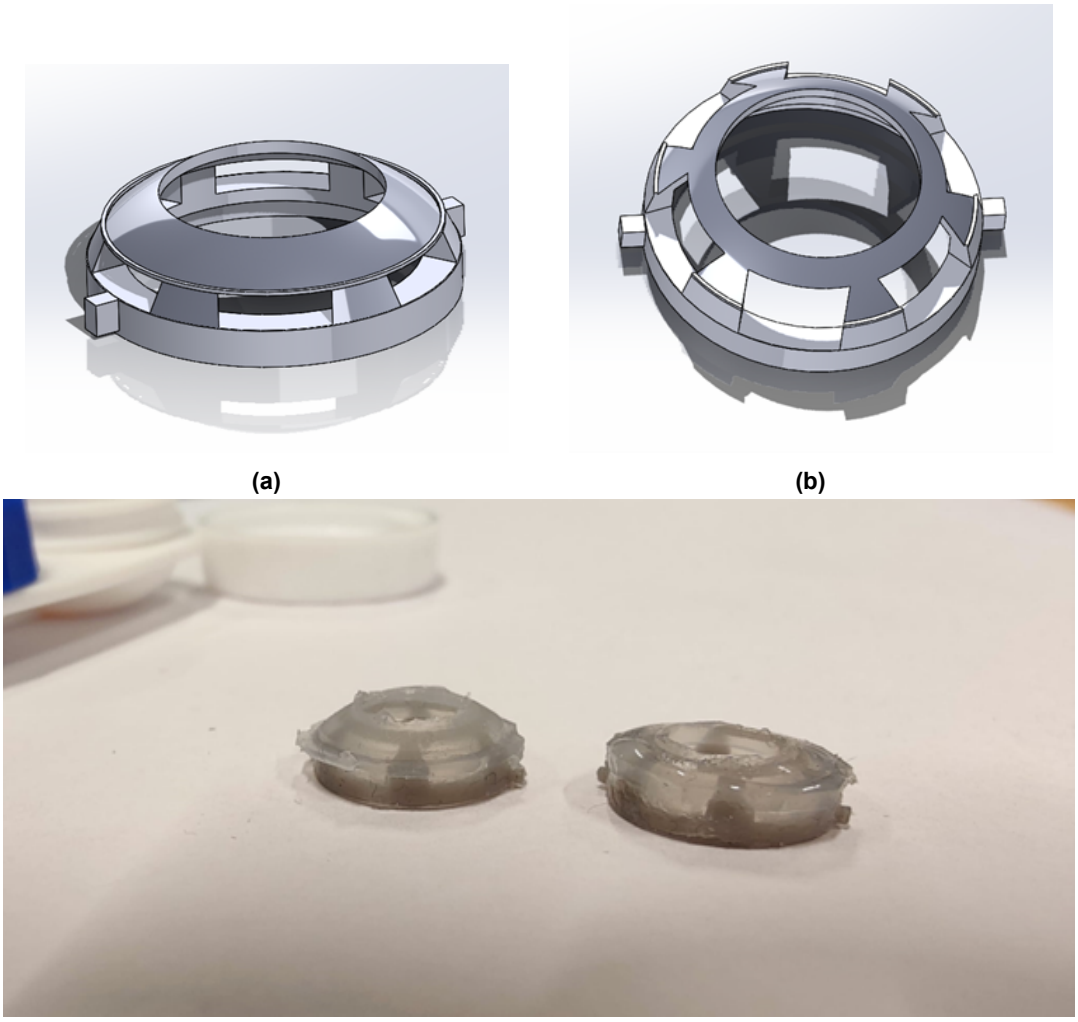

Figure 3.10: Versions of corneal pieces - (a) older version, (b) newer version, and (c) corneal pieces (newer version) with silicone membrane around it

the anterior chamber. When placed accurately, these windows align exactly at the location where the keratome is used in a real human eye during surgery. The number of windows and their sizes can be varied as long as the dome ring can be securely held. The entire piece is coated with silicone to replicate the incision of the cornea as well as be the contact point which when interacted with, pushes the eyeball about the tension elements. Figure 3.10 shows the old and the new design versions of the component.

The lens and capsular membrane bag around it are replaced by a hydrogel slice and eggshell membrane. These two are kept on the raised platform in the circular ridge on the top of the eyeball piece. The membrane needs to be held under tension without any wrinkles, even during the capsulorhexis activities. The friction between the membrane and the cornea piece held by the notch of the eyeball piece and the downward force by the cap should provide enough grip to hold the membrane under tension.

3.7. Tolerances and fixtures

The tolerance for the flat surfaces coming in contact with each other and lock is about 0.05-0.07 mm. This is visible between the base-tension element and corneal cap–eyeball notch contacts.

The tolerance between two concentric circular contacts is 0.1 (diametrically). This is visible between contacts between the spherical steel ball-eyeball-lower eyeball plate, pins between the eyeball-lower eyeball plate, and the circular ring of corneal piece-eyeball contacts. These contacts were determined by trial and error while exploring the usage of lubricants, adhesives, and filler materials between the fixture surfaces. Compliant features were tried and tested but were not achievable due to their delicate structures and sizes.

Permanent fixtures: The steel ball is fixed to the central pillar of the base piece and is never moved. Therefore, it is fixed with superglue. This fixture process needs to be done with caution to not spread the superglue over the top surface of the steel ball as it might hinder the movement of the eyeball.

Temporary fixtures: The prototype allows the user to use tension elements of different stiffnesses according to their need. The contact between the tension elements and the slots in the base is temporary and is generally held firmly in place using a filler such as thin paper.

The corneal piece and the eyeball are held together with a pin-notch setup. The capsular membrane also acts as a filler material which further reduces the space (tolerance) between the pieces so that pieces are held firmly. Before the notch feature was introduced, cyanoacrylate glue was used to hold the corneal piece along with the membrane within the straight slot of the eyeball. This glue does not harden as quickly as the superglue as it takes about 60-75 minutes to harden in damp surroundings. The high viscosity and the stickiness of the glue were responsible for filling in the thin gaps and prevented the pieces from falling off rather than the hardening property. This allowed the user to install the pieces at least 30 minutes in advance before the trials began and clean the pieces after the trials within the time window.

The pin contacts between the eyeball and the lower eyeball plate can either be permanent or temporary depending upon the usage. Although there is no practical need to separate these pieces while performing different trials, the user might be interested in using the base-tension elements-steel ball-lower eyeball plate arrangement as a flexible stand that can hold different attachable eyeball models. Both cases were considered while designing the pieces. A super glue would ensure a permanent fixture and a small paper filler would provide a more temporary fix. Cyanoacrylate glue is not recommended for temporary fixtures as the residue might harden and damage or block the pin-slot provision over time.

3.8. Full model overview

Figures 3.11a and 3.11b shows the exploded and assembled views of the prototype. The whole prototype fits into a cylinder of 70 mm and a height of 50 mm. It weighs about 60 grams. Figures 3.12a, 3.12b, and 3.12c show the prototype in use.

Note: All the major dimensions of the parts can be found in Appendix B.

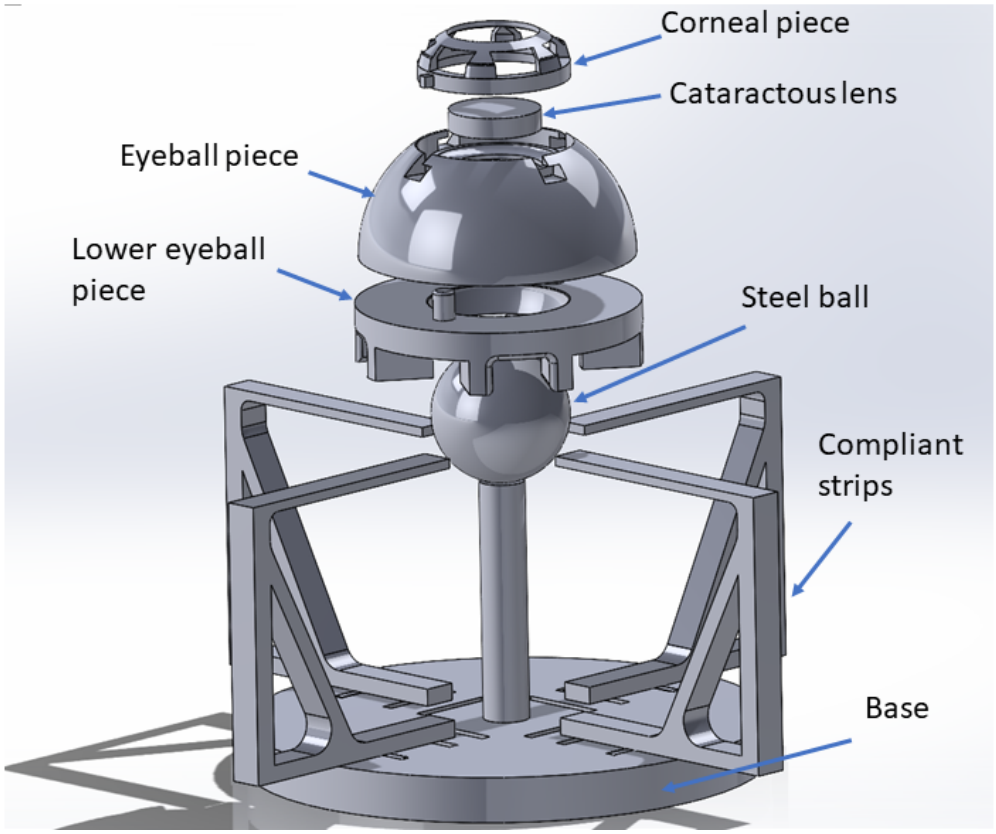

(a)

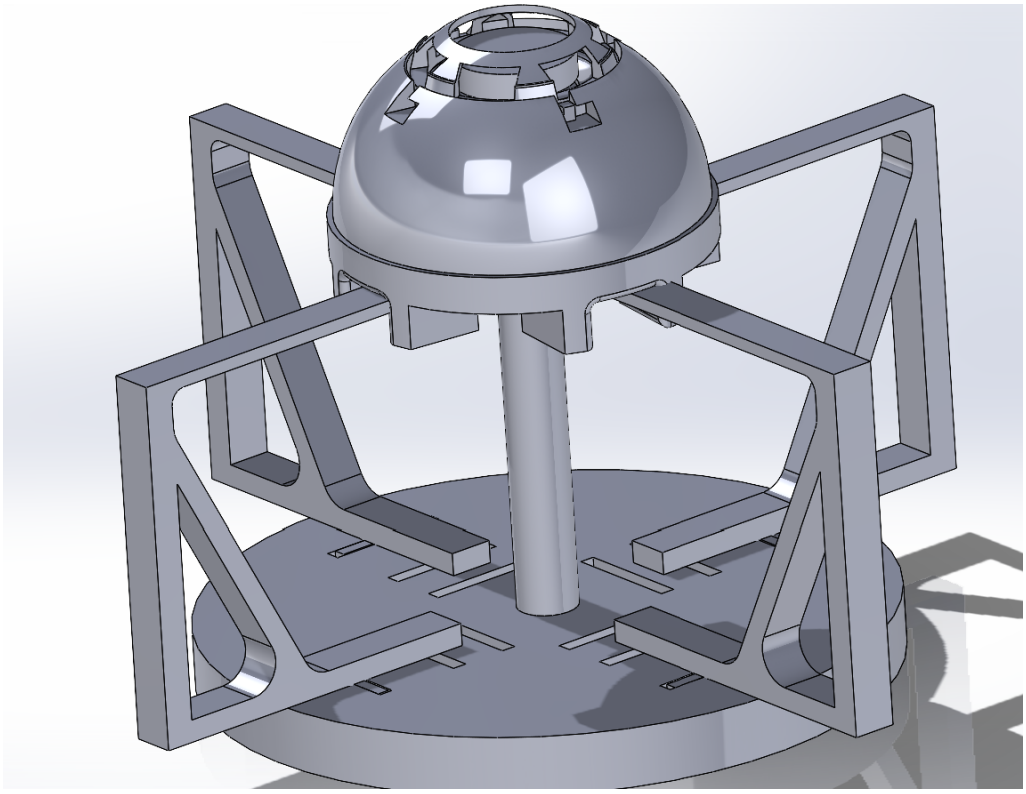

(b)

Figure 3.11: Full model views of the prototype.

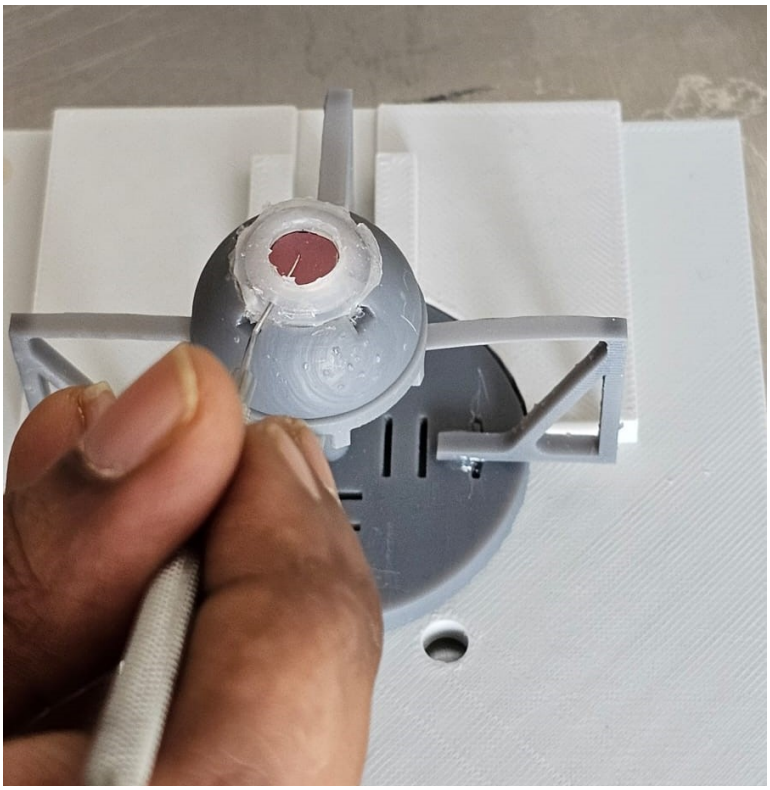

(a)

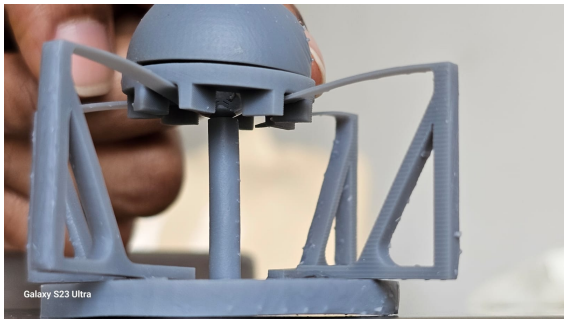

(b)

(c)

Figure 3.12: Prototype images (a) incision check (without any liquids or contact lens), (b) side view, and (c) close-up view over complete corneal chamber with plastic film instead of eggshell membrane

.

4

Materials and preparation

The choice of the materials for specific components of the model depends on several factors as listed below:

1. *Properties:* All the materials chosen must have almost the same material properties as that of the tissue in the human eye or when used as a component, give the desired response.

2. *Availability/resource management:* The chosen material should not be too difficult to obtain in the setting being used. This is particularly important since it is difficult to get certain materials in LMICs due to the availability or the high cost of purchase, especially if they are under the 'consumables' type. This often rules out materials that have the exact properties required as they cannot be used practically due to cost/ availability.

3. *Method of preparation:* Since the intended purpose is in a medical facility, the method of preparation must either be simple or be made using existing machines in the laboratory. Components that use simpler materials but need to be prepared using specific highly sophisticated machines are not desired. Off-the-shelf materials are deemed to be better due to their standard properties and relative ease of use with little preparation.

Assumption: Most of the parts are done on a 3D printer and it is assumed that the 3D printer is used in the medical facility. The 3D printer used for this prototype is Formlabs Printer because of the dimensions of the smaller parts being used. This 3D printer is not commonly used currently in medical universities, especially in the LMICs but based on the technological advancements and use of other additive manufacturing research in the medical domain, this type of printer may be fruitful in the years to come.

4.1. Structural components

Most of the structural components and the molds for the corneal structure are made on Formlabs 3D printer using the Draft resin [72]. It is the most common and standard resin used by the printer. Its material specification is listed in Table 4.1.

Table 4.1: 3D printing material properties

Property	**Value**
Ultimate tensile strength	52 MPa
Tensile modulus	2.3 GPa
Flexural modulus	2.3 GPa
Elongation	4%

One of the listed disadvantages of using this material is the slight unreliability of the specific mechanical properties [73]. This is especially crucial to consider while making the tension elements of the desired shape since the final component might have a small deviation from the theoretical value. The surface quality of printed components was also checked and found to be within acceptable range with little friction. The printing specification is as given in Table 4.2.

Table 4.2: 3D printing specifications

Specification	**Value**
Software and version	PreForm version 3.32.0
Layer thickness	0.05 mm
Print setting	Default
Supports	Yes
Post curing setting	Full post-cure
Post cure time	60 minutes
Post cure temperature	60 degrees C

4.2. Ball joint

The ball joint attached to the base is a standard stainless-steel ball-bearing of 12 mm diameter. Since there are no large magnitudes of normal reaction forces in the joint, the exact material of the ball bearing does not matter if the surface is smooth.

4.3. Corneal tissue

The 3D-printed corneal piece needs to be coated with a membrane that can interact with the surgical tools at the user's disposal while training on the prototype. The incision and the movement of the tools happen across the corneal membrane. The trainee must be able to feel the same resistance provided by a real cornea while working on the prototype. PMMA [74] and silicone are the most commonly used artificial cornea substitutes for experimental studies. Although PMMA is transparent and may have sufficient structural strength to not need the underlying 3D-printed corneal piece for rigid support, the manufacturing process for small parts with tight tolerances is difficult. Silicone membranes are easier to mold into smaller and thinner shapes. They are also hydrophobic and have low surface tension when in contact with water. This combined with its self-closure tendency (for small clean cuts) helps to replicate the self-sealing nature of a real cornea and prevents water spillage from surgical puncture sites. These sites are also very easy to repair by adding a tiny amount of silicone resin on it and curing it. Figure 3.10c (Chapter 3) shows the membrane over the corneal piece.

For the prototype, PlatSil Gel-00 from Polytek Development Corp. is used. The reason for using this specific silicone over other varieties is its ability to be moldable into thin membranes without any deformities or tears. The material properties are as shown in table 4.3 [75].

The membrane is translucent after curing. Therefore, a view window is made at the top of the dome ring for visibility.

4.4. Corneal cover

In a real human eye, the entire cornea is transparent. During the surgery, the microscope is facing directly into the eye from the top and the view window to look at the cataractous lens is as big as the dilated pupil. Ideally, the corneal membrane in the prototype is supposed to be

Table 4.3: Materials properties of the silicone resin

Specification	Value
Mix Ratio by Volume	1A:1B
Pour time	6 minutes
Demold time	30 minutes
Cured Color	Milky white
Viscosity	22,000 cP
Elongation	1.275%
Tensile strength	154 psi
Die B tear strength	56 pli

completely transparent, which is not the case with the silicone used as the part is translucent when ejected from the mold. Since all the surgical tool interactions take place through the windows beneath the dome ring, a clear dome-like section can attached at the top of this structure for visibility. The size of this opening should be at least as big as the pupillary dilation, which is about 8 mm [60]. There was a choice of either using some products off the shelf or choosing a specific material and preparing it in a particular shape. Based on the talks with experts in the field of materials, specifically plastics, and silicone, it was found that a transparent component with the required dimensions without aberrations, bubbles, or defects is very difficult to consistently make using regular setups. Therefore, the focus was directed towards finding the component in the common market or the medical facility. A hard contact lens was found to be very suitable for this purpose due to its exact shape and optical clarity. However, it has not been used in the current prototype because it is difficult to obtain, especially without a prescription and an appointment with the optician even for a default lens and it is quite expensive per pair. The next alternative was a soft contact lens which was available very easily and inexpensive. The contact lens used in the prototype is a daily contact lens bought from a local store. The exact power of the lens does not matter for its purpose in the prototype.

The soft contact lens off the shelf has two major problems. Although it has the right height, the base diameter of the lens was 13.4 mm, slightly higher than the anatomical value on which the holder was designed. Therefore, the lens needs to be cut carefully into the shape desired using a cutting tool (See appendix). The second problem was that the lens was too weak to retain its dome shape when placed on the corneal piece for an extended time, as shown in Figures 4.1a and 4.1b. Even when the prototype is fully assembled and the anterior chamber filled with water, the contact lens placed over the circular orifice would flip outwards. Gluing the lens to the corneal piece does not alleviate the trouble either. This problem was ascertained to be because of the water-air surface disparity between the two lens surfaces. Similar observations were made when the anterior chamber was filled with saline solution while the outer surface was exposed to air or water drops. This is determined to be due to diffusion along with unequal stretching of the lens- the surface in contact with low concentration solution (or water between air-water separation) tends to expand more than the other side and hence the lens dome flips. This issue can be solved by using the same liquid used in the anterior chamber to wet the lens from the outside drop by drop every 2 minutes or so to keep the surface hydrated.

4.5. Capsular membrane

The anatomical capsular membrane covering the lens is held in the eye by the zonules and ciliary muscles. In the prototype, the membrane must be stretched without premature tears or

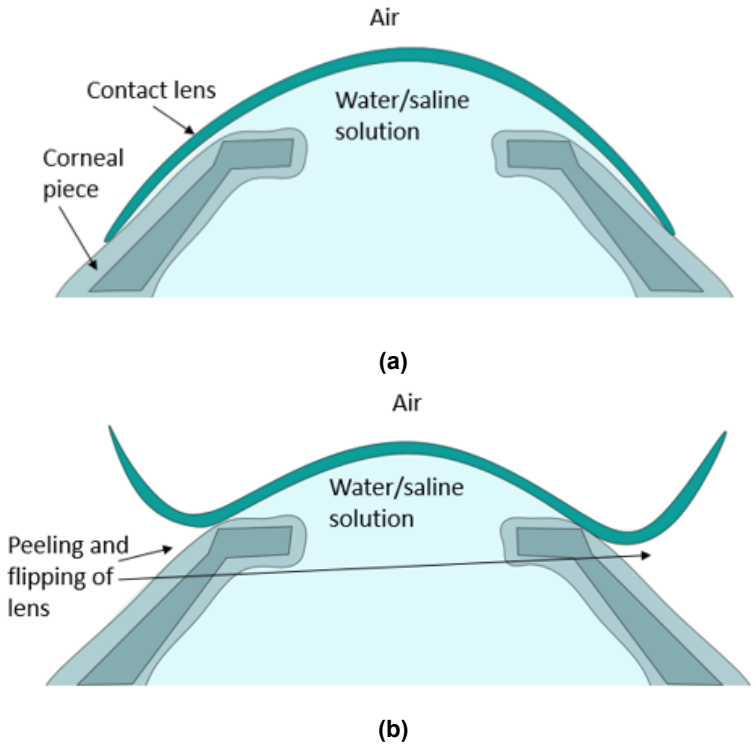

Figure 4.1: Contact lens peeling and flipping.

wrinkles as shown in Figure 2. There are very few works of literature that discuss the use of phantom capsular membrane materials in phantom eye projects. Almost all the materials and chemicals the authors mention are chosen based on the setup-specific thin-film manufacturing methods such as physical/chemical vapor deposition and spin coating. While the membranes they replicated using these methods and materials are of high quality, both in terms of comparable thickness and tear strength, there are several reasons why they were not used in this project. Firstly, the setups required for making these membranes may not be available in a medical teaching facility in LMICs. Secondly, the capsular membrane to be used in this prototype is the only part that needs to be replaced after every trial (in case of severe failure, the hydrogel lens may need to be replaced too, but not too often). Therefore, problems associated with material cost and availability might cause issues.

Alternatively, an off-the-rack choice of membrane material is more suited for this component- something that is thin (in the range of 20 - 40 microns), has similar tensile properties, and tears in a similar manner when operated on by surgical instruments. Plastic films had the right thickness but were too tough and stretchy since they were manufactured to not tear easily. Eggshell membranes have been widely discussed to be used for imitating the peeling of the internal limiting membrane (ILM) during vitreoretinal surgery. A study in 2023 [76] showed the usage of eggshell membranes having properties similar to the anterior capsular membrane in the human eye. This is supported by another study [77] which claims that the surgeons also agreed that this membrane can be used to train both anterior eye capsulorhexis as well as ILM peeling in the posterior eye. Dr. Thomas (collaborator) and Dr. Efe (surgeon for surgical trial) also supported this claim. Therefore eggshell membrane was chosen to be used to imitate the anterior capsular membrane in this project.

A small hole is made in the raw egg from the side and the contents are removed, leaving out the shell with its internal membrane intact. The shell is then kept in boiling water for about 1

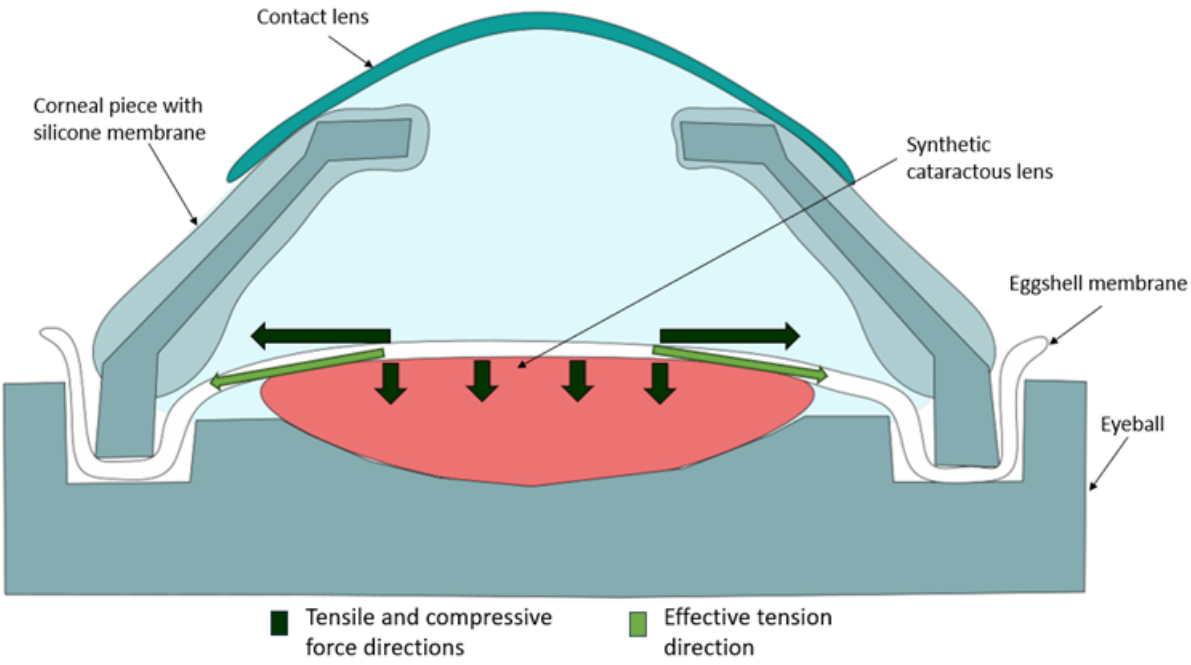

Figure 4.2: Tension and stretch direction of the capsular membrane in the prototype (tolerances are exaggerated).

minute to sterilize it. The papers do not specify how exactly the membranes are extracted from the eggs. A weak acid such as store-bought vinegar is used to dissolve the eggshell leaving behind the membrane relatively intact. The shells are dipped in vinegar overnight as the shells dissolve or crumble away, depending upon the concentration of acetic acid in vinegar. The eggshell membrane can be easily separated from the remnants of the shell and be stored in fresh vinegar or saline solution (PBS) for usage. The membranes need to be used within 48 hours of the preparation process to avoid decomposition.

4.6. Cataractous lens

The anatomical lens in the eye exerts tension on the capsular membrane, which keeps it stretched firmly. While the posterior segment of the anatomical lens is bulging, the anterior part is much flatter. During the capsulorhexis procedure, the lens acts as a semi-hard medium on which the procedure can be carried out. The exact color of the phantom lens does not matter as long as one can differentiate between the membrane boundaries and the lens in the prototype.

One of the prime candidates for the materials is hydrogel as it can achieve the required stiffness while also being squishy while maintaining its shape. Figure 4.3 shows the hydrogel 'Orbeez' used in the prototype. Orbeez are commercially available hydrogel balls made up of Sodium polyacrylate and can absorb a large amount of water to increase in volume [78]. It is often used in soilless plant pots, crafts, and other recreational activities while being very cheap. During the usage of orbeez in this project, it was found that cutting the fully swollen hydrogel with a very sharp knife and keeping it in a small tightly sealed humid container will let it retain its shape for months at a time. While the dehydrated beads are hard and brittle, the fully swollen orbeez ball is firm and bouncy. The stiffness can be toned up by dehydrating the piece and locked by sealing it in the container until it is used. The slice used in the prototype is about 1-2 mm thick, 8 mm in diameter, and flat on top.

The other material suitable for the lens is the silicone used for the corneal tissue. Unlike hydrogel, silicone pieces cannot be fragmented and are tough to tear apart. Since the capsulorhexis training does not involve lens dissection and cracking, both materials can be used for the training, depending upon the case study. The hydrogel lens is squishier than the silicone counterpart. The silicone cataract lens is made using a tray-shaped mold having circular holes to be filled. The final lens is flat and has a thickness of 1-1.5 mm, 8 mm in diameter.

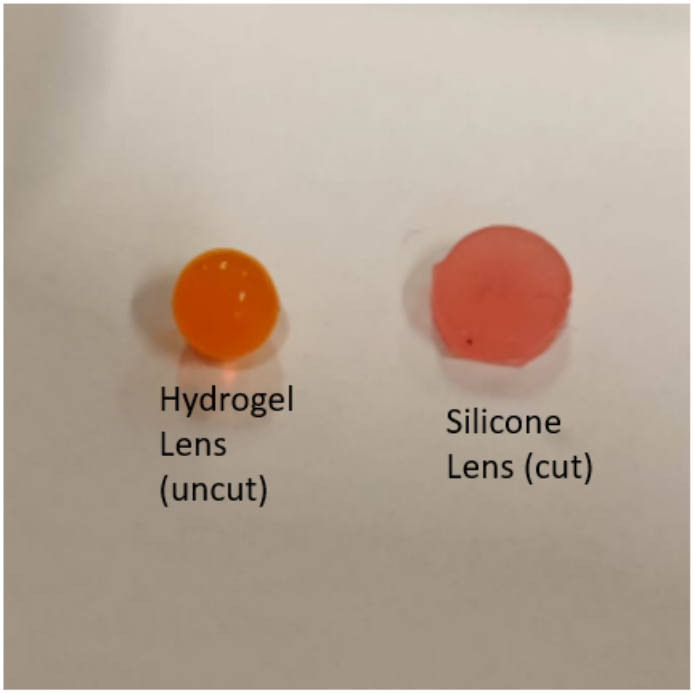

Figure 4.3: Cataractous lens choices

Note: Assembly of all the parts and steps to prepare silicone parts can be found in Appendix A.

5

Experimental setups, protocols, and verification

Electronic components: FUTEK force sensor was used to measure the contact force between the probe and the specimen. The sensor had a range of 0 to 1 N with 1000 divisions, which had been calibrated by adjusting the resistance of the signal conditioner using standard weights [pics in appendix]. A Micro-Epsilon optoNCDT 1302 laser displacement sensor was used to measure the precise linear motion of the stage. This sensor had a range of 20 millimeters. Both the displacement and the force sensors were connected to the Scaime CPJ RAIL signal conditioner (green box), which in turn was connected to the NI USB-6008 Multifunction I/O device which worked as an analog-digital converter (white box) connecting the sensors to the computer via a USB cable.

Softwares: The sensor data were gathered and processed using the NI LabVIEW 2018 (64-bit) student edition. The program file containing the block diagrams, codes, and controls used to obtain the raw data was provided by Jacques Brenkman from the Meetshop at 3ME. The overview of the block diagram is shown in Figure 5.1.

The recorded data is stored as an Excel file with 5 columns, each for time (ms), Force (volt-

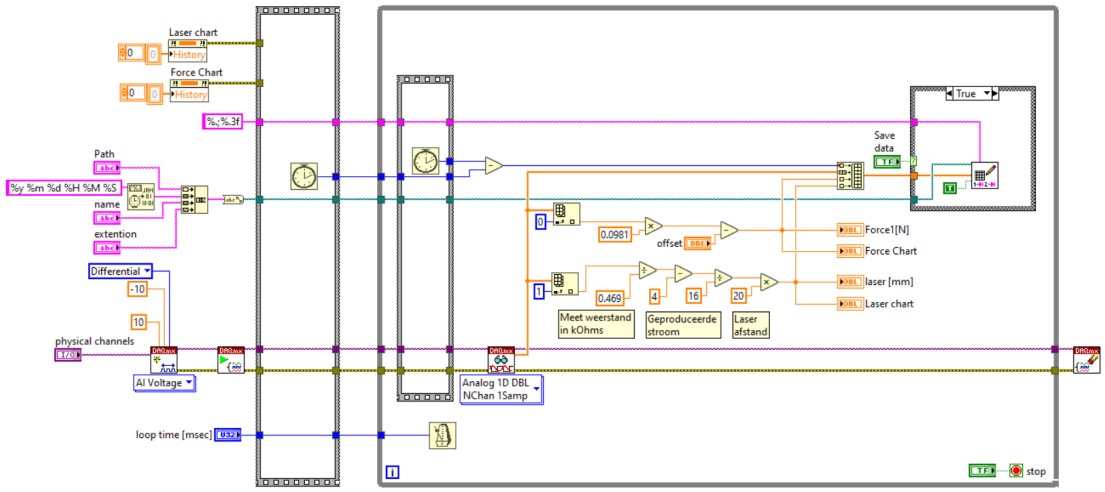

Figure 5.1: Block diagram of the LabVIEW file

age), displacement (voltage), Force (N), and displacement (mm) respectively.

MATLAB version R2022b was used to extract the raw data, process it, and obtain the graphical and numerical stiffness values. A simple script was written to extract the force and displacement data from columns 4 and 5 respectively and the results were plotted and compared. For each graph, the slope was calculated at the initial 10 degrees to obtain their corresponding stiffnesses.

Testing rig setup: A 200x200 mm PMMA board with slots was cut using a laser cutter which

served as a true base for the setup. Two long steel columns with square cross-sections were attached underneath the PMMA base to elevate it and provide a good grip. A THORlabs manual linear stage with Mitutoyo linear screw handle of 0-25 mm range and 0.01 least count was attached on the PMMA base with M6 screws and nuts. A platform for the force sensor and a laser sensor holder were 3D printed using PLA and were attached to the PMMA base. The sensors were attached to these provisions. Depending upon the experiment, either an angled baseplate to hold the whole prototype or a perpendicular platform to hold the individual tensile elements were attached to the linear stage with screws. The angle of the baseplate for the prototype was set to +15 degrees towards the force sensors to increase the working range of the setup.

5.1. Preliminary experiments

5.1.1. Stiffness of a single compliant strip

Objective:

1. To compare the experimental stiffness of complaint strips of varying thicknesses.
2. To find the effect of varying the speed of platform motion.
3. To compare the variation in the stiffness and Force-displacement profile after 20 cycles of loading and study the mode of failure for compliant strips of varying thickness.

Setup and experiment:

Three samples from each of the compliant strips of thicknesses 0.5 mm, 0.85 mm, and 1 mm. Setting three ranges of speed and calculating the rotations of the micrometer per second to achieve these linear speeds, which in this case is '0.5' cycle/s for 0.25 mm/s (slow), '1' cycle/s for 0.5 mm/s (medium/ standard) and '2' cycles]/s for 1 mm/s (fast). A special platform to hold the compliant strip in the intended position as shown in Figure 5.2a and 5.2b. The point of contact between the probe and the compliant strip should be the same as that between the strip and the lower base of the eyeball in the complete setup. Force value 'Fs' is obtained from the force sensor. For the sake of comparison with the complete setup in the following secondary experiment, the angular deflection is calculated with the distance 'R_1' which is the distance between the center of the steel ball and the point of contact of the lower eyeball plate and strip instead of the length of the cantilever strip. 'R_1' is also the same as the radius of the eyeball and the point of incision on the slots of the corneal eyepiece which is 12 mm. The distance 'S_1' is the distance moved by the probe, which is the same as the linear movement of the point of contact in the full model assuming the arc length is the same as the linear movement. This is shown in Figure 6.12a.

The angular distance θ is calculated using the formula-
S_1=R_1.sinθ

The stiffness of the strip 'K_s' in g/deg is calculated using the formula-
K_s= ΔFs/$\Delta\theta$ *101.9716

Experiment:

1. A single compliant strip of a particular thickness is held on the platform of the testing rig in such a way that the probe is perpendicular to the strip. Sensors are set up to monitor the forward movement of the strip on the platform. The platform is moved forward for 5 mm at medium speed and the data is recorded. Then the platform is brought back to the initial position and is repeated two more times. This step is carried out on the other two

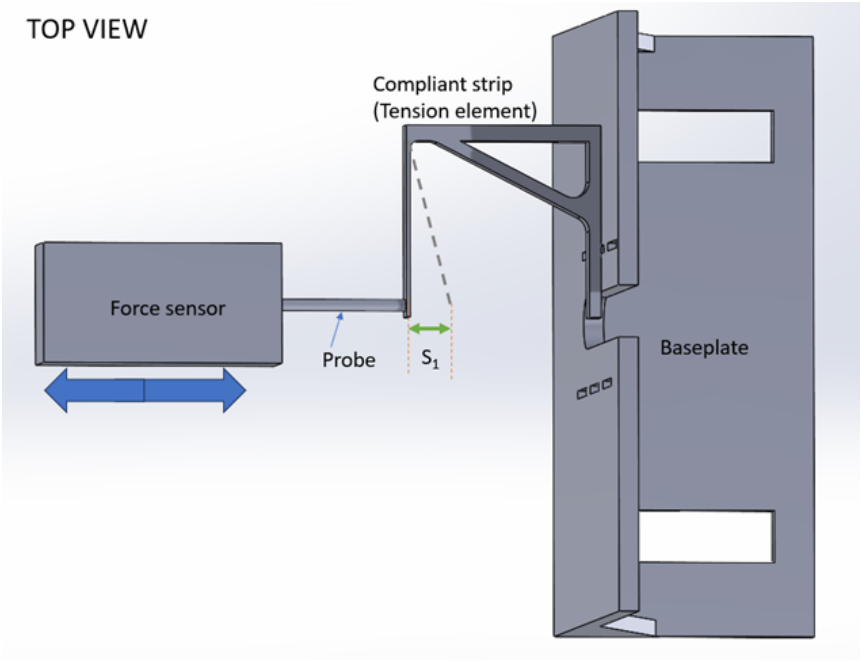

(a)

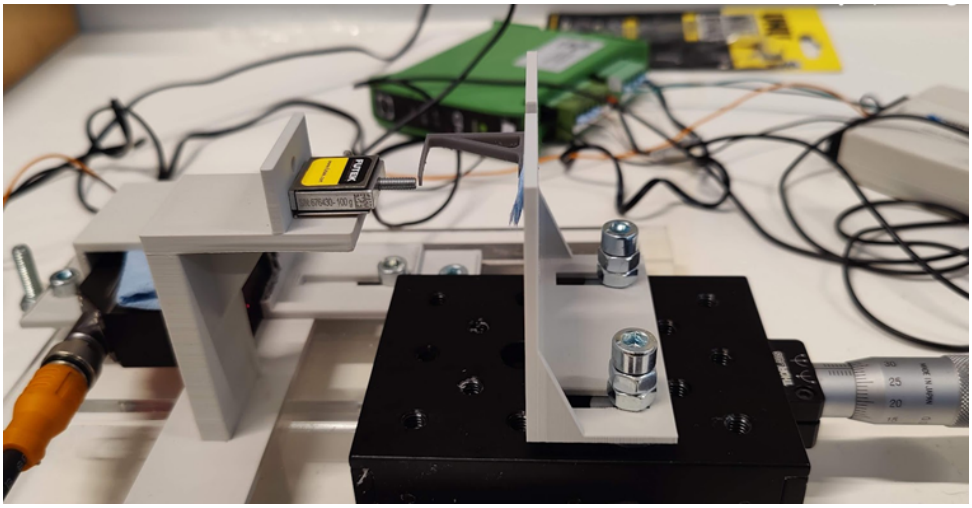

(b)

Figure 5.2: Preliminary experiment setup.

strips of different thicknesses.

2. A new compliant strip of 0.85 mm thickness is placed on the platform and step 1) is performed again at a slow and fast speed; each being conducted thrice on the same strip. This is done to avoid the deviations arising from minor thickness variations from multiple samples. The mean values of the plot points of each speed category are calculated and graphically represented.

3. The specimens used in step 1) are loaded onto the testing setup and the 0-5 mm back-and-forth movement is carried out another 16 times at medium speed. On the 20th cycle, the data is recorded as the specimen moves from the rest to the final position until the failure is observed (break, yield or locking). This step is conducted for compliant strips

of other thicknesses using samples used in Step 1.

5.1.2. Tear, fit, and water retention test of the silicone ring

Test 1: Fit the corneal cap on the eyeball. Using a keratome, a horizontal incision is made through the window and poked through it. If the silicone film does not tear beyond the incision hole, the test is considered a pass.

Test 2: After test 1, a micro forceps or any such capsulorhexis needle is inserted into this cut and the capsular membrane is torn or wiggled. If the membrane does not slip off, this test is a pass.

Test 3: All the tools are removed, and water is filled in from the dome top and covered with the lens piece. If there is no leaks, the test is a pass.

5.2. Secondary Experiment: Torsional stiffness test of the setup

*Objective:*To determine the torsional stiffness of the eyeball movement in all directions (major and minor) along with the twist and to plot it on the graph.

Prerequisites: The contact surfaces need to be smooth to reduce friction as much as possible. The laser displacement sensor should be aligned in such a way that the total motion of the platform is within the range of the sensor.

Setup: The prototype with 0.85 mm compliant strips is securely held on the baseplate of the testing rig as shown in Figure 5.3. In the first run, the force-sensing probe is aligned to one of the four major directions of the tilt. An attachment is chosen which is either blunt, blade, or rod-shaped and is fitted on the tip of the probe tip. The point of contact of the probe tip on the dummy eyepiece is defined and measured from the center of the metallic ball of the joint and named 'R_2' whose value is 16 mm. The platform on the setup has a forward default tilt of 15 degrees and hence the protruding flat contact area of the eyeball is at this angle to the probe. This pre-tilted design makes sure that the probe does not slide off too much along the contact surface during the experiment.

Experiment: The probe is pushed against the contact surface in an incremental step rate of 0.5 mm/s and the force values 'F_{tot}' are recorded in N. As the eyeball tilts, the distance covered by the platform is recorded/ monitored by the laser displacement sensor which is later converted to angular movement. (Conversely, the linear distance of the probe motion 'S_2' can be approximated to the arc length due to the small functional range of the prototype and the angle be found by the formula-

S_2=R_2.sinθ

The prototype is then turned towards other major and minor directions and the steps are repeated. The probe location is changed to measure the torsional stiffness in the restricted twist motion.
After obtaining the force-displacement data, the torsional stiffness in N/deg, further converted to gram force per degree (g/deg) over the functional range-

K_{tot}= /$\Delta F_{\text{tot}}/\Delta\theta$ * 101.9716*Z

Here Z is the ratio R_2/R_1. This is added in the formula since there is an offset between the

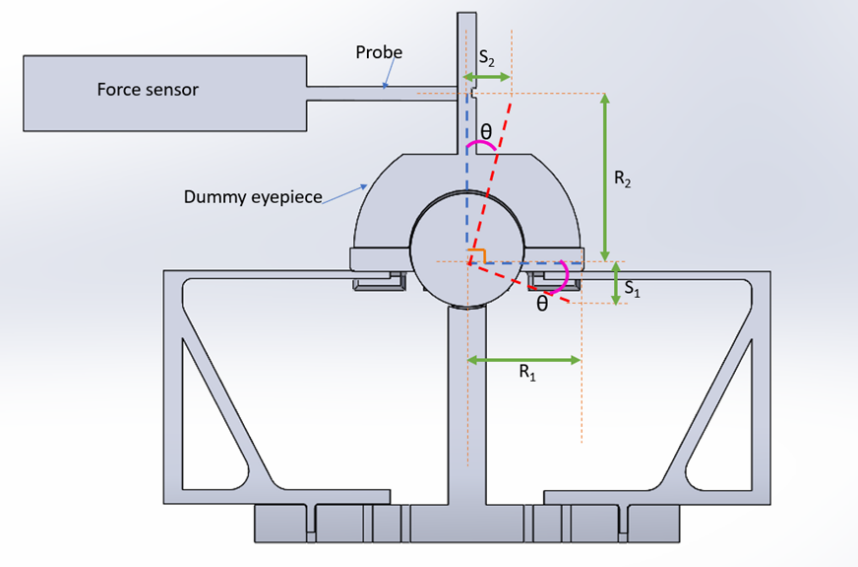

(a)

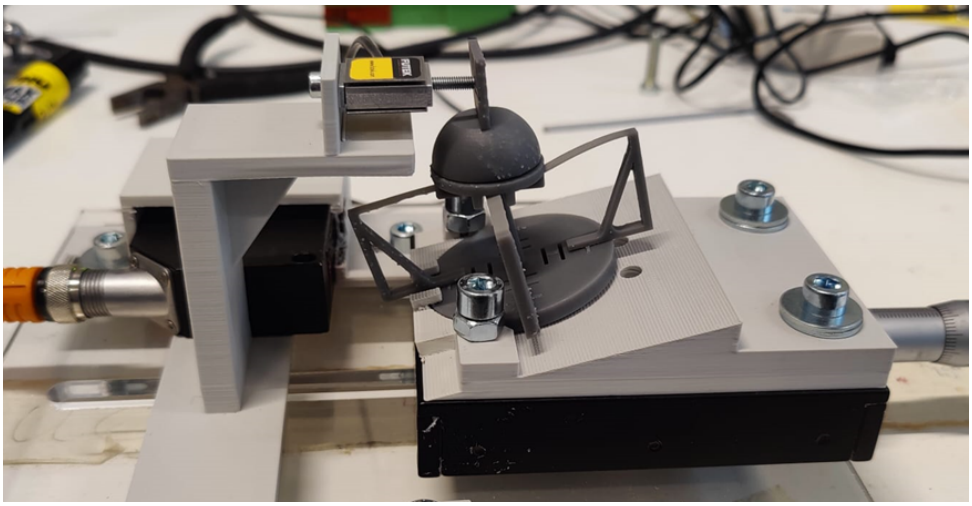

(b)

Figure 5.3: Secondary experiment setup.

actual corneal eyepiece piercing point (which is designed to be the same as R_1) and the point at which the probe pushes the plate on the dummy eyepiece. The value of Z is 1.3333. The slip distance of the probe on the plate is ignored Due to the small functional probe movement range of 5 mm, the deviation of the strip is small, therefore an average torsional stiffness value can be assigned in each direction and plotted on the radial plot graph.

5.3. Clinical Evaluation

Objective: To check whether capsulorhexis and associated surgical procedures be carried out on the prototype by a qualified and experienced surgeon in a real cataract surgery situation.

Experimental setting: The trial was carried out at a wet lab facility provided by Dutch Ophthalmic Research Centre B.V. The wet lab provided a surgical setting with an operation theatre style setup of bed and surgical microscope suitable for eye surgery. The room had multiple cameras and the sessions could be recorded. The trial was conducted by Dr. Efe, a cataract

surgeon with more than 15 years of experience. A tray with all the necessary tools was kept by the surgeon's side.

Pre-trial orientation: A brief presentation was given to the surgeon to showcase the prototype and the objectives. A consent form was given to the surgeon as well the DORC person in charge and overseeing the trial – Mart Gahler regarding the trials, questionnaire, aspects of biological tissue in the prototype, and handling of the trial results in the form of audio, and video, and written feedback. The surgeon was made aware of the possible failures of the prototype during the trials such as parts falling off, liquid leakage, and radial tear or membrane slip. A questionnaire containing 15 questions (shown in Chapter 6) each of which can be rated as either 'needs improvement' or 'functional' was given to the surgeon for his reference.

Trial and post-trial: The prototype was assembled and placed on the table under the microscope while the cameras began to record. A live feed from the microscope was made visible on the LCD screen next to the setup. Due to the relatively simple and safe procedure, everyone was present in the wet lab next to the surgeon during the trial, with each question from the questionnaire being raised as the procedure continued. The surgical instruments on the tray chosen for the trial were a stab knife 15 degrees (also called a keratome), a standard cystotome made by bending the tip of a needle on a syringe, a Mohr Capsulorhexis forceps intraocular style (23 gauge / 0.6 mm), and a syringe containing viscoelastic liquid, also called Ophthalmic Viscosurgical Device (OVD). The trial was conducted as a regular surgery until the completion of the capsulorhexis stage was completed either successfully or unsuccessfully, all while the doctor gave feedback at each step. After the trial, the surgeon filled up the questionnaire while also giving his critical insight into each component of the prototype as well as explaining why certain points were graded high or low in the questionnaire. The trial concluded with the surgeon giving his recommendations on how to improve the prototype in certain aspects (the unedited questionnaire is attached in the appendix).

5.4. Validation by training surgeon

Pretext: After the clinical evaluations were done and the results were obtained, the prototype underwent a few minor changes to address the concerns. These involve either the setup steps (addressed in Chapter 3 under 'Tolerances and fixtures'), processing such as further reducing eggshell membrane thickness, or use of contact lenses as discussed in Chapter 4. The new version was now packed and sent back to Dr. Thomas in India for further analysis as a training surgeon (henceforth called a trainer).

Objective: To assess whether the prototype is suitable for training purposes by a trainer. Feedback from the trainer after the tests was to be conveyed to the author.

Validation trial: Apart from carrying out the capsulorhexis procedure similar to the previous trial on their own, the trainer would perform other checks and trials. The author had briefly suggested some of the checks to be done which the trainer interpreted and expertly tested along with his own trials. These are as follows:

1. Ease of assembly- checks to determine how comfortable and repeatable the assembly of the prototype is designed to be.
2. Functionality check- checking the appropriate strength to move/support the moving parts (under various tension element stiffnesses). It also involves checking the range of the

eyeball's movement.

3. Visibility of the anterior chamber under the microscope- similar to the clinical trials. The ability to use Methylcellulose (for developing countries) in the presented model to fill the anterior chamber apart from regular saline water.
4. Possible use of dyes to stain the capsular membrane.
5. Paracentesis- A procedure wherein the anterior chamber is either drained or pressurized to maintain the maintain the intraocular pressure (IOP) using syringes.
6. Maneuverability- ability of the cannula to move appropriately in this eye model.

6

Results and discussions

The range for calculating the stiffness was between 2- and 10 degrees of flexion. The initial point was set to 2 degrees and not the origin because of the small yet sudden shifts along the Y-axis between 0-2 degrees. This variation is likely due to the sudden contact with the probe. In most of cases, the first major slip at the contact point between the probe and the surface occurred after 10 degrees of flexion. The results of the experiments are as follows.

6.1. Preliminary experiments

6.1.1. Change in thickness of the compliant strip

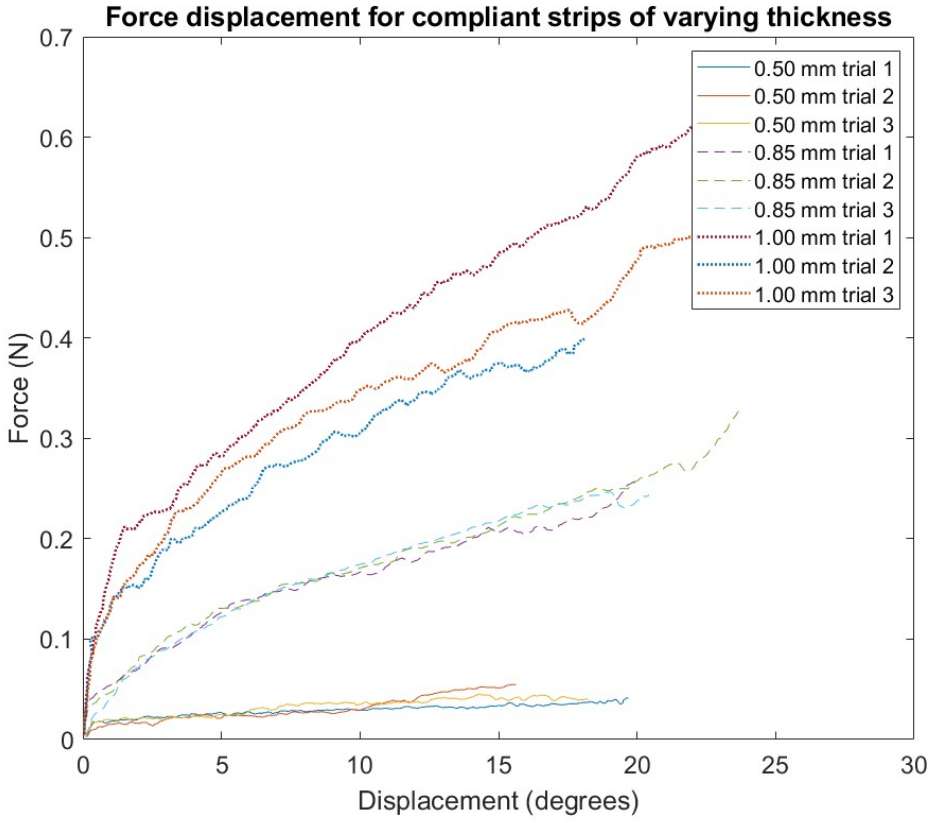

Figure 6.1: Force-displacement behavior for compliant strips of varying thickness.

Figure 6.1 shows the trend of the force-displacement behaviors of the batches of different thicknesses. The mean stiffnesses of each of the batches were as shown in Table 6.1.

The apparent standard deviation of the stiffness values of each group could be mainly due to the small deviations in the thickness of each strip in a batch and up to some extent the surface roughness between the probe and the contact surface of the strip. The thickness of the

Table 6.1: Variation of stiffness values for batches of strips having different thickness

Thickness of the strip (mm)	Stiffness values (g/deg)
0.50	0.17 ± 0.05
0.85	1.16 ± 0.14
1.00	2.52 ± 0.13

strips greatly influences their stiffness values. By comparing the desired range of the stiffness values in the anatomical eye, we see that the stiffness values between 0.85 mm and 0.5 mm strips are suitable for the prototype if the strips are printed using this specific material.

During the two separate surgeons' trials conducted at the later stages of experimentation, they were given all three options to choose to attach to the testing prototype.

6.1.2. Changing the speed of the platform motion

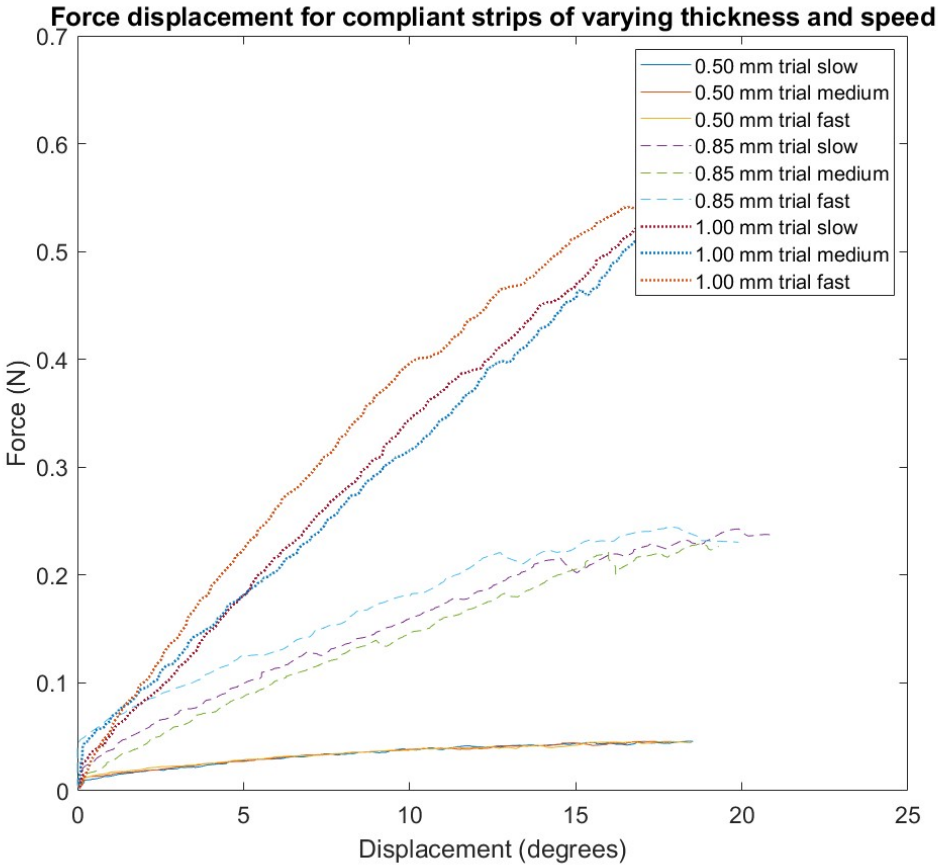

Figure 6.2: Force-displacement behavior for compliant strips for varying thicknesses and speeds.

Figure 6.2 shows the trend of the force-displacement behaviors of the batches of different speeds on the same strip of 0.5, 0.85, and 1 mm thickness. The stiffness values of each speed batch are as shown in Table 6.2.

From the table, we can see that the stiffness for the fastest batch is lower than the other

Table 6.2: Variation of stiffness values for different thickness strips at varying speed

Thickness of strip (mm)	Stiffness values (g/deg)		
	Slow	**Medium**	**Fast**
0.50	0.26	0.19	0.13
0.85	1.29	1.25	0.97
1.00	3.08	2.72	2.61

two batches. This effect is more profound upon reducing the thickness of the strip. The major slips occur beyond 10 degrees of displacement. A faster speed leads to the slip occurring sooner between the probe and the bent specimen.

A change of specimen of the same batch is likely to have the same or more deviation from the mean stiffness value as compared to speed and therefore the speed test is done on the same compliant strip. While the average difference in stiffness values at different speeds from multiple specimens of the same thickness would have given a definitive percentage increase/decrease, all three samples of different thicknesses show the same trend and hence this trend can be generalized.

During an actual training session or a live surgery, the incision tools are moved through the cornea at a medium-fast speed. The capsulorhexis and the tissue fragment handling speed are at a slow-medium speed. This of course depends on person to person and their level of expertise.

6.1.3. Variation in the stiffness profile after 20 cycles of loading

Figure 6.3 shows the compliant strip behavior after 20 cycles of repeated loading when loaded to maximum deflection at medium speed. The full behavior of the strips shows the characteristic nonlinear behavior of the structure. The stiffness values calculated by the slope of the curves for the first 10 degrees of each batch are shown in Table 6.3.

Table 6.3: Variation of stiffness values for different thickness strips at 20^{th} cycle

Thickness of the strip (mm)	Stiffness values (g/deg)
0.50	0.23
0.85	1.41
1.00	2.85

The stiffness values for each batch have increased slightly over their mean values (compared with Table 6.1. This may be due to the strain-hardening effect due to repeated loading although the manufacturer of the resin material has not specified the exact reason for this. Unlike the other trials which were stopped abruptly on purpose when the probe had moved linearly by 5 mm, specimens in this trial were tested up to their limits but only on their respective 20^{th} cycles and data were recorded. The absolute range of the compliant strip has been seen to increase by increasing the thickness of the strip.

The mode of failure observed for all the specimens irrespective of their thickness was locking/slipping due to flexion beyond its range as seen in Figure XXs. Beyond this position, the

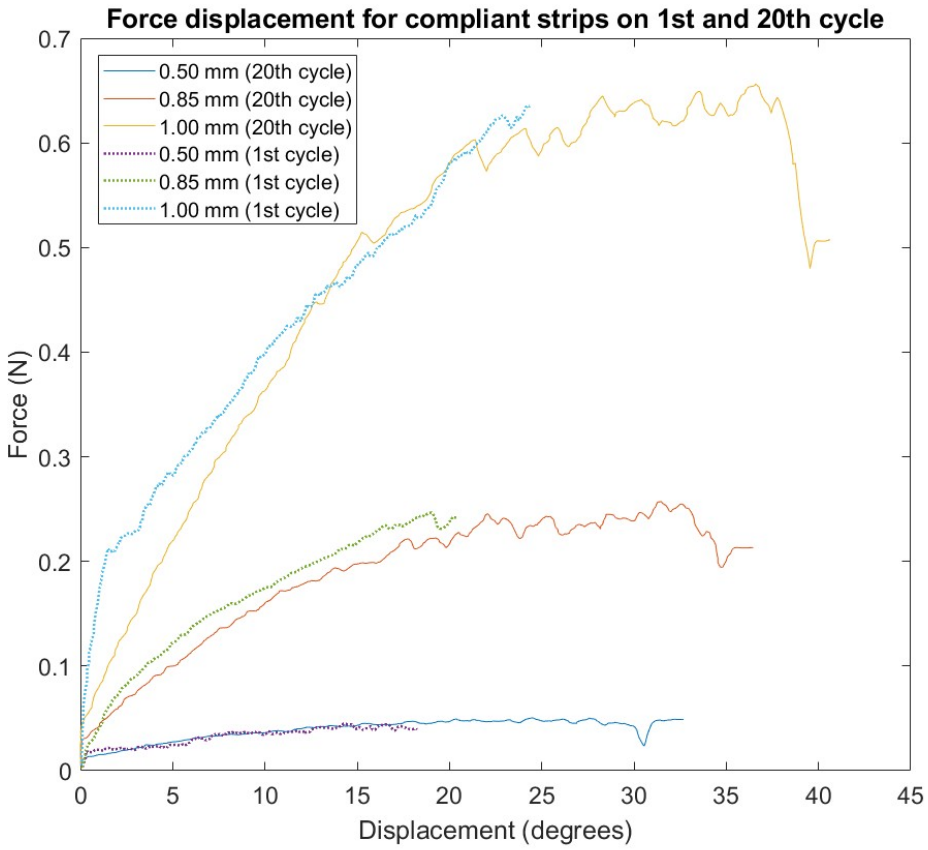

Figure 6.3: Force-displacement behaviour of compliant strips of varying thicknesses on 1^{st} and 20^{th} cycle

probe could no longer push the strip, which is like the failure seen in the complete prototype.

It is highly unlikely that the repeated loading of the complaint strips would have any significant effect on the outcomes of the speed test. This effect would be a fraction of the deviation of the stiffness values seen in the table.

During these three experiments, it was observed that the recoil of the compliant strips was slow after the maximum load applied was removed, especially for the final millimeters to straighten. This was exacerbated during the repeated loading cycles with each intermittent waiting time prolonged as the cycle number increased. In an automated testing rig designed for fatigue life, this might come up as an issue since the strip might not always be in sync with the speed of the probe unless the strip is held firmly at the tip.

Due to the very low number of cycles in this experiment, it is not possible to specify the cycle life of the compliant elements of different thicknesses. Since the failure is not a complete breaking of the strip but more of a plastic deformation, it is possible to reuse the compliant elements a few more times after bending the strips carefully in the reverse direction and holding them for some time in that state. This is not a sure-shot method of reusing the elements and therefore is not recommended unless replacements are not available. The stiffness is also

likely to change depending on the extent of flexion and usage. Based on the observations throughout the project, the thicker compliant strips lasted significantly longer than the thinner ones with the least residual deflection.

In all three trials, the data from testing the 0.5 mm had a lot of scattering despite using the default filter. While some of this could be attributed to the manual motion of the linear stage and the internal vibrations in the screw system, most of it is because the recorded data is only a few magnitudes higher than the least count of the force sensor over the entire duration of the trial. Additional filters were put on the data to smoothen it to get the stiffness data.

6.1.4. Other preliminary experiments:

The incision test on the partially assembled portion of the prototype was a pass. The incision wound did not spread beyond the site. Any deliberate attempts to tear were localized to that particular window in the corneal piece. The incision site on the window was then also found to be completely sealable when a bit of uncured silicone was put along the cut which shows that the ports could be reused at least a few more times.

The tool penetration and the membrane grip test were a pass. A 27-gauge needle bent in the shape of a cystotome was inserted into the partially assembled portion of the eye through the previous incision site. The corneal piece was held firmly in its place and the membrane did not slip. No visible wrinkles on the eggshell membrane were seen even in the presence of water in the anterior chamber.

The leak test was a pass. Once the corneal piece was held in place securely, the membrane provided filled up the gap between the two interlocking pieces. The water did not leak through the gaps or the incision cuts when the top of the corneal piece was covered with a lens and in the absence of any external pressure on the corneal surface mainly due to surface tension. It was seen that if the anterior chamber was pressurized, a small bead of water would leak from the gap between the corneal piece and the eyeball, especially near the notches. This could be fixed by using a tiny amount of cyanoacrylate glue that would block the gap due to its viscosity.

6.2. Secondary experiment

The force-displacement behavior for the individual arms made of 0.85 mm compliant strips are as shown in Figure 6.4.

‘Direction 1’, ‘direction 2’, ‘direction 3’, and ‘direction 4’ are the major direction stiffnesses whereas stiffnesses ‘direction 12’, ‘direction 23’, ‘direction 34’, and ‘direction 41’ are the stiffness of the prototype in the direction between the arms, also known as minor direction stiffness. The values of these are given in the Table 6.4.

It is seen that all the compliant strips (arms) have stiffness values within the acceptable ranges of 0.65 to 1.5 g/deg as shown by the anatomical details. The results also verify that the principle of the parallel spring system incorporated in the model – the minor direction stiffness is almost the sum of the stiffnesses of the pair of arms. The discrepancies are mostly because of tilting the default eyeball more towards the weaker arm instead of strictly being 45 degrees to each arm. The radial plot in Figure 6.5 shows the mean stiffness variation along

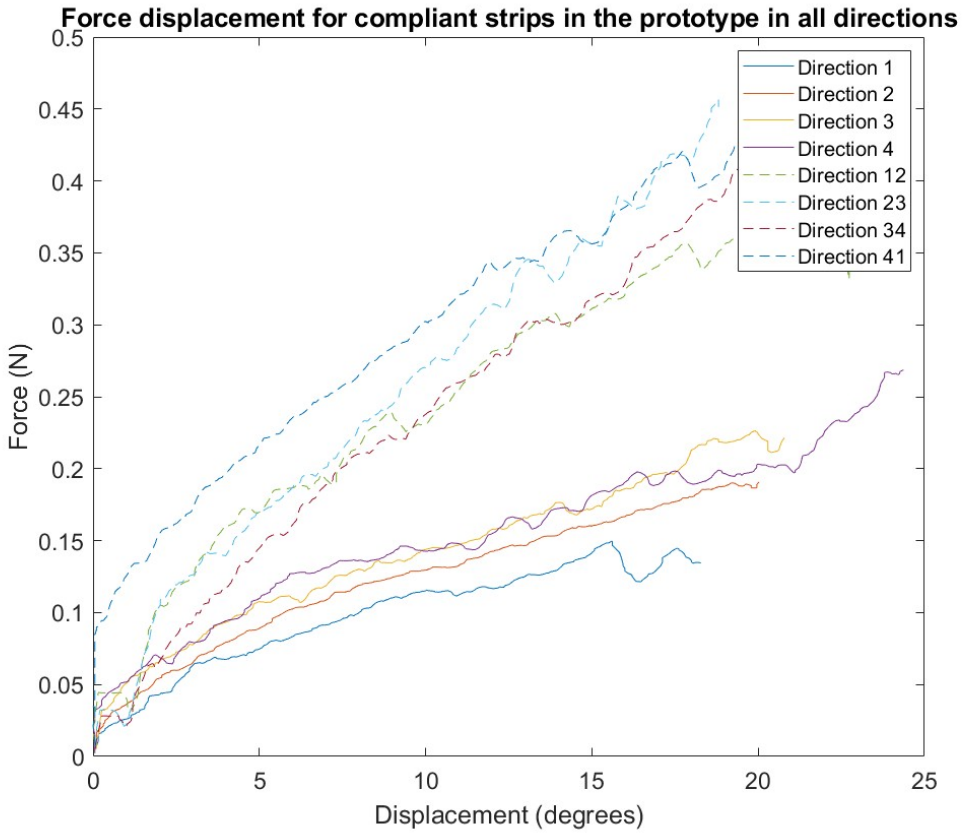

Figure 6.4: Force-displacement behavior for compliant strips in the prototype for all directions.

Table 6.4: Stiffness values of the compliant arms in the prototype in all directions

Name of the arm or direction	Stiffness value (g/deg)
Direction 1	1.29 ± 0.06
Direction 2	1.09 ± 0.15
Direction 3	1.14 ± 0.11
Direction 4	1.13 ± 0.09
Direction 12	1.92 ± 0.06
Direction 23	2.45 ± 0.15
Direction 34	2.52 ± 0.19
Direction 41	2.49 ± 0.11

all 8 directions.

Effect of friction

During the first few attempts of conducting the trials, the data was highly affected by many unexpected oscillations in the force-displacement behaviors. It was later found out that the small residuals along the edges of the compliant strip, the rim of the lower eyeball plate, and the inner spherical surface of the eyeball in contact with the steel ball led to friction between the

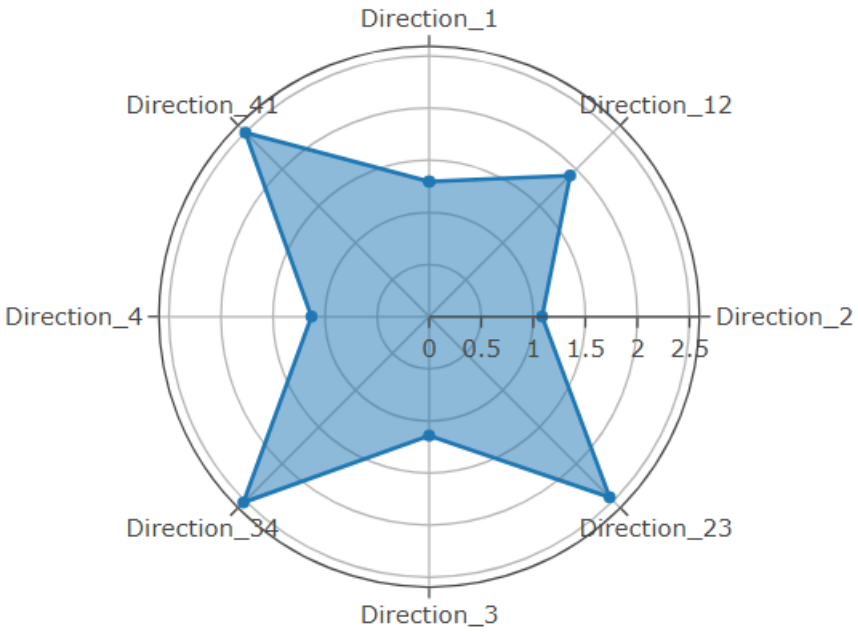

Figure 6.5: Stiffness of 0.85 mm thick tension element model in all directions (g/deg).

contact surfaces. The friction between either the inner eyeball surface or the rim of the lower eyeball plate and the steel ball often leads to directions resisting the motion more than the rest. Rust on the surface of the steel ball due to improper use of lubricants would also have a similar effect. Lubricants were initially applied on the spherical surfaces which increased the initial pushing force due to the thin film surface tension between the steel-plastic surfaces. Thus, they were not used.

The tiny stubs of the support structure remnants on the edges of the compliant strip interfered the most as the source of friction, especially when the eyeball was pushed along the minor direction as they came in contact with the walls of the ridge underneath the lower eyeball plate. This effect was reduced by a significant amount after filing the edges.

Effect of creep

During the repeated loading experiment, the compliant strips regained their original shape in a brief period after the load was removed in each cycle. This, however, is not the case for structural deformity due to creep. In an assembled prototype, the compliant strips are under a bit of pretension as they are being pushed against the lower eyeball plate. Over time, creep sets in, and the pretension is lost as the compliant strip retains its bent shape as shown in Figure 6.6. The findings were based on a fully built prototype which was left unattended for over a month. The strips did not revert to their straight cantilever position. This effect is more profound in thinner compliant strips as their stiffness is very low.

Therefore, it is suggested to disassemble the tension elements from the prototype during the storage period.

Figure 6.6: Effect of creep due to continuous loading over a month (left one is the unused piece, right one is the deformed piece after a month)

6.3. Cost estimation

Table 6.5: Cost analysis table

Process/ component	**Retail cost**	**Cost per prototype (Approx)**	**Source**
3D printing			
Material- V2 draft resin (inclusive of support structures, molding parts, and at least 1 spare piece for the corneal piece and each batch of tension element)	163 EUR/litre	15-20 EUR	[79]
Silicone membrane			
Material cost	60 EUR/kg	1-1.5 EUR	[80]
Processing cost	NA	NA	-
Miscellaneous – stirring stick, cup, release agent (per use), gloves, dye (per use), etc.	2 EUR (approx.)	2 EUR	-
Steel ball	1.5 EUR/piece	1.5 EUR	[81]
Contact lens (daily)	7.5 EUR for 15 pieces	0.5 EUR (for single layer) and 1 EUR (for double layer)	[82]
Miscellaneous (per use) - egg, glue, vinegar		2-3 EUR	-
Total Cost		20-30 EUR	

One of the main objectives of the project was to make the final prototype as cost-efficient as possible. One of the main assumptions is that a suitable 3D printer is available at the facility, or such options are available nearby so that the printing cost could be paid on an hourly basis and the amount of material consumed. Discussion was held with the workshop technicians at IWM in TU Delft regarding the costs associated with 3D printing based on European market prices. Although an exact rate (EUR/hour) was not obtainable, it is estimated to be less than or equal to the material cost. The material cost may also be much lower than that stated in the table if the parts are made with other draft resins.

Table 6.5 gives an overview of the cost per prototype. The post-processing is done by the user and therefore this cost is not added to the overview. The cost of accessories such as surgical tools and blades for cutting the 3D support structures off the parts are not included.

6.4. Clinical Evaluation

6.4.1. Assessment overview

The original questionnaire was initially unclear to the surgeon, especially the 'sufficient' and 'functional' columns of assessment. He suggested combining the two columns into the 'acceptable' column so that the questionnaire has a standard 'yes/no' format with some explanation of grading under certain objectives. The filled table is as presented as Table 6.6 where the chosen option is highlighted in green.

Table 6.6: Assessment Table. (Green = selected)

Pre-trial checks:			
Tools used: Cystotome (21G), micro forceps (23G Mohr), and keratome			
Thickness of beams used: Medium (0.85 mm)			
Lens used/unused: Yes			
Dye used/ unused: No			
(Additional comments can be given to the * marked criteria, if needed)			
Sr. No.	**Criteria**	**Needs Improvement**	**Acceptable**
1	Compatibility with the tools	No	Yes
2	Compatibility with the microscope and clarity of cornea	No	Yes
3	Model behavior during the trial	Frequently gets stuck or parts falling off	Behavior similar to that of the intact eye or gets stuck sometimes
4	Ease of tool movement within the eye	Not easy	Easy
5	Movement of the eye muscles associated with the level of mistakes	Little to no similarity to human eye movement	Considerably similar to human eye movement
6	Range of motion	Less than actual	Similar or close
7	Stiffness of the eye	Different	Similar or close

8	Anatomical similarity (dimensional)*	Many inconsistencies (>4)	Few or no inconsistencies (<=4)
9	Anatomical similarity (tissue texture) *	Many inconsistencies (>4)	Few or no inconsistencies (<=4)
10	Ease of corneal incision	Difficult	Easy and similar
11	Access to the site of capsulorhexis	Difficult	Easy and similar
12	Ability to do CCC*	Difficult	Easy and similar
13	Possibility of complications (tear)	High	Low
14	Aqueous humor leakage	High	Low
15	Time for completion of the procedure compared to standard trial	Considerably more time than usual	Similar or slightly more time than usual

There were a few concerns raised during the trial and these were briefly discussed by the surgeon during and after the trials were finished. It was concluded that the prototype was acceptable if the problems that became evident during the trials were fixed. Some of these problems were fixed during the trials immediately while the others involved either a design change or improving the material being used. The whole trial session was recorded, and this video has been attached to the appendix (as a hyperlink/repository) after approval from DORC as well as the surgeon.

It should be noted that the outcomes of the trials were obtained first and then the design and the materials chapters were updated based on the findings and suggestions of the surgeon- the permanent fixing of the eyeball, dying the synthetic cataractous lens or membrane red (or using a colored hydrogel slice) and the separation of the eggshell membrane layers using hot and cold water baths.

6.4.2. Concerns

There were 4 problems faced by the surgeon while performing capsulorhexis on the prototype and each of these shall be explained in detail.

1) Parts falling off – During the initial part of the trial, the first incision made in the corneal piece by the keratome knocked off the loosely held eyeball off the lower eyeball plate as shown in Figure 6.7.

It should be noted that the eyeball was fixed by jamming a thin piece of paper between the pin connections and the surgeon was made aware of the possibility of this happening before the trial began. The surgeon was given the option of either being intervened to reattach the same eyeball back, continuing the trial in that state by carefully balancing it using the other hand, or fixing it firmly using super glue. The eyeball was reattached twice during the trial and the surgeon finally decided to continue the trial despite the eyeball being loosely attached.

After the trial ended, a brief discussion was held where another prototype was fitted with

Figure 6.7: Eyeball falling off

the eyeball using the super glue to test the flexural behavior of the compliant elements in the model (0.85 mm was preferred). The surgeon suggested that he felt it was better to permanently fix the eyeball to the lower piece as he felt there was no need to keep it separable according to him.

2) Contrast – The surgeon found that it was difficult to find the initial cut made by the cystotome on the membrane as the membrane and the silicone lens were both white. The visuals seen under the microscope and on the screen were too white. Figures 6.8a and 6.8b show the surgeon using the incision that he already made earlier by using the cystotome to raise the membrane flap for the video. During the entire trial, no dye was used to stain the membrane primarily because, according to the surgeon, it is generally expensive to be used during such trials and not used typically in many developing countries.

The surgeon suggested to either stain the eggshell membrane or the lens with either a red or a dark blue pigment while preparing them to develop the contrast in the final model.

3) Glare – The surgeon mentions that it was difficult for him to see the incision marks on the membrane as there were a lot of glares in the anterior chamber of the eye as shown in Figure 6.9a. It should be noted that the contact lens was not placed over the eyeball by the surgeon when he mentioned this. The light from the microscope would enter the top of the eyeball and would scatter everywhere inside the anterior chamber. This does not happen in a real eye because of the curved shape of the cornea which bends all the light rays towards the lens through the pupil. The surgeon then keeps a single layer of the contact lens over the corneal piece and finds out that the glare disappears instantly as shown in Figure 6.9b.

It should be noted that this effect was more pronounced due to the nature of OVD being used instead of water or saline solution. The lens flipped during this stage of the trial, but the surgeon did not consider it a problem as it did not hinder his trial without any glare.

4: Membrane too thick and rigid – The surgeon felt that the eggshell membrane used

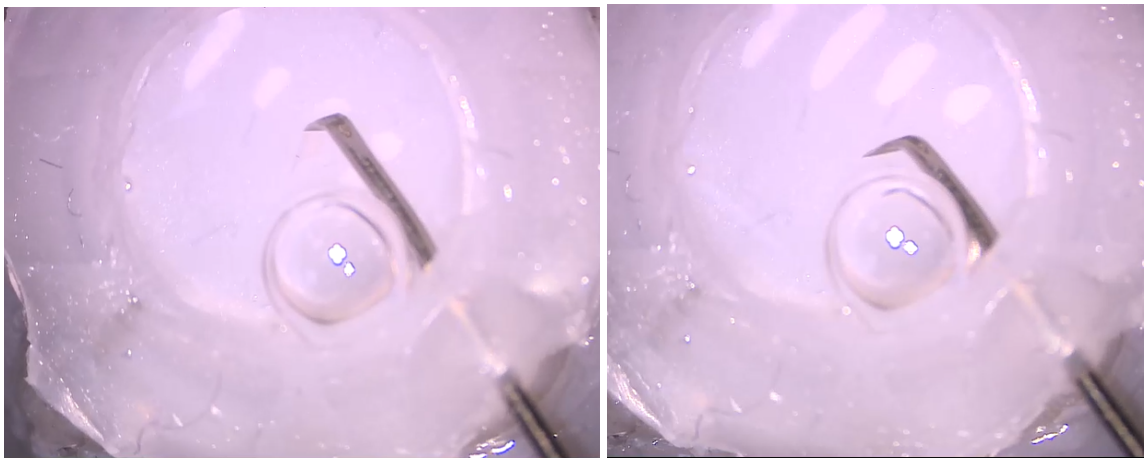

(a) (b)

Figure 6.8: (a) and (b) Lack of contrast between the membrane and the underlying lens.

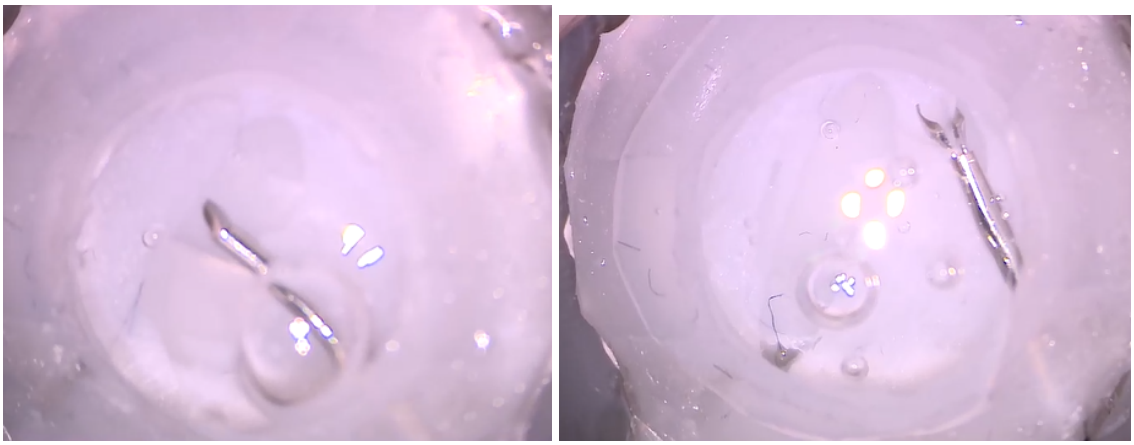

(a) (b)

Figure 6.9: (a) View on screen without the lens on the corneal piece, and (b) view on screen with the lens on the corneal piece

in the prototype during the trial was too thick to be held firmly with the micro forceps. This not only impacted the grip he had on the membrane while performing the CCC but it also led to the membrane being too rigid. According to the surgeon, the rigidity of the membrane makes the tear go radially outwards rather than traveling along the path of the forceps circularly. He also stated that more force than usual is required to tear it, which makes it difficult to control the motion of the tool. Figure 6.10a shows the radial tear in the membrane during the trial.

The solution to this problem was to make the membrane thinner. The surgeon quickly pointed out that the eggshell membrane had at least two layers in it and had delaminated during the trials. This was further verified by the author by further studying the anatomy of hen eggshells- they typically have two layers which are almost indistinguishable for the bare eye [83]. The superficial layer is thin and clear (approx. 22μm) while the bottom layer is slightly thicker and cloudy (approx. 48μm). When asked to try to tear the thinner superficial layer of the delaminated membrane, the surgeon said that he felt it was now very similar to an actual human capsular membrane. Figure 6.10b shows the two delaminated layers of the membrane plucked out during the trial.

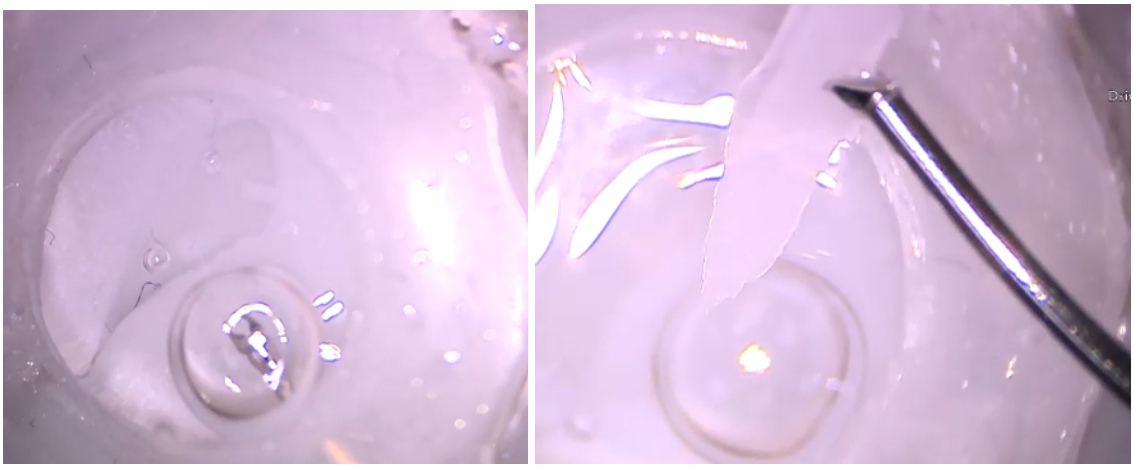

(a) (b)

Figure 6.10: (a) Radial tear, and (b) delaminated layers of the eggshell membrane.

The surgeon was also advised to use the hot-cold thermal shock process while preparing the membranes to get the thinner layer more easily. This method was later tried and found to be a success. The materials chapter mentions this part which came as an outcome of this trial.

6.4.3. Implications

The approval from the practicing surgeon on the prototype meant that it was suitable for trying out the capsulorhexis step by considering it as an alternative to the human eye. However, the trial does not point to whether the prototype is suitable or not for training the students. This had been made clear by the surgeon before the trials commenced since the training with such models is often accompanied by the curriculum and the experience of the trainer.

The trial played a great role in getting feedback directly from the surgeon in real-time while being present at the site. The critical flaws became apparent only when it was examined by such professionals and their suggestions were very exact from a practical perspective. The video of the trial is very crucial information for this project and served as the intermission for further development before the last trials since this final testing planned is taking place in India by Dr. Thomas and recording the functioning of the prototype would be difficult if not cumbersome.

6.5. Validation by the training surgeon

Dr. Thomas (henceforth called trainer in this and the following subsections) carried out several minor tests over several weeks by himself along with his own students and professional colleagues. The validation process involved introspection of the pure design of the model, consistency of the model properties to the specific requirements, suitability of the model in the current curriculum, comparison of the prototype with other prototypes (if any), mock training exercises under his supervision, drawbacks, and rooms for improvement in the prototype. The trainer's response was very positive towards the design of the prototype with some room for improvement. The results of these were discussed online comprehensively.

6.5.1. Structural flaws and improvement in the design of the training model

The trainer pointed out four structural flaws in the design he felt he needed to address. The first major flaw was the eyeball falling off the lower eyeball plate during training. This was also seen during the surgical trials before (see Figure 6.7). Although the problem was assumed to have been solved by gluing the pieces together, the trainer was a bit opposed to this idea. The trainer felt that it would be better for the prototype to be divided into a common flexible base and variable half-eyeball halves that can be swapped when needed and treated as separate entities, especially from the perspective of future progress. The glue, when used improperly, could also affect the movement of the eyeball as a whole. The design was then modified a changing the duel pin design on the lower plate, which could now 'fit and twist' securely into the grooves at the mating surface of the eyeball piece as shown in Figures

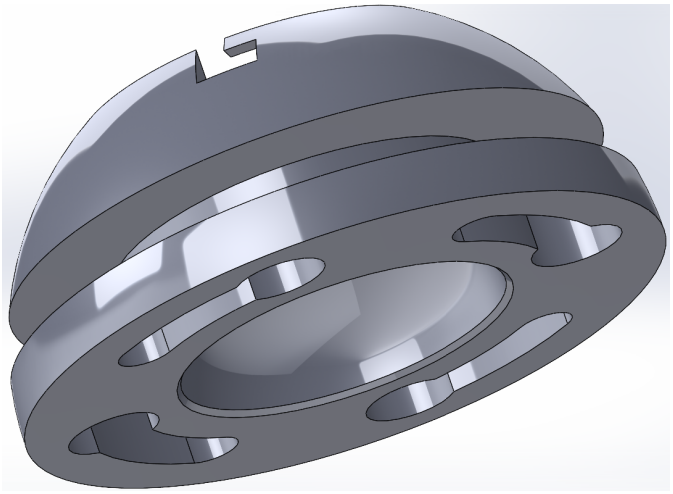

(a)

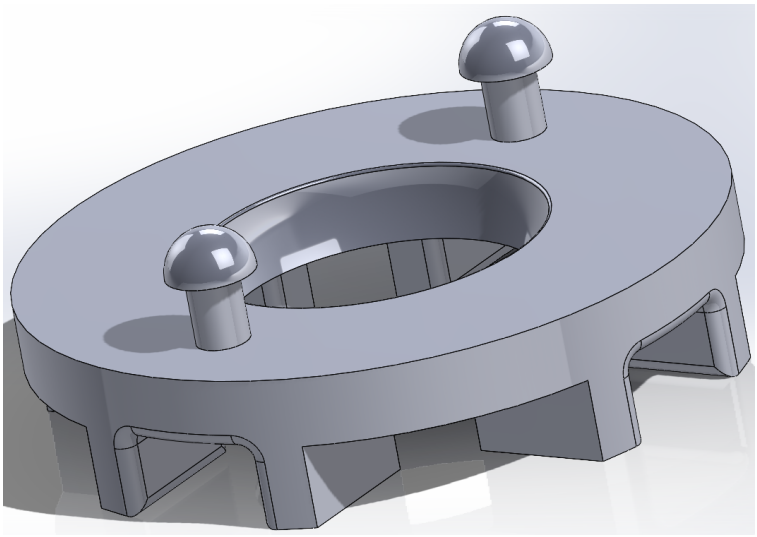

(b)

Figure 6.11: Modified eyeball and lower plate.

The second major flaw involved the compliant strips falling out of the ridges in the lower plate. The prototype was designed to have a functional range of 20 degrees from the vertical in all directions, with all the mechanical analysis done within this limit. As discussed earlier

in previous chapters, this limit was chosen as it was well within the maximum range of the movement when done by the expert surgeon. During surgical trials, the surgeon also felt and agreed the range was well within his expertise. However, the trainer pointed out that sometimes the trainees do tend to make major mistakes during their practices in the initial stages by pushing the eyeball well over 40 degrees or even more. As a result, the eyeball would flex so much that the other free strips would jump out of the ridges of the lower eyeball plate and get stuck. This might involve the overly strained strip to break. Although some modifications were proposed to alleviate either the short-range or the jumping ”out and sideways” issues of the strip as shown in Figures [[figure]], addressing both at the time was not possible without totally overhauling the design. Therefore, this is one of the fundamental limitations of the proposed prototype.

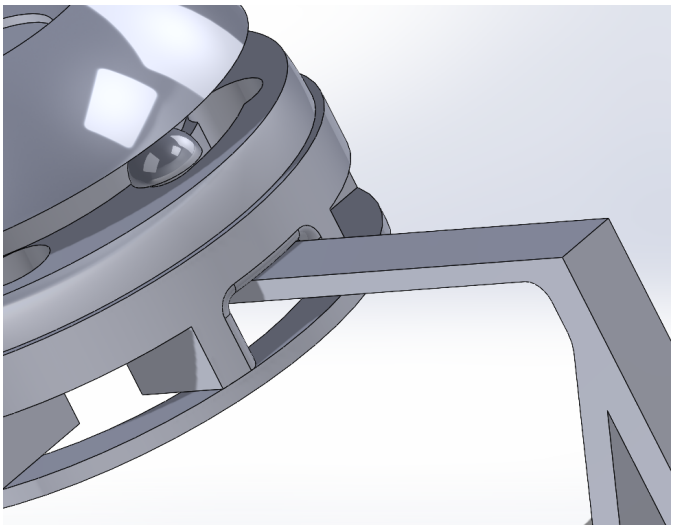

(a)

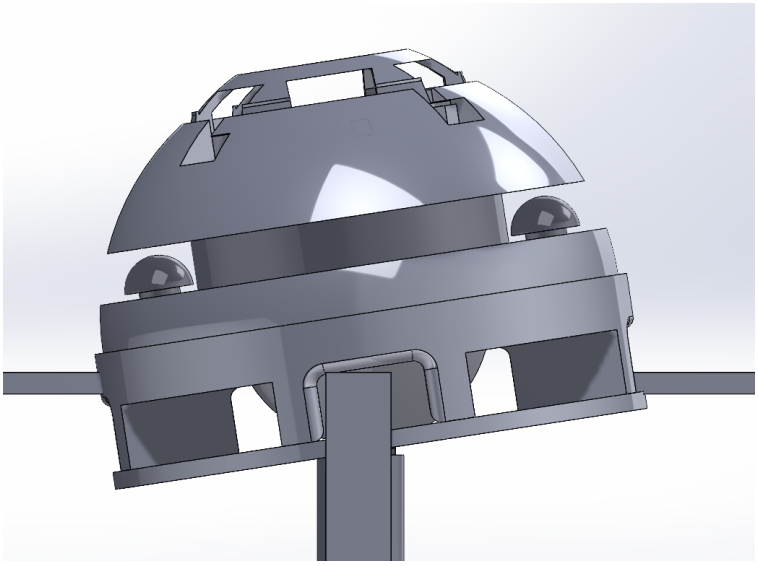

(b)

Figure 6.12: (a)Additional attachement to the lower eyeball plate, (b) range of movement (figure does not show flexing of the strips)

There was a minor flaw that involved the grip over the stretched eggshell membrane by

the corneal piece in the anterior chamber of the model. The trainer felt that the membrane would slip sometimes when the capsule-tearing part of the capsulorhexis step was carried out. This was overseen during the surgical trials as the surgeon tore off the membranes when they were thicker and the author did not have the necessary instruments or proper training in capsulorhexis to know whether such slips could be reproduced. While the membrane delaminating step was introduced in the material preparation guidelines, the tolerances of the corneal piece and the eyeball were adjusted. This validation trial made it clear that this was not enough. Many ideas were discussed and the parts were designed. Small teeth-like projections (about 0.1mm in depth) beneath the corneal piece were made to improve the grip as seen in Figure [[figure]]. Applying a minute amount of cyanoacrylate glue on the toothed edge of corneal tissue and pressing it on the stretched eggshell membrane to partially cure before loading this on the eyeball is also expected to work. There was an option of adding a rubber-like cushion like a sealing ring between the membrane-corneal piece junction to pinch down but because the slip arises from inherent tolerance of the manufacturing process (few tens of micrometers) and packing material at this scale is not very practical, it was not not considered in this study. Other minor changes were made to make the mating parts in the model a bit sturdier.

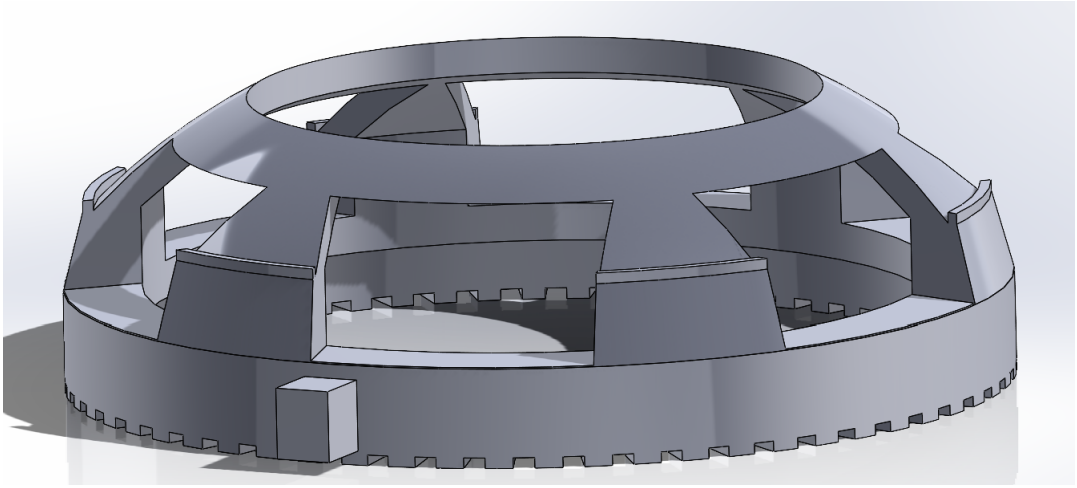

Figure 6.13: Modified corneal piece with teeth

The proposed modified prototype after the feedback from the surgeon is shown in Figure [[figure]]. A few cross-sectional views are in the appendix (Figures [[figure]] and [[figure]])

6.5.2. Positive remarks

Apart from the flaws, the trainer was impressed with the rest of the features. The cornea design was very suitable for the training. Although the surgeon in the surgical trial was indifferent towards this approach, the trainer appreciated the window-shaped design. He reasoned that each of those windows could serve different purposes or training opportunities- some covered in silicone membrane while others be left clear. The silicone membrane chosen was also very similar to the corneal tissue when penetrated with different surgical tools at his disposal. The clarity of the chamber under the microscope was also very good with minimal glare for both Methylcellulose as well as saline water. Although paracentesis was not possible as the IOP could not be increased or decreased since the lens was not attached, he acknowledged that the current model was not designed for such tests as it focused only on globe movement and capsule tearing. The chamber dimensions were akin to the human eye and the tools like

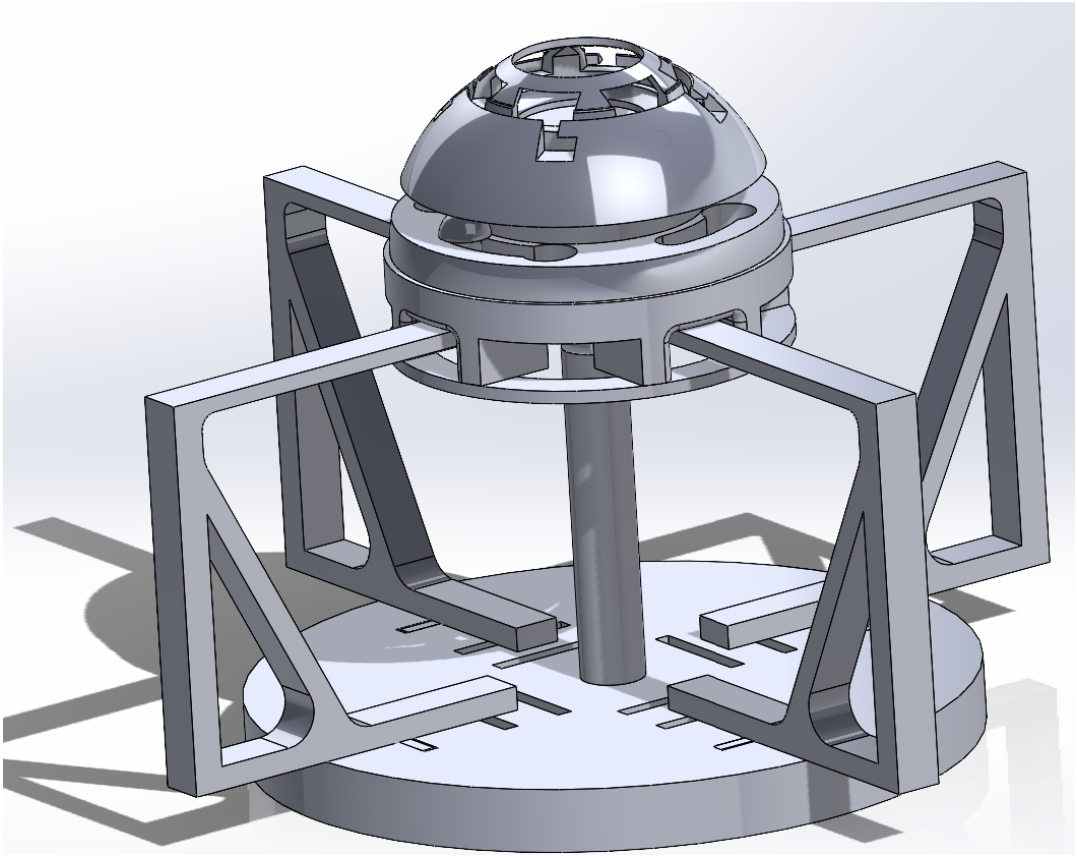

Figure 6.14: Modified prototype design

canula and forceps could be moved very appropriately.

For the limited range the model was designed for, the trainer acknowledged that the force and tension he and his students felt while moving the eyeball were similar to that of the human eye system for compliant strips of thicknesses between 0.5-0.85 mm, which was similar to the findings from the mechanical analysis. After each trial, the damage to the strips was minimal and within acceptable limits. The modular approach of the prototype was simple and easy to install without much hassle. This was especially important because there were several customization options available based on the training needs as well as storage and disassembly (as mentioned in the 'effects of creep' subsection in previous parts of this chapter). A few parts were expected to break by accident, especially the compliant strips either by rough handling by the students, manufacturing issues, or uneven/excessive loading - the trainer felt the overall design allowed easy replacement.

6.5.3. Proposed training methodology

Talks were had with the trainer about the possibilities of including the prototype and the training methods on it in the curriculum, at least in a closed and controlled manner. His response was very positive- there have been almost no models for globe stability training while the students can perform cataract surgery steps that are human eye-like when compared to the proposed prototype model. For this reason, as a professor and an examiner himself, Dr. Thomas suggested that the current training model could be incorporated after the 6 months of the first year of the 3-year course of ophthalmology course. This period is generally when the student has grasped the basics of surgery and undergone several animal eye training in the wet lab ex-

periments. The proposed model of training will fall into the dry lab training which immediately precedes the first human trials, therefore bridging the gap between the static animal eyes and dynamic human eyes. Mistakes are evident at this stage of transit and the proposed model acts well for its part to be a buffer, helping them hone their skills.

6.5.4. Recommended design changes for future improvements

The trainer supports the claim that there is a lot of potential in the current model for future work. A completely sealed cornea with a clear silicone membrane covering even the empty top of the corneal piece with no aberrations from molds would be the ideal design for many training procedures, including capsulorhexis and paracentesis. Some changes to the silicone/hydrogel lens material may make the model suitable for the rest of cataract surgery procedure training. A synthetic version of the eggshell membrane that has the same properties and a simpler preparation method would be useful as it makes the setup process simpler. Covering the half eyeball with proper surface tissue-like material can be good for suture training. 3D printing materials that have similar properties yet are cheaper can make the prototype even more accessible. A lot of isolated eyeball models could be made that could sit on the same globe movement system designed for this project.

6.6. Limitations of the project and experiments

There are a few limitations of this project and the nature of experiments, as listed:

- The design's range of motion was limited between -20° and +20° in all directions, which was lower than the total range the trainer desired.
- Exact theoretical calculations and finite element modelling were not performed to get the ideal thickness of the compliant strips for printing.
- Capsular membrane studies and exploration were limited by the availability of suitable testing machines. The choice of material was based solely on the research articles and their findings.
- Mechanical trials could have been completely automated instead of relying on the manual movement of precision guides.
- The capsulorhexis part of the validation trial was not a complete success. However, the trainer viewed this to be due to the membrane and less about the design.
- Re-validation trials of the modified prototype design were not carried out due to the nature of this project. However, the final design changes were communicated to the trainer.

6.7. Accomplishment of the set requirements

In this final section, the author addresses how the all requirements set at the beginning of the project are met to varying extents.

The proposed prototype has been successfully able to suit the requirements of the globe stability training- with all the movements and resistances replicated as close to a real eye. The eyeball design has achieved a very high level of anatomical similarity, except for the functioning of the capsular membrane.

The model is suitable for repeated usage with several features that allow for the repair and replacement of single or multiple-use materials. They can be easily built with the availability of a 3D printer and cost as low as 20-30 Euros per model. The model is customizable and the redesigned final model can be split to use the entire half eyeball as a static setup if needed.

7

Conclusion

This thesis project focused on designing and creating a training model of the anterior human eye for ophthalmology students to hone their skills in cataract surgery. The resulting final prototype sheds light on the often-overlooked field of eye phantoms, especially for training purposes. Through thorough iterations of several quantitative and qualitative assessments by various certified professionals, this very first model of its kind has achieved its distinction in achieving most, if not all the goals of this project. While the principal necessities of the prototype such as anatomical similarity and training capabilities had been achieved, the secondary obligations such as cost-effectiveness, fabricability in low-resource settings, and customizability have also been accomplished. While this project narrowed down to very specific steps of cataract surgery, there are a lot of doors waiting to be opened in this field using the final model presented in this project. Many design ideas are yet to be explored to improve the outcomes of the current model. Designing better corneal surfaces, creating synthetic substitutes for the membranes used in this project, and exploring alternative designs to attain better flexibility would be a few suggestions the author would like to put forward as possible directions for future works. The author hopes that future developments in eye-training phantom models would be competitive if not better than its alternatives.

References

[1] Serge Resnikoff et al. “Global magnitude of visual impairment caused by uncorrected refractive errors in 2004”. In: *Bulletin of the World Health Organization* 86.1 (2008), pp. 63–70.

[2] Nation Eye Institute. *What is cataract?* 2023. URL: https://www.nei.nih.gov/learn-about-eye-health/eye-conditions-and-diseases/cataracts#:~:text=Most%20cataracts%20happen%20because%20of,lens%20%E2%80%94%20known%20as%20a%20cataract (visited on 01/16/2024).

[3] Frank J Giblin. “Glutathione: a vital lens antioxidant”. In: *Journal of Ocular Pharmacology and Therapeutics* 16.2 (2000), pp. 121–135.

[4] Mohamed Abou Shousha and Sonia H Yoo. “Cataract surgery after pars plana vitrectomy”. In: *Current opinion in ophthalmology* 21.1 (2010), pp. 45–49.

[5] Hitoshi Shichi. “Cataract formation and prevention”. In: *Expert opinion on investigational drugs* 13.6 (2004), pp. 691–701.

[6] NHS. *Age-related cataracts*. 2020. URL: https://www.nhs.uk/conditions/cataracts/ (visited on 01/16/2024).

[7] Noha Mohamed Mohamed, Eman Shokry Abdalla, and Hanaa Hamdy Ali. “Quality of life of elderly patients with cataract”. In: *Zagazig Nursing Journal* 14.1 (2018), pp. 118–132.

[8] Maria Vittoria Cicinelli et al. “Cataracts”. In: *The Lancet* 401.10374 (2023), pp. 377–389.

[9] Junaid Khan and Subhojit Shaw. “Risk of cataract and glaucoma among older persons with diabetes in India: a cross-sectional study based on LASI, Wave-1”. In: *Scientific Reports* 13.1 (2023), p. 11973.

[10] Vincent DJ-P Dubois and Andrew Bastawrous. “N-acetylcarnosine (NAC) drops for age-related cataract”. In: *Cochrane Database of Systematic Reviews* 2 (2017).

[11] Christopher T Leffler et al. “The history of cataract surgery: from couching to phacoemulsification”. In: *Annals of Translational Medicine* 8.22 (2020).

[12] Geetha Davis. “The evolution of cataract surgery”. In: *Missouri medicine* 113.1 (2016), p. 58.

[13] Partha Biswas et al. “Residency Evaluation and Adherence Design Study III: Ophthalmology residency training in India: Then and now–Improving with time?” In: *Indian Journal of Ophthalmology* 66.6 (2018), pp. 785–792.

[14] Rohit Khanna, Siddharth Pujari, and Virender Sangwan. “Cataract surgery in developing countries”. In: *Current opinion in ophthalmology* 22.1 (2011), pp. 10–14.

[15] GW Eye Associates. *Cataract surgery*. URL: https://www.gweye.com/procedures/cataract-surgery (visited on 01/16/2024).

[16] Tony D Glover and Gheorghe M Constantinescu. “Surgery for cataracts”. In: *Veterinary Clinics of North America: small animal practice* 27.5 (1997), pp. 1143–1173.

[17] Carolyn E Kloek et al. “A broadly applicable surgical teaching method: evaluation of a stepwise introduction to cataract surgery”. In: *Journal of Surgical Education* 71.2 (2014), pp. 169–175.

[18] Sharon Nobuntu Maseko, Diane van Staden, and Euphemia Mbali Mhlongo. “The rising burden of diabetes-related blindness: A case for integration of primary eye care into primary health care in eswatini”. In: *Healthcare*. Vol. 9. 7. MDPI. 2021, p. 835.

[19] Suresh K Pandey and Vidushi Sharma. “Ophthalmology training and teaching in India: How these young ophthalmologists can become leaders of tomorrow?” In: *Indian Journal of Ophthalmology* 66.10 (2018), p. 1517.

[20] Javed Farooqui. “Postgraduate training program in ophthalmology in India: What’s lacking?” In: *Journal of Clinical Ophthalmology and Research* 3.2 (2015), pp. 111–111.

[21] Parikshit Gogate et al. “Residency evaluation and adherence design study: Young ophthalmologists’ perception of their residency programs–Clinical and surgical skills”. In: *Indian journal of ophthalmology* 65.6 (2017), p. 452.

[22] Susan Lewallen et al. “Non-physician cataract surgeons in Sub-Saharan Africa: situation analysis”. In: *Tropical Medicine & International Health* 17.11 (2012), pp. 1405–1408.

[23] Ministry of Health and Government of India Family Welfare. *NATIONAL ELIGIBILITY CUM ENTRANCE TEST (UG)*. June 28, 2023. URL: https://www.gweye.com/procedures/cataract-surgery (visited on 01/16/2024).

[24] New Delhi All India Institute Of Medical Sciences. *Syllabus for ophthalmology*. URL: https://www.aiims.edu/aiims/academic/aiims-syllabus/Syllabus%20-%20MBBS.pdf (visited on 01/16/2024).

[25] ANOUSHKA KAPILA, HARA PRASAD MISHRA, and NANDINI UPADHYAY. “Understanding the Facets of Service Bond for Medical Graduates and Post-Graduates in India”. In: ().

[26] Ministry of Health and Government of India Family Welfare. *Online NEET – PG Seats Allotment process*. January 17, 2024. URL: https://mcc.nic.in/pg-medical-counselling/ (visited on 01/16/2024).

[27] Elisabeth M Feudner et al. “Virtual reality training improves wet-lab performance of capsulorhexis: results of a randomized, controlled study”. In: *Graefe’s Archive for Clinical and Experimental Ophthalmology* 247 (2009), pp. 955–963.

[28] Mary K Daly et al. “Efficacy of surgical simulator training versus traditional wet-lab training on operating room performance of ophthalmology residents during the capsulorhexis in cataract surgery”. In: *Journal of Cataract & Refractive Surgery* 39.11 (2013), pp. 1734–1741.

[29] Madeleine Selvander and Peter Åsman. “Virtual reality cataract surgery training: learning curves and concurrent validity”. In: *Acta ophthalmologica* 90.5 (2012), pp. 412–417.

[30] Bonnie An Henderson et al. “Stepwise approach to establishing an ophthalmology wet laboratory”. In: *Journal of Cataract & Refractive Surgery* 35.6 (2009), pp. 1121–1128.

[31] Sehrish Nizar Ali Momin et al. “Surgical training in ophthalmology: Role of EyeSi in the era of simulation-based learning”. In: (2022).

[32] Amar Pujari et al. “Animal and cadaver human eyes for residents’ surgical training in ophthalmology”. In: *Survey of Ophthalmology* 67.1 (2022), pp. 226–251. ISSN: 0039-6257. DOI: https://doi.org/10.1016/j.survophthal.2021.05.004. URL: https://www.sciencedirect.com/science/article/pii/S0039625721001223.

[33] Chee Kiang Lam, Kenneth Sundaraj, and Mohd Nazri Sulaiman. “A systematic review of phacoemulsification cataract surgery in virtual reality simulators”. In: *Medicina* 49.1 (2013), p. 1.

[34] Vijay Kumar Dada and Narottama Sindhu. “Cataract in enucleated goat eyes: training model for phacoemulsification”. In: *Journal of Cataract & Refractive Surgery* 26.8 (2000), pp. 1114–1116.

[35] Shameema Sikder, Khaled Tuwairqi, Eman Al-Kahtani, et al. “Surgical simulators in cataract surgery”. In: (2013).

[36] Rajeev Sudan et al. “Formalin-induced cataract in goat eyes as a surgical training model for phacoemulsification”. In: *Journal of Cataract & Refractive Surgery* 28.11 (2002), pp. 1904–1906.

[37] S Farzad Mohammadi et al. “Sheep practice eye for ophthalmic surgery training in skills laboratory”. In: *Journal of Cataract & Refractive Surgery* 37.6 (2011), pp. 987–991.

[38] William F Maloney, Deborah Hall, and Dean B Parkinson. “Synthetic cataract teaching system for phacoemulsification”. In: *Journal of Cataract & Refractive Surgery* 14.2 (1988), pp. 218–221.

[39] UK Phillips studio. *Cataract eyes*. 2020. URL: `https://phillipsstudio.co.uk/cataract-eyes/` (visited on 01/16/2024).

[40] Eyecre.at GMbH. *Eye 4 cataract*. 2023. URL: `https://www.eyecre.at/shop/eye4cataract/` (visited on 01/16/2024).

[41] Carmelo De Maria et al. “Phantoms in medicine: The case of ophthalmology”. In: *Biomedical Science and Engineering* 3.1 (2019).

[42] Christoph Beck et al. “Low-cost head phantom for the evaluation and optimization of RF-links in ophthalmic implants”. In: *Biomedical Engineering/Biomedizinische Technik* 58.SI-1-Track-O (2013), p. 000010151520134377.

[43] Santosh G Honavar. “Steps to standardize ophthalmology residency programs in India”. In: *Indian Journal of Ophthalmology* 66.6 (2018), p. 733.

[44] Accreditation Council for Graduate Medical Education. *Common Program Requirements*. 2023. URL: `https://www.acgme.org/programs-and-institutions/programs/common-program-requirements/` (visited on 01/16/2024).

[45] Inessa Bekerman, Paul Gottlieb, Michael Vaiman, et al. “Variations in eyeball diameters of the healthy adults”. In: *Journal of ophthalmology* 2014 (2014).

[46] Kishore Cholkar et al. “Eye: Anatomy, physiology and barriers to drug delivery”. In: *Ocular transporters and receptors*. Elsevier, 2013, pp. 1–36.

[47] Jada Morris et al. “Proteomics of pseudoexfoliation materials in the anterior eye segment”. In: *Advances in protein chemistry and structural biology* 127 (2021), pp. 271–290.

[48] Helga Kolb. “Gross anatomy of the eye”. In: (2011).

[49] Do A Robinson. “The mechanics of human smooth pursuit eye movement.” In: *The Journal of Physiology* 180.3 (1965), p. 569.

[50] DS Childress and RW Jones. “Mechanics of horizontal movement of the human eye”. In: *The Journal of Physiology* 188.2 (1967), pp. 273–284.

[51] Kenneth W Wright. “Anatomy and physiology of eye movements”. In: *Pediatric Ophthalmology and Strabismus*. Springer, 2003, pp. 125–143.

[52] Sepehr Feizi et al. “Central and peripheral corneal thickness measurement in normal and keratoconic eyes using three corneal pachymeters”. In: *Journal of ophthalmic & vision research* 9.3 (2014), p. 296.

[53] Ying Hon et al. “In vivo measurement of regional corneal tangent modulus”. In: *Scientific reports* 7.1 (2017), p. 14974.

[54] William J Dupps Jr and Steven E Wilson. “Biomechanics and wound healing in the cornea”. In: *Experimental eye research* 83.4 (2006), pp. 709–720.

[55] Louise Pellegrino Gomes Esporcatte et al. “Biomechanical diagnostics of the cornea”. In: *Eye and vision* 7.1 (2020), p. 9.

[56] Jason Porter et al. “Separate effects of the microkeratome incision and laser ablation on the eye’s wave aberration”. In: *American journal of ophthalmology* 136.2 (2003), pp. 327–337.

[57] Veena Bhardwaj and Gandhi Parth Rajeshbhai. “Axial length, anterior chamber depth-a study in different age groups and refractive errors”. In: *Journal of clinical and diagnostic research: JCDR* 7.10 (2013), p. 2211.

[58] Neil Lagali et al. “Laser-Scanning in vivo Confocal Microscopy of the Cornea: Imaging and Analysis Methods for Preclinical and Clinical Applications”. In: Mar. 2013, pp. 51–80. ISBN: 978-953-51-1056-9. DOI: 10.5772/55216.

[59] Kambiz Thomas Moazed and Kambiz Thomas Moazed. “Iris Anatomy”. In: *The Iris: Understanding the Essentials* (2020), pp. 15–29.

[60] H Kenneth Walker, W Dallas Hall, and J Willis Hurst. “Clinical methods: the history, physical, and laboratory examinations”. In: (1990).

[61] Rafael Iribarren. “Crystalline lens and refractive development”. In: *Progress in retinal and eye research* 47 (2015), pp. 86–106.

[62] Weirong Chen, Xuhua Tan, and Xiaoyun Chen. “Anatomy and Physiology of the Crystalline Lens”. In: *Pediatric Lens Diseases* (2017), pp. 21–28.

[63] J Bours, HJ Födisch, and O Hockwin. “Age-related changes in water and crystallin content of the fetal and adult human lens, demonstrated by a microsectioning technique”. In: *Ophthalmic research* 19.4 (1987), pp. 235–239.

[64] RF Fisher. “The elastic constants of the human lens”. In: *The Journal of physiology* 212.1 (1971), pp. 147–180.

[65] Homayoun Tabandeh, Graham M Thompson, and Peter Heyworth. “Lens hardness in mature cataracts”. In: *Eye* 8.4 (1994), pp. 453–455.

[66] Susanne Krag and Troels T Andreassen. “Mechanical properties of the human lens capsule”. In: *Progress in Retinal and Eye Research* 22.6 (2003), pp. 749–767.

[67] Brian P Danysh et al. “Contributions of mouse genetic background and age on anterior lens capsule thickness”. In: *The Anatomical Record: Advances in Integrative Anatomy and Evolutionary Biology: Advances in Integrative Anatomy and Evolutionary Biology* 291.12 (2008), pp. 1619–1627.

[68] Lee Ann Remington. “Chapter 5 - Crystalline Lens”. In: *Clinical Anatomy and Physiology of the Visual System (Third Edition)*. Ed. by Lee Ann Remington. Third Edition. Saint Louis: Butterworth-Heinemann, 2012, pp. 93–108. ISBN: 978-1-4377-1926-0. DOI: https://doi.org/10.1016/B978-1-4377-1926-0.10005-0. URL: https://www.sciencedirect.com/science/article/pii/B9781437719260100050.

[69] Thomas Kuriakose. “Examination of Lens”. In: *Clinical Insights and Examination Techniques in Ophthalmology*. Singapore: Springer Singapore, 2020, pp. 143–148. ISBN: 978-981-15-2890-3. DOI: 10.1007/978-981-15-2890-3_12. URL: https://doi.org/10.1007/978-981-15-2890-3_12.

[70] written by Anna Barden All about vision. *Eye muscles and their functions*. 2023. URL: https://www.allaboutvision.com/eye-care/eye-anatomy/eye-muscles/ (visited on 01/16/2024).

[71] Won June Lee et al. “Differences in eye movement range based on age and gaze direction”. In: *Eye* 33.7 (2019), pp. 1145–1151.

[72] Formlabs. *Draft Resin*. 2024. URL: https://formlabs.com/eu/store/materials/draft-v2-resin/ (visited on 01/16/2024).

[73] Formlabs. *Using Draft Resin*. 2024. URL: https://support.formlabs.com/s/article/Using-Draft-Resin?language=en_US (visited on 01/16/2024).

[74] Thomas D Lenart et al. “A contact lens as an artificial cornea for improved visualization during practice surgery on cadaver eyes”. In: *Archives of ophthalmology* 121.1 (2003), pp. 16–19.

[75] Polytek Development corp. *PlatSil Gel-OO*. 2024. URL: https://polytek.com/platsil-gel-oo (visited on 01/16/2024).

[76] Kerstin Lebahn et al. “Determination of material properties from tissue samples of low strength and size”. In: *Current Directions in Biomedical Engineering*. Vol. 9. 1. De Gruyter. 2023, pp. 427–430.

[77] Ali Üneri et al. “New steady-hand eye robot with micro-force sensing for vitreoretinal surgery”. In: *2010 3rd IEEE RAS & EMBS International Conference on Biomedical Robotics and Biomechatronics*. IEEE. 2010, pp. 814–819.

[78] TheRoundup Org. *What Are Orbeez Made Of Are They Biodegradable*. 2024. URL: https://theroundup.org/what-are-orbeez-made-of-are-they-biodegradable/ (visited on 01/16/2024).

[79] Formlabs. *Draft resin-store*. 2024. URL: https://formlabs.com/eu/store/materials/draft-v2-resin/ (visited on 01/16/2024).

[80] Schminkengrime. *PlatSil Gel-OO*. 2024. URL: https://schminkengrime.nl/polytek-platsil-gel-00-silicone-1kg (visited on 01/16/2024).

[81] Romijn Hardware Tools bv. *KOGELS STAAL*. 2024. URL: https://www.romijn.nl/kogels/733949-558-kogels-staal.html#/212-diameter_mm_ab-120 (visited on 01/16/2024).

[82] Etos. *Soft Daily Lenses*. 2024. URL: https://www.etos.nl/producten/etos-zachte-daglenzen--400-111158804.html (visited on 01/16/2024).

[83] AH Parsons. “Structure of the eggshell”. In: *Poultry Science* 61.10 (1982), pp. 2013–2021.

A

Appendix: Parts creation and assembly steps

A.1. Molding the silicone membrane membrane on corneal piece

1. Make sure the tweezers, mold, clean corneal piece, mold cap, release spray, cup, stirrer, and silicone resin (PlatSil -00 A and B) are all available. (Figure A.1)

Figure A.1

2. Spray the release agent of the mold and the mold cap.(Figure A.2)

Figure A.2

3. Mix the resin mixture 1:1 scale in a cap using a stirrer and place it in a vacuum chamber to degas it.(Figure A.3)

Figure A.3

4. After degassing for a minute, carefully pour a small amount of the silicone resin mixture into the mold.(Figure A.4)

Figure A.4

5. Press the corneal piece into the filled mold till it overflows.(Figure A.5)

Figure A.5

6. Add some more resin on top of the setup to form a layer and then place the cap on it and press.(Figures A.6 and A.7)

Figure A.6

Figure A.7

7. Add some coloring pigment into the remaining silicone and pour it into the lens tray to create a batch of cataractous colored lens
8. Let the silicone harden over 5-6 hours and gently remove all the pieces from the mold. Make sure to remove extra materials to fit into the parts perfectly.

A.2. Prototype setup guide

Full set overview: The following pictures are of the package sent to Dr. Thomas. The package has multiple copies of each part necessary to assemble at least 2 whole prototypes alongside the spare parts (except eggshell membranes and liquids).

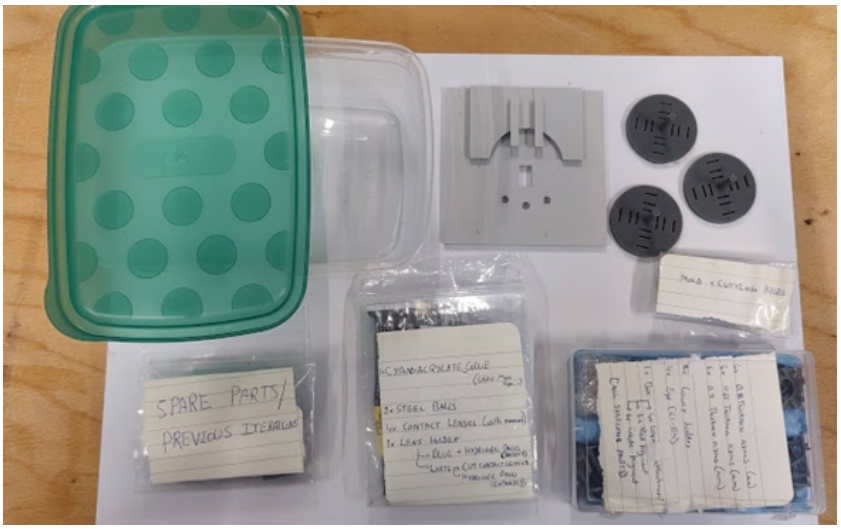

Figure A.8: Full Kit

(a) (b) (c)

Figure A.9: Full kit

Setup steps: The following steps are to be followed to build the prototype. Some steps may also have a tip written next to it which can be implemented by the user in case it is necessary.

1. The lower eyepiece is cleaned and placed on the base through its central pillar with the pins facing upwards. The steel ball is attached to the tip of the base pillar using a single drop of superglue. Care must be taken to not spread the glue over the other surfaces of the ball. (Figure A.10)

Figure A.10

2. The spherical hollow surface of the eyeball and ball are cleaned. The two alternate holes of the eyeball are either stuffed with a very thin piece of paper (as shown in the image below) or glued for temporary or permanent fixtures respectively. If glue is used, care must be taken as to not add excessive glue as it might spread out of the pinhole and stick to the ball. The paper filling must not extend over the hollow surface of the eyeball as that might hinder the free movement of the eyeball over the steel ball. (Figure A.11)

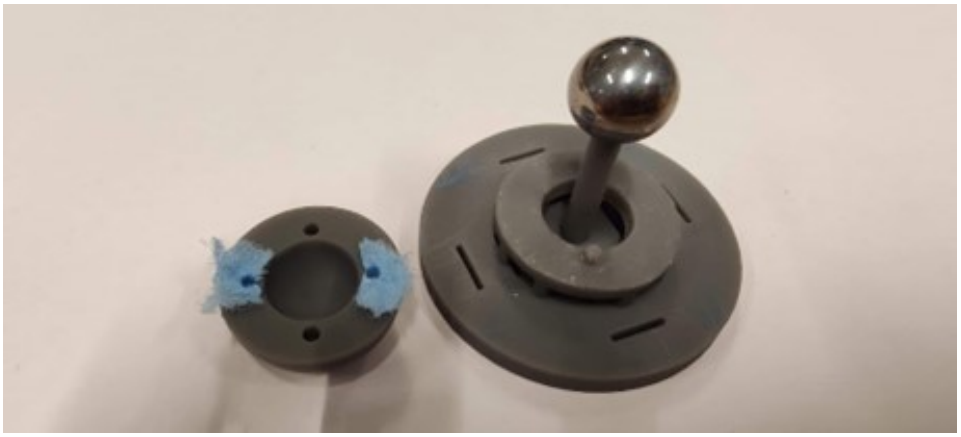

Figure A.11

3. Attach the eyeball firmly to the setup and check if the eyeball can move about freely. Check if the attachments are firm. There might be some gap between the eyeball and the lower eyeball piece, which can be ignored if the pieces are held firmly.(Figure A.12)

Figure A.12

Tip: if the temporary fixture is loose, 4 tiny bits of strong adhesive tape can be fixed over the lower surface of the lower eyepiece avoiding the grooves in which the tension elements sit and the eyeball.

4. The cataractous lens made of either silicone (as shown in the figure below) or sliced hydrogel is placed in the top central groove of the eyeball piece. Make sure that the size of the lens is such that it fits well in the grove and is not too thick. (Figure A.13)

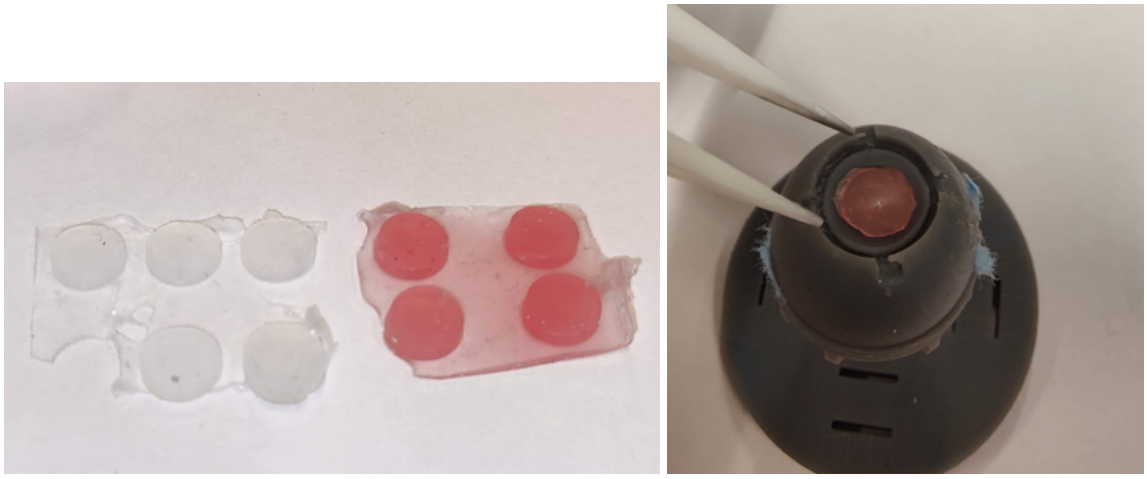

(a) (b)

Figure A.13

5. The thin eggshell membrane is placed over the setup and is held firmly while stretching it over the top part of the eyeball in such a way that there are not wrinkles over the lens. (The image below shows a plastic wrapper instead of the eggshell membrane due to reasons regarding the filming premise and cleanliness). (Figure A.14)

(a) (b)

Figure A.14

6. The corneal piece is placed over the stretched membrane using the other hand and pressed down in the circular groove of the eyeball gently with a thumb from the top or forceps on the pins of the piece. Care must be taken as to not push too hard with the thumb on the dome ring or forceps on the pins as they might break. When the pins are in the notch and the corneal piece leveled, the pins are pushed anticlockwise using a sharp tool, again carefully without breaking the pins. This should lock the corneal piece in place. (Figure A.15)

(a) (b)

Figure A.15

7. A set of 4 tension elements of suitable stiffness is picked from the selection. A thin piece of paper is wrapped in a ‘U’ shape on the lower part of each tension element. The tension elements are then attached using fingers to the slots in the base one at a time in such a way that each cantilever strip can slide into the rectangular groove of the lower eyeball piece when the eyeball bends. Do not use glue as prolonged tension in the strips might cause them to bend and deform. Hold the eyeball firmly and trim down the excessive eggshell membrane protruding outwards using a sharp scalpel if needed (scratches on the eyeball do not damage the prototype’s functioning). (Figure A.16)

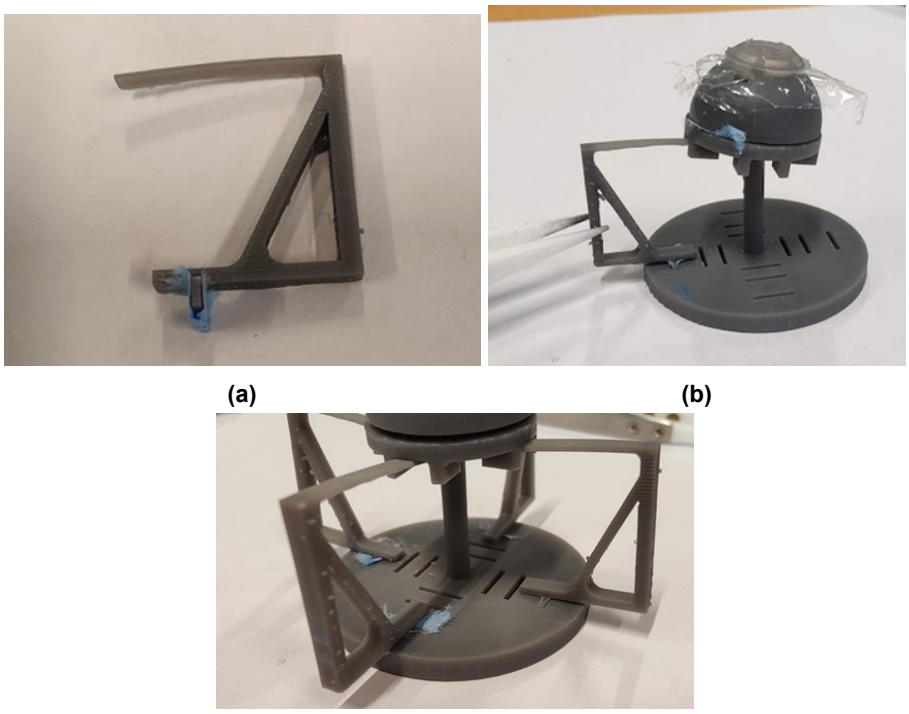

(a) (b)

(c)

Figure A.16

To remove the tension elements, use a sharp tool or forceps to push the element from the bottom of the base slot until the piece is free to fall off. Do not pull out with the fingers as they will break (Figure A.17)

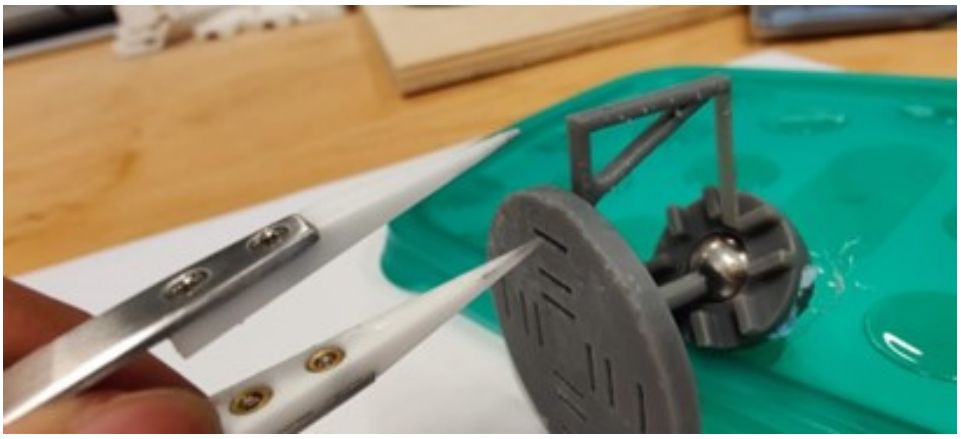

Figure A.17

8. Slide the setup into the semicircular slot of the white baseplate and make sure everything is firmly held. (Figure A.18)

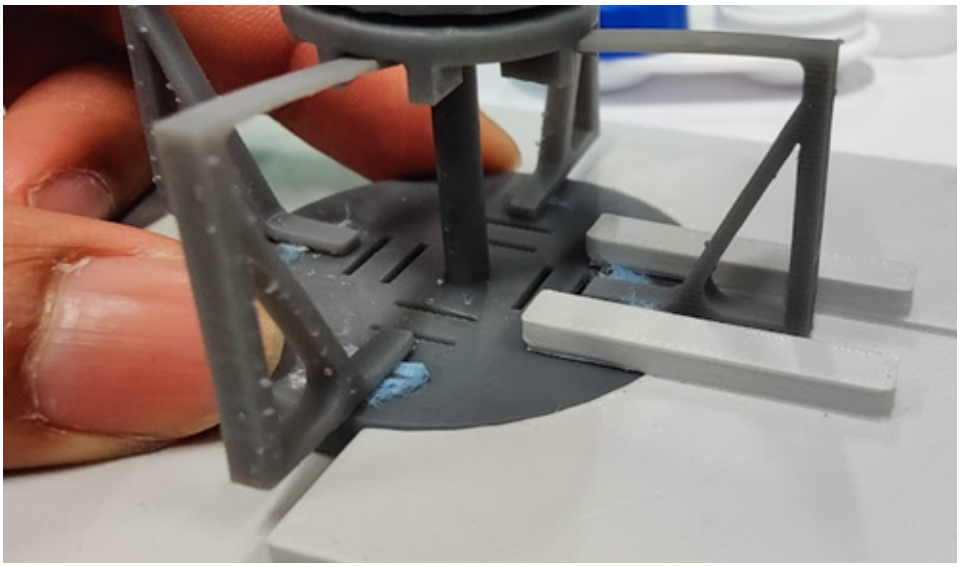

Figure A.18

9. Add water to the anterior chamber using a syringe until there is a convex surface of water. Check for any type of leaks around the circumference of the corneal piece and the notches. Check for any wrinkles over the cataractous lens. (Figure A.19)

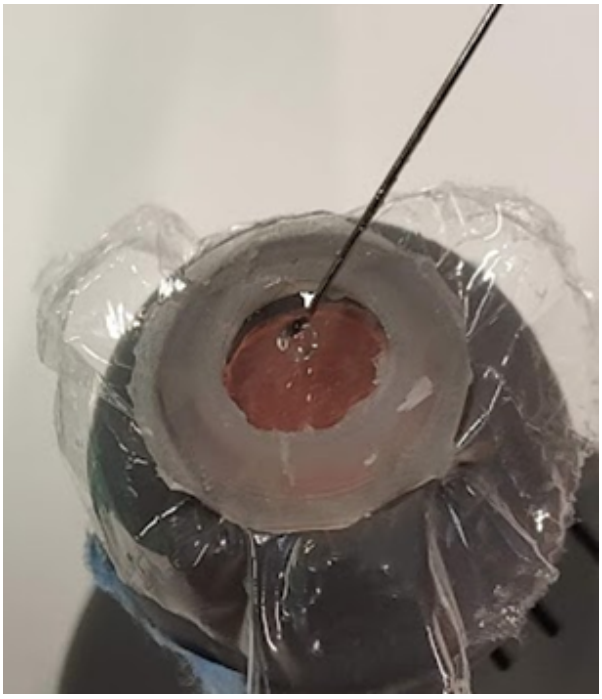

Figure A.19

Tip: If there are any leaks about the notches, add a drop of cyanoacrylate glue. This glue will not harden for at least an hour if the surfaces are wet or humid. The glue can also be applied on the circular underside of the corneal piece in step 6 if the tension of the capsular membrane is not enough. After the usage, clean the residual glue completely using a scalpel or a sharp tool.

10. The lens is placed over the corneal piece and the water surface carefully. The small air bubble can be removed during training if needed. Add a drop of water (or the same solution used in the anterior chamber) on the outer surface of the lens soon after the placement and every 1-1.5 minutes. If the lens flips, adding this water and maintaining the water level in the anterior chamber should get it back to its normal position. (Figure A.20)

(a) **(b)**

Figure A.20

B

Appendix: Major dimensions of prototype and graphs

B.1. Dimensions

Cross-sectional view:

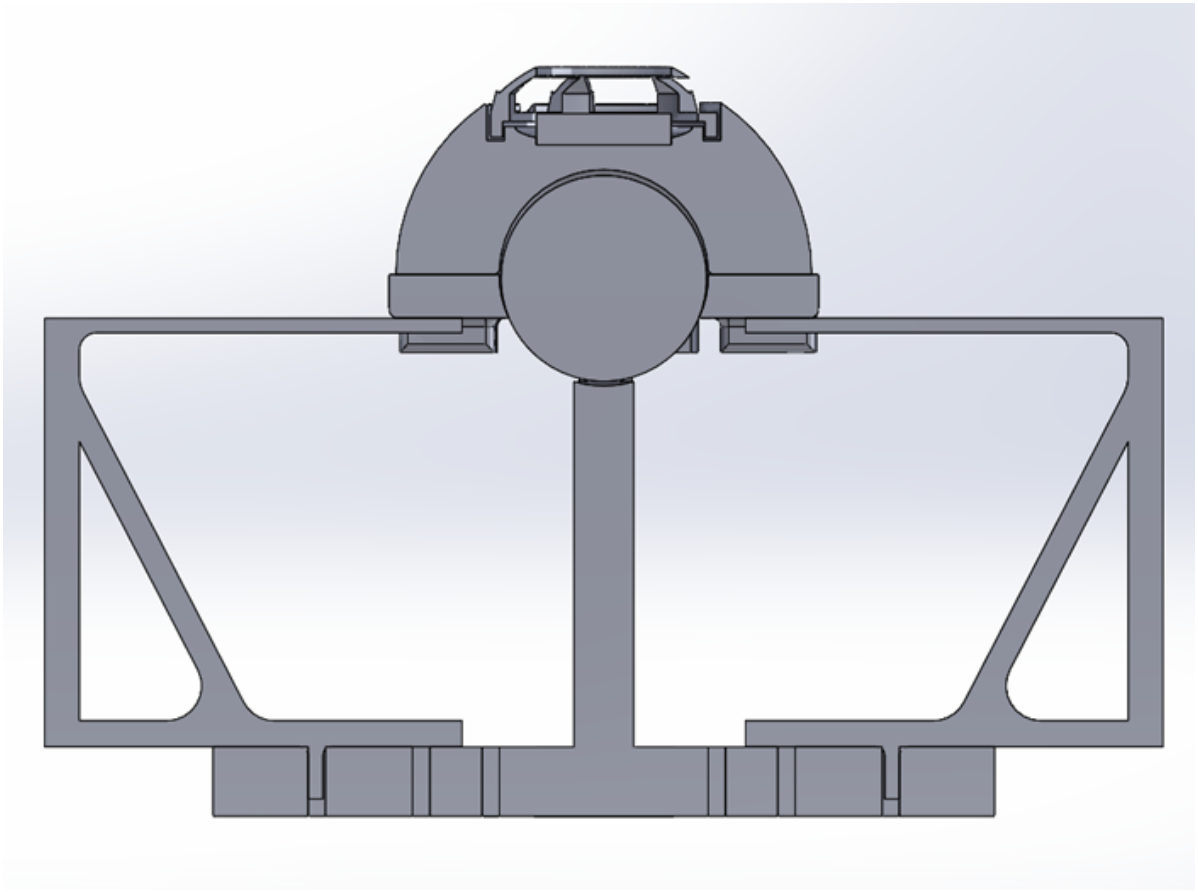

Figure B.1

Major dimensions:

- Eyeball diameter: 24 mm

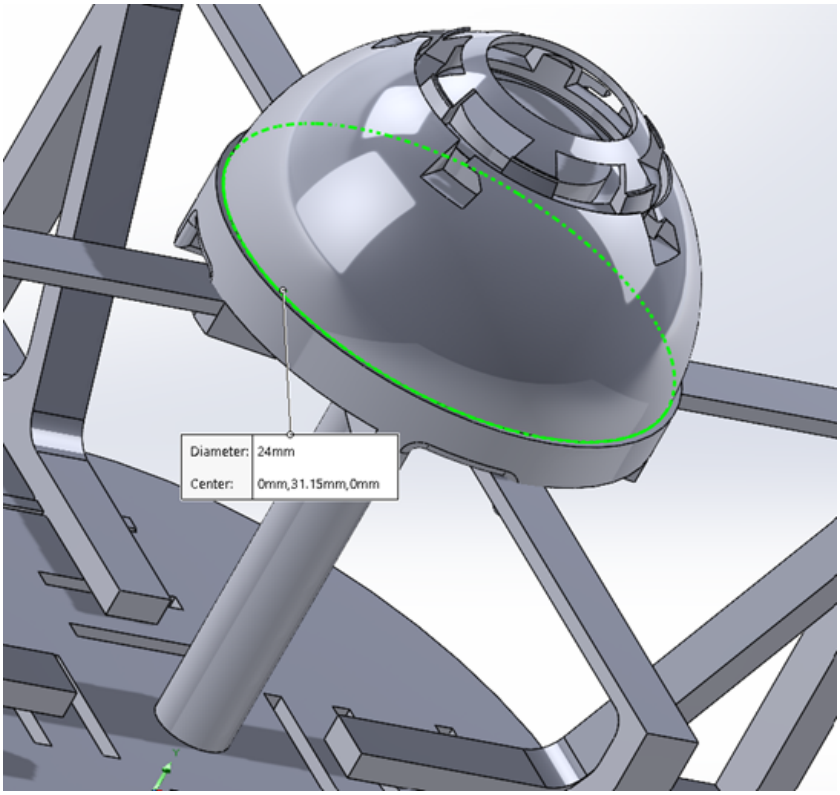

Figure B.2

- Workable cornea diameter: 11 mm (internal diameter ignoring the wall thickness)

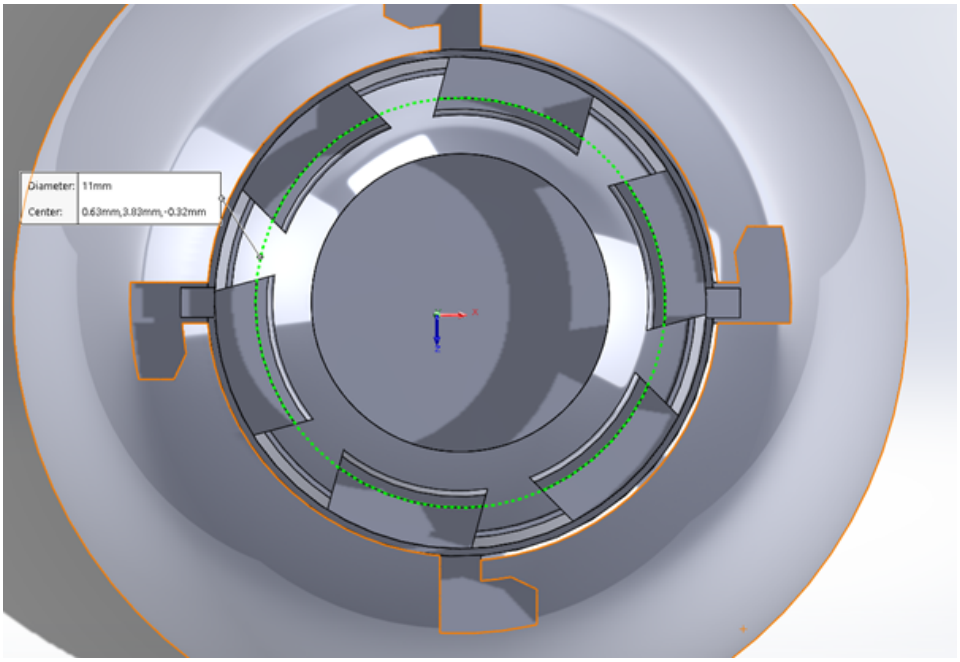

Figure B.3

- View window (pupil dilated) diameter: 8 mm

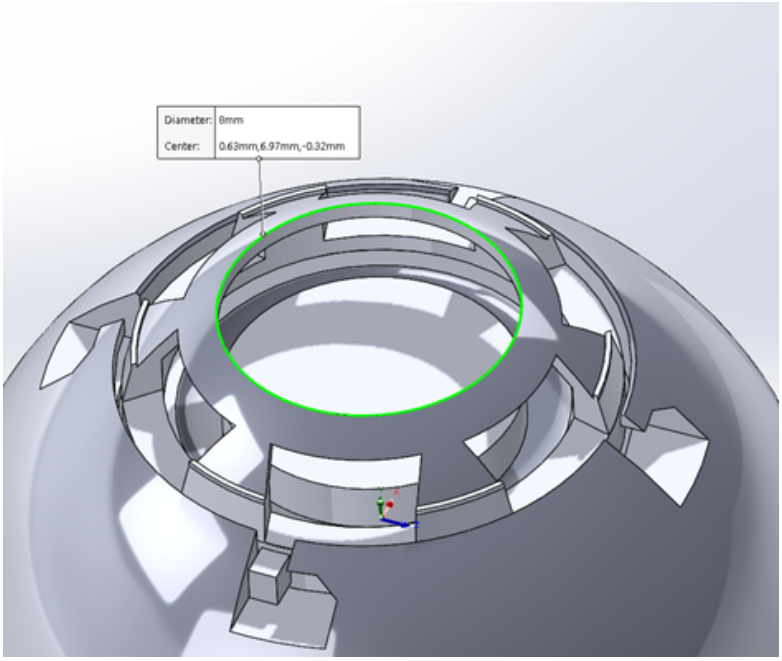

Figure B.4

- Anterior chamber depth: 2.06 mm+ 0.62 mm = 2.64 mm (ignoring the lens dome and membrane thickness). [lens can be made thinner to increase ACD].

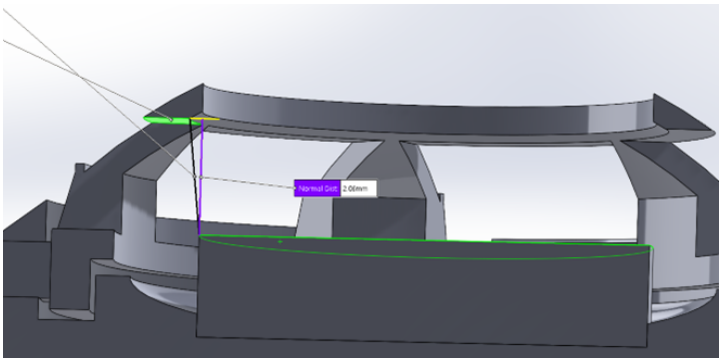

(a)

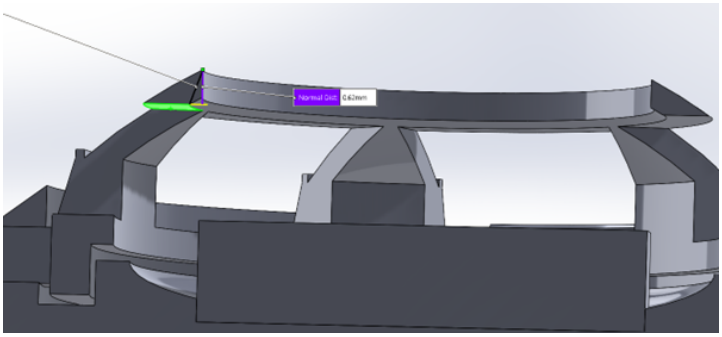

(b)

Figure B.5

- Vertical distance between the lens capsule surface and point of entry: 0.64mm.

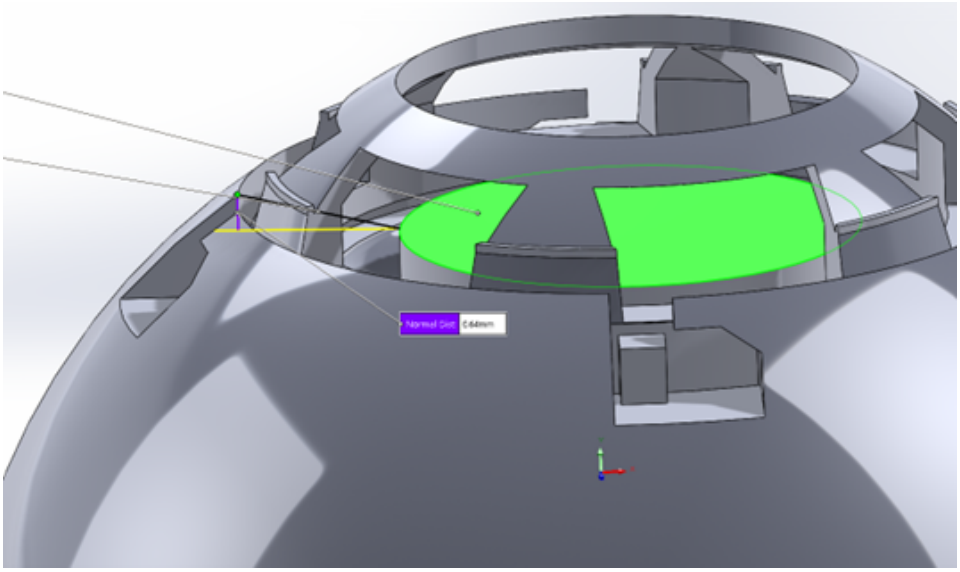

Figure B.6

- Actual lens thickness: 1.8 mm, diameter: 8 mm, Workable lens thickness: 0.75 mm, diameter: 8 mm

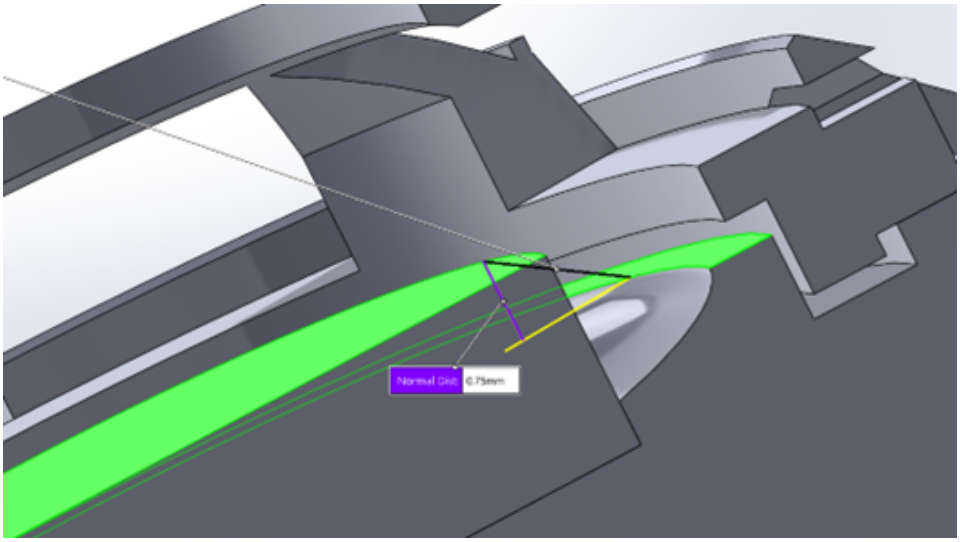

Figure B.7

- Number of ports: 6; Angular orientation between two ports: 60 degrees [of which two opposing ports are along major direction (either up/down or left/right)]

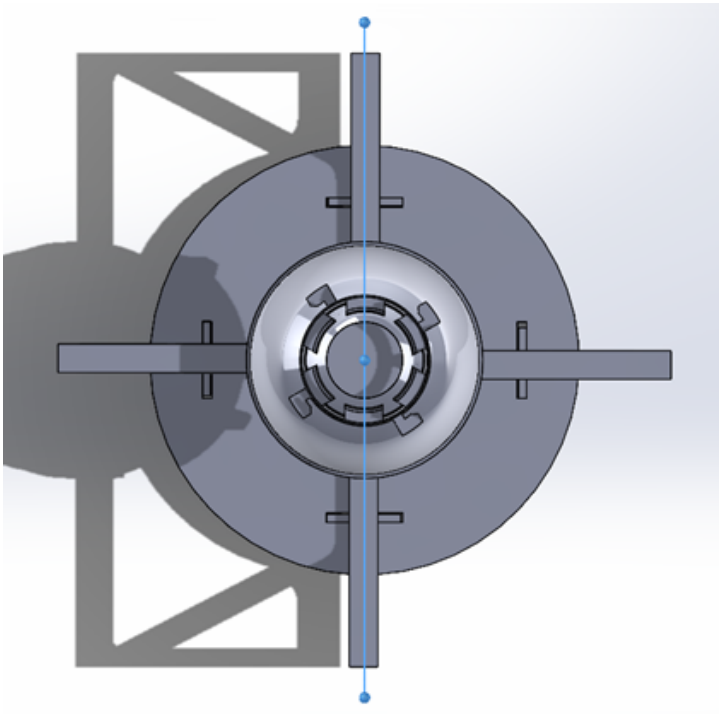

Figure B.8

- Wall thickness at incision (ignoring silicone overlay): 1mm

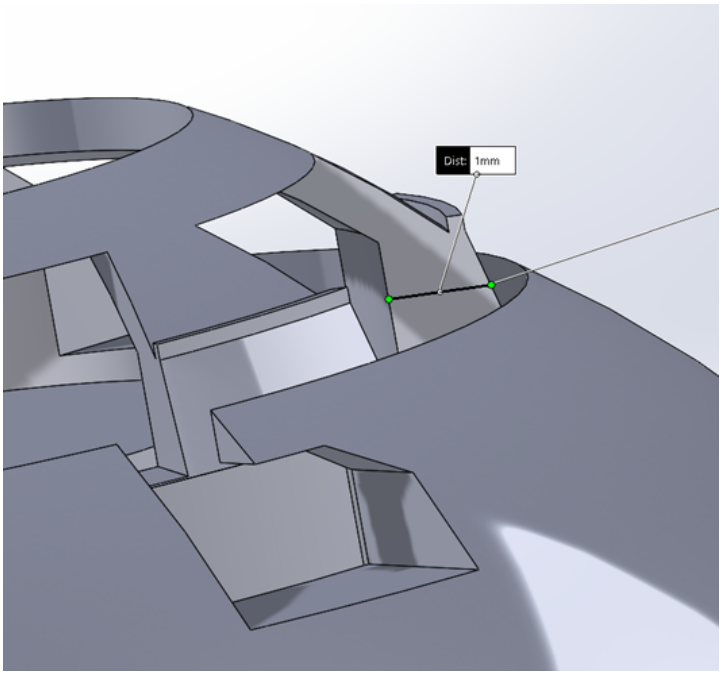

Figure B.9

- Workable Incision port size: 4 mm x 1.42 mm

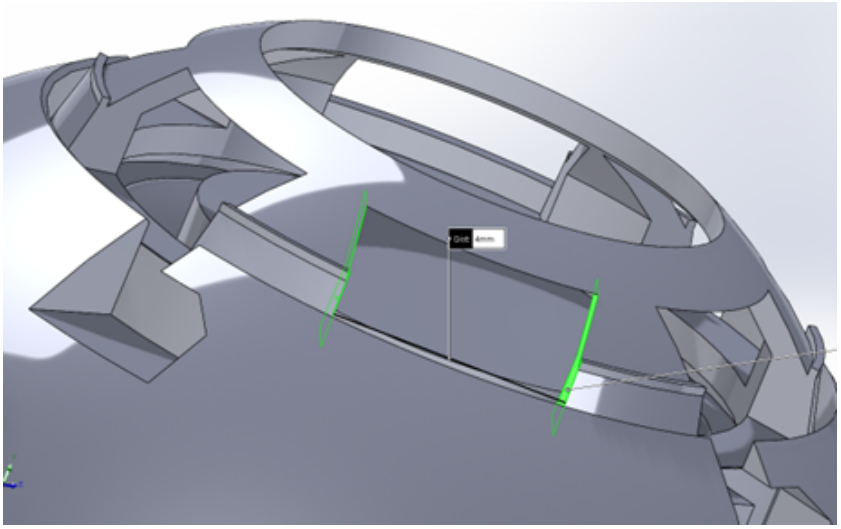

(a)

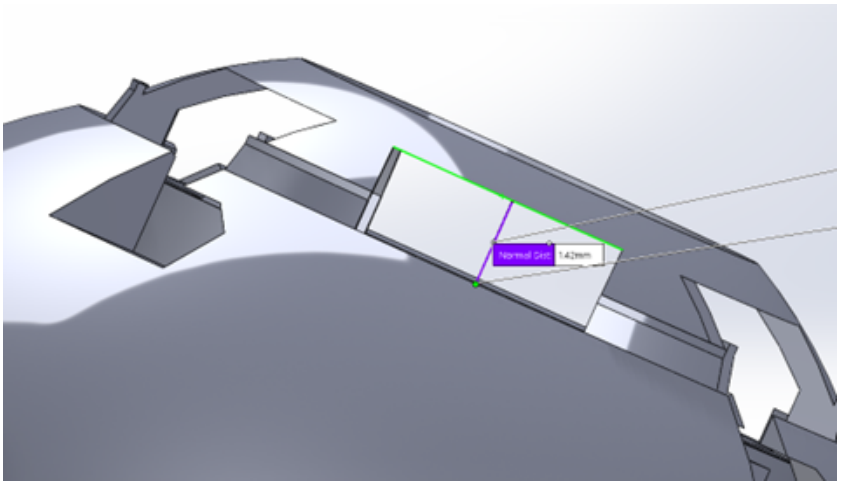

(b)

Figure B.10

- Cornea piece with different model eyeballs (with and without notches).

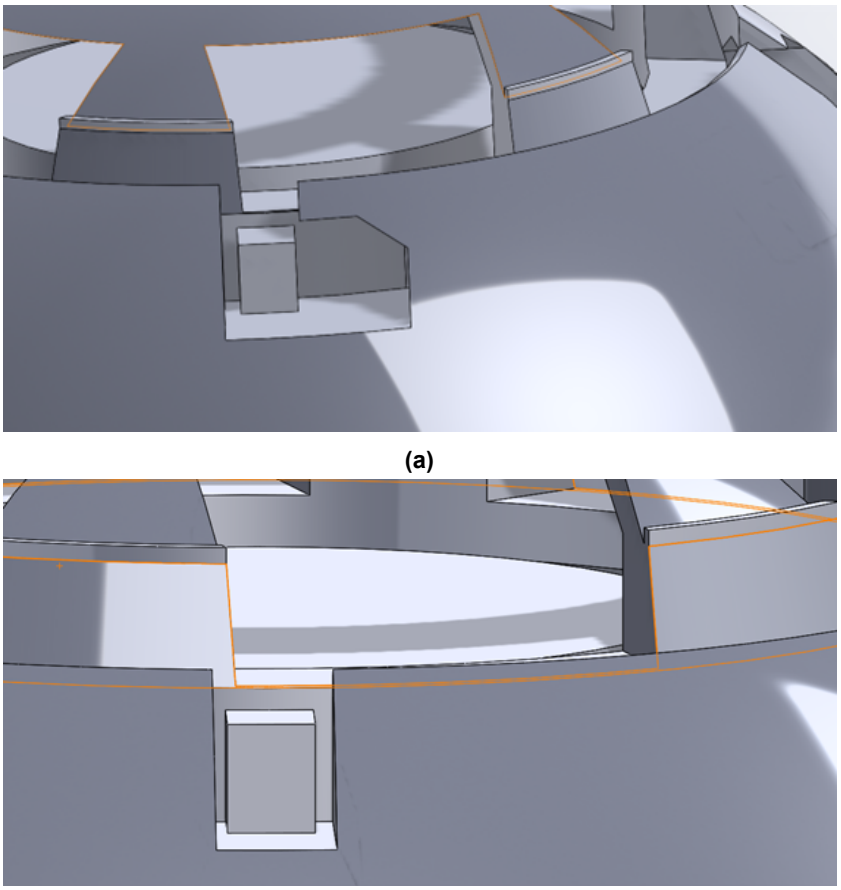

(a)

(b)

Figure B.11

B.2. Additional graph

Cyclical loading of 0.5mm thickness strip: The following graph shows the hysteresis of the strip as it underwent 20 loading cycles during the mechanical trials. The data captured is for the 10 cycles and it is visible that the hysteresis is visible as the loop.

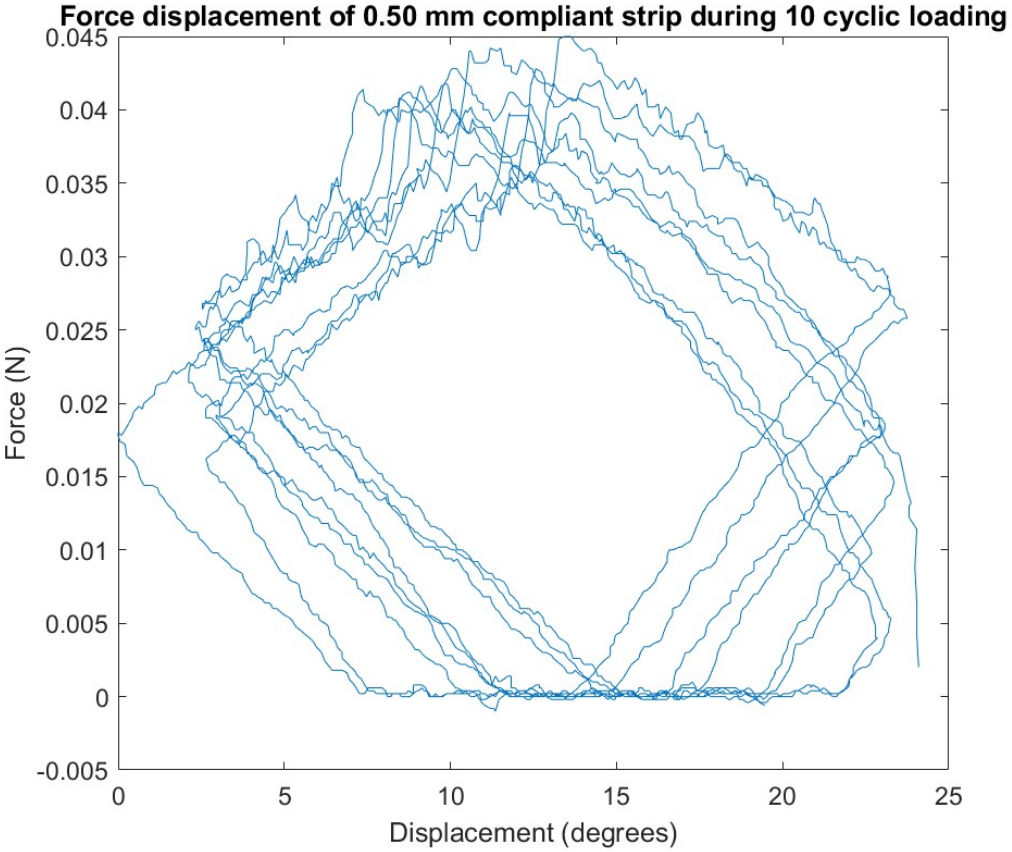

Figure B.12: Hysteresis loop of 0.50 mm compliant strip under 10 cyclic loadings.